

CAKE FILTRATION AT HIGH BIOMASS NITROGEN REMOVING SYSTEMS

by

Burcu Özdemir

B.S. in Environmental Engineering, İstanbul University, 2000

M.S. in Environmental Engineering, Marmara University, 2003

Submitted to the Institute of Environmental Sciences in partial fulfillment of
the requirements for the degree of

Doctor

of

Philosophy

in

Environmental Technology

Boğaziçi University

2013

ACKNOWLEDGEMENTS

I would like to begin by expressing my deep appreciation to my advisor, Prof. Orhan Yenigün for giving me the opportunity of working with him. I am thankful for his support and guidance as well as for his trust in me. I would like to acknowledge Prof. Ahmet Saatçı and his pantyhose joke, saying that nevermind the filter media, cake formed on the media will do all filtration, you can even use a vuggy material as thin as a pantyhose. I did not use pantyhose but his words deeply inspired me while I was developing the cake filtration unit. I am thankful for his support and guidance starting from the very first days of my Masters program. I would also like to thank Prof. Ayşen Erdinçler; our talks helped me to mold my view and avoided me from being superficial in some analyses.

I would like to acknowledge Istanbul Water and Sewerage Administration (İSKİ) and Paşaköy wastewater treatment plant. I would like to thank Ali İnci, former manager of the plant for İSKİ, Dr. Mehmet Emre Baştopçu, general manager of Kuzu Group, Filiz Veznikli, former manager of the plant for Kuzu Group, Bahadır Bozkır, former construction manager of Kuzu Group, for the construction of the pilot plant in 2007. I would also like to acknowledge Sanda Kıray and Ian Hume for supplying the membranes and information. I would like to thank Adem Aydın and his team for all mechanical works and for his endless patience in me. I would like to thank Halil Batan, Barış Şen and their team for all electrical works, especially Baris Şen, who also gave life to my automation scenario; I thank for their endless patience in me. I would also like to thank Hale Uğurcu, former laboratory manager of Kuzu Group and laboratory assistants Ümit Şahin and Adem Hasırcı for helping me in sampling. I would like to acknowledge Özge Pulanay for helping me with the initial filtration experiments. I am thankful to all maintenance team and shift men, who helped to maintain the pilot plant and kept the pilot plant running. Also, I would like to acknowledge

everyone under the roof of İSKİ, who has been asking me whether ‘the pantyhose’ accomplished.

I am thankful to Assoc.Prof. Bülent Mertoğlu and his team for helping me with the molecular work that also helped me to develop the structure of my thesis and the methods for understanding the high biomass systems.

I am thankful to Prof. Slawomir Hermanowicz for having me as a part of his group and for being a sincere help. Working in his laboratory, has been a great opportunity for deeper understanding of membrane fouling and more importantly gave me a chance to study more on filtration mechanisms. I would also like to acknowledge Prof. Lisa Alvarez Cohen for her help on questioning and analyzing the molecular data.

I would like to acknowledge Kuzu Group, where I worked as a process and design engineer, for my financial support. I would like to acknowledge my other financial supporters as a student and a researcher: The Scientific and Technological Research Council of Turkey (TÜBİTAK) and Engineering Research Support Organization (ERSO) of University of California at Berkeley.

I appreciate tremendous help of my family. I would like to thank my late father for being the greatest father and I would like to thank my mother for being the greatest mother. I would like to acknowledge Alp; he has been the greatest support in everything. I am thankful for his endless mentoring and his encouraging way. I would like to express my deepest respect.

Finally, I would like to acknowledge Starbucks Beyođlu; the team and all guests provided the best study environment for me that really helped me to concentrate and focus on my work while I was having trouble during my pill treatment for almost the last two years.

ABSTRACT

Pilot scale cake filtration biological reactor (CFBR) and membrane bioreactor (MBR) were operated (capacity: 100 m³/d) for 26 months. The system was evaluated according to conventional cake filtration theory using its plots of V vs. t and t/V vs. V . Standard blocking model plots of CFBR were compatible ($R^2 > 0.95$) for the initial period; the latter was best fitted to the cake filtration model ($R^2 > 0.99$). The linearity between t/V and V was observed individually, showing a change of filtration characteristics at the transition point. Results of a particular period (six months) with complete sludge retention were presented to state the sludge production pattern and, the activity and diversity of nitrogen converters. The average sludge yield reached equilibrium after day 105 (0.25 kg_{MLSS}/kg_{COD}, MLSS~15,000 mg/L). Volatile portion of mixed liquor suspended solids (MLVSS/MLSS) increased–decreased–increased and stabilized around 0.57. Inert material stabilization showed that inerts could be degraded at sufficiently long SRTs. The nitrifier population was adversely affected by gradually increased biomass with insignificant effluent quality change. However, coexistence of aerobic and anaerobic ammonia oxidizers in a partially aerated system was confirmed. The total operation cost of such high biomass filtration system could be 9–15 percent less than that of a biological nutrient removal (BNR) plant because of the decreased expenses for sludge disposal.

ÖZET

Pilot ölçekli kek filtrasyon biyolojik reaktör (CFBR) ve membran bioreaktör (MBR) üniteleri (kapasite: 100 m³/gün) 26 ay boyunca işletilmişlerdir. Sistem konvansiyonel kek filtrasyon teorisine göre $V-t$ ve $t/V-V$ grafikleri kullanılarak değerlendirilmiştir. CFBR için, başlangıç periyodu standard bloke modeli ile uyumludur ($R^2 > 0.95$); sonraki period için kek filtrasyon modeli en iyi sonucu vermiştir ($R^2 > 0.99$). Periodlar ayrı ayrı değerlendirildiğinde, t/V ve V arasında doğrusal ilişki vardır; ilk period sonunda lineerlikten sapma noktası filtrasyon karakteristiğindeki değişimi göstermektedir. Çamurun bütünüyle sistemde bekletildiği, altı aylık bir dönemde, çamur üreme süreci ve azot gideren organizmaların faaliyet ve çeşitlilikleri değerlendirilmiştir. Sistemdeki çamur üremesi 105 gün sonra denge koşullarına ulaşmıştır. Askıda katı madde içerisindeki uçucu (MLVSS/MLSS) oranı atmış–azalmış–yeniden artmış ve 0.57 civarında dengelenmiştir. İnert madde stabilizasyonu, inertlerin yeterince uzun çamur yaşlarında ayrışabileceklerini göstermiştir. Çıkış kalitesine önemli etkisi olmamasına rağmen, nitrifikasyon organizmalarının faaliyet ve çeşitlilikleri, giderek artan biyokütle konsantrasyonundan olumsuz etkilenmiştir. Sonuçlar, kısmen havalandırılan sistemde, aerobik ve anaerobik amonyak yükseltgeyici organizmaların birarada bulunabileceklerini doğrulamıştır. Böyle bir yüksek biyokütle filtrasyon sisteminin işletme maliyeti, herhangi bir biyolojik nütrient giderim (BNR) tesisine göre yüzde 9–15 azaltacaktır.

TABLE OF CONTENTS

ACKNOWLEDGEMENTS	iii
ABSTRACT	vi
ÖZET	vii
LIST OF FIGURES	xi
LIST OF TABLES	xiv
LIST OF SYMBOLS / ABBREVIATIONS	xv
1. INTRODUCTION AND SCOPE	1
1.1. Sludge Disposal in Activated Sludge Plants	2
1.2. Problems of Sludge Disposal	3
1.3. Scope	3
2. BACKGROUND AND LITERATURE REVIEW	6
2.1. Introduction	6
2.2. Filtration Principles	7
2.3. Cake Filtration	9
2.3.1. Sludge Cake Formation	10
2.3.2. Pressure Drop through the Filter Cake	11
2.3.3. Filtration Experiments and Expressing the Performance	16
2.4. Filtration Mechanisms	20
2.4.1. Complete Blocking Filtration Law	21
2.4.2. Intermediate Blocking Filtration Law	24
2.4.3. Standard Blocking Filtration Law	28
2.4.4. Cake Filtration Law	31
2.5. Membrane Bioreactors	35
2.5.1. Technology Implementation	37
2.5.2. Membrane Materials	39

2.5.3. Membrane Configurations	40
2.5.4. Membrane Fouling	41
2.5.5. MBR Operation	43
2.5.6. Bio-treatment in MBR	45
3. THE PILOT UNIT - CAKE FILTRATION BIOLOGICAL REACTOR (CFBR) AND MEMBRANE BIOLOGICAL REACTOR (MBR)	49
4. EVALUATION OF CAKE FILTRATION BIOLOGICAL REACTORS (CFBR) VERSUS MEMBRANE BIOLOGICAL REACTORS (MBR) IN A PILOT SCALE PLANT	60
4.1. Introduction	60
4.2. Materials and Methods	62
4.2.1. Theoretical Section	62
4.2.2. Experimental Section	65
4.3. Results and Discussion	66
4.3.1. Bioreactor Performance	66
4.3.2. Filtration Analyses in Laboratory and SS Removal Efficiency of the Cloth Filter	68
4.3.3. Filtration Analyses in the Pilot MBR/CFBR	75
4.3.3.1. Trans-Membrane Pressures (TMP) and Flux Variations	76
4.3.3.2. Pressure Drop across Cloth Filter and Flux Variations	82
5. SLUDGE PRODUCTION AND DEGRADATION AT HIGH BIOMASS SYSTEMS WITH COMPLETE SLUDGE RETENTION	90
5.1. Introduction	90
5.2. Materials and Methods	92
5.2.1. Control Parameters	92
5.2.2. Determination of the Sludge Production	91
5.3. Results and Discussion	97
5.3.1. Evaluation of Sludge Production in the Bioreactor	97
5.3.2. Effect of Complete Sludge Retention on Nitrogen Converters	107
6. INVESTIGATION OF NITROGEN CONVERTERS IN HIGH MLSS SYSTEMS	112

6.1. Introduction	112
6.2. Materials and Methods	113
6.2.1. Sampling from the Pilot bioreactor	113
6.2.2. DNA Extraction and PCR Amplification	114
6.2.3. Real-time PCR	114
6.2.4. Cloning and Sequencing Analysis	116
6.3. Results and Discussion	116
7. HIGH BIOMASS FILTRATION SYSTEMS: ENERGY AND COST ANALYSIS OF SLUDGE PRODUCTION	126
7.1. Introduction	126
7.2. Operational Cost Calculations	129
7.2.1. Pilot Plant Operation Costs	129
7.2.2. Full-scale Operation Costs	130
7.3. Results and Discussion	135
7.3.1. Bioreactor Performance and Energy Consumption	135
7.3.2. Sludge Yield in the Bioreactor	136
7.3.3. Effect of Biomass Filtration Instead of Gravity Removal in Final Clarifiers	136
8. CONCLUSIONS	145
REFERENCES	148

LIST OF FIGURES

Figure 2.1. Schematic diagram of cake formation and growth	12
Figure 2.2. Drivers of membrane technology implementation	39
Figure 2.3. Nitrification/denitrification MBR plant scheme	41
Figure 3.1. General overview of the Paşaköy WWTP	50
Figure 3.2. General overview of fine screens, grit chamber, Parshall flume and the pilot plant (A: Membrane permeate line B: Cloth filter permeate line)	50
Figure 3.3. Atelier and on-site construction of the pilot unit	51
Figure 3.4. General overview of the membrane bioreactor and the cloth filter (The cloth filter is located within the reactor close to the membrane plates)	53
Figure 3.5. Coarse bubble diffusers (left) and diffuser piping (right)	54
Figure 3.6. Control room: power panel, data logger, blowers and permeate instruments (left); permeate line in detail (right)	54
Figure 3.7. Construction steps of the cloth filter unit	56
Figure 3.8. Microstructure of the cloth filter	57
Figure 3.9. Clean water test and sludge seeding	58
Figure 4.1. Stabilised cake layer on the cloth filter	67
Figure 4.2. Permeate SS results of pilot scale cloth filter	69
Figure 4.3. Permeate SS results of laboratory scale cloth filter	70
Figure 4.4. Experimental data of constant-pressure filtration used in the laboratory study at $p_o = 800$ Pa. The 1.6% activated sludge samples from return activated sludge (RAS) of the full-scale plant and the pilot plant were filtered and the medium was composed of two layers of polyester filter Plot of V vs. t (a) Plot of t/V vs. V (b)	71
Figure 4.5. Plot of V vs. t (a) and t/V vs. V (b) Experimental data of constant-pressure filtration used in the laboratory study at $p_o = 800$ Pa. Different concentrations of activated sludge samples from the pilot plant and 1.6% return activated sludge (RAS) of the full-scale plant were filtered in the	

lab-scale unit and the medium was composed of two layers of polyester filter	73
Figure 4.6. Flux decline rate for MBR/CFBR and RAS sludge filtration: (a) complete blocking model, (b) intermediate blocking model (c) standard blocking model, and (d) cake filtration	74
Figure 4.7. Fouled membrane cartridges in the first run	76
Figure 4.8. Change of the trans-membrane pressure (Pa) of the membranes with respect to operation time (hours)	78
Figure 4.9. Change of the flux ($L h^{-1} m^{-2}$) membranes with respect to time (hours)	78
Figure 4.10. Flux decline rate for MBR at the initial filtration: (a) complete blocking model, (b) intermediate blocking model, (c) standard blocking model, and (d) cake filtration	79
Figure 4.11. Flux decline rate for MBR at the latter filtration: (a) complete blocking model, (b) intermediate blocking model, (c) standard blocking model, (d) cake filtration	81
Figure 4.12. Plot of flux ($L h^{-1} m^{-2}$) decline vs. t and V vs. t for the first and second runs of the CFBR	83
Figure 4.13. Plot of V vs. t (a) and t/V vs. V (b) Experimental data of the CFBR at $p_o = 20$ kPa	86
Figure 4.14. Pressure difference (Δp , Pa) of filtration, cake resistance (Δp_c , Pa) on cloth and cumulative filtration volume (m) vs. time (hours). Experimental data of the CFBR at $p_o = 20$ kPa	87
Figure 4.15. Flux decline rate for CFBR: (a) complete blocking model, (b) intermediate blocking model, (c) standard blocking model, cake filtration	88
Figure 5.1. Mass balance diagram	94
Figure 5.2. Observed sludge yield coefficient (Y_{obs} , $kg_{MLSS} kg_{COD}^{-1}$) with increasing MLSS concentration in the pilot plant	100
Figure 5.3. The correlation of $Y_{obs,B}^{-1}$ vs. μ^{-1}	100
Figure 5.4. Sludge yield in the bioreactor. MLSS (1) and MLVSS (1): MLSS and MLVSS yield in the first 90 days; MLSS (2) and MLVSS (2): MLSS	

and MLVSS yield in the latter period	102
Figure 5.5. Cumulative inorganic material load to the bioreactor and the amount of inorganic sludge accumulated in the bioreactor	104
Figure 5.6. Organic loading rate to the reactor	106
Figure 5.7. Inert material removal in the pilot unit	108
Figure 5.8. Variations of MLVSS/MLSS ratio and the AmoA enzyme (copy numbers/mL extracted MLVSS)	109
Figure 5.9. Variations of MLVSS/MLSS ratio and 16S rRNA (gene copy numbers/mL extracted MLVSS)	111
Figure 6.1. A simple box-flow diagram of the pilot unit	115
Figure 6.2. Neighbor-joining phylogenetic tree of AOB sequences generated from <i>amoA</i> gene. The significance of each branch is indicated by bootstrap values (1,000 replicates). The scale bar represents 0.05 inferred substitutions/nucleotide positions	125
Figure 7.1. The P&I diagram of the pilot plant	131
Figure 7.2. Block diagram of the BNR plant	132
Figure 7.3. Distribution of important items in total operation cost for Option 1	142
Figure 7.4. Distribution of electricity costs for Option 1	142
Figure 7.5. Distribution of important items in total operation cost for Option 2	143
Figure 7.6. Distribution of electricity costs for Option 2	143
Figure 7.7. Distribution of important items in total operation cost for Option 3	144
Figure 7.8. Distribution of electricity costs for Option 3	144

LIST OF TABLES

Table 2.1. Membrane filtration types	36
Table 3.1. Membrane specifications	55
Table 3.2. Cloth filter specifications	55
Table 4.1. Filtration models and fouling mechanisms	65
Table 4.2. The raw water and effluent quality for CFBR	68
Table 5.1. Some sludge yield (Y_{max}) and decay rate (b) values given in literature	101
Table 6.1. Primer sets used in conventional and real-time PCR assays	117
Table 6.2. Average influent and effluent wastewater characteristics in the pilot tank	118
Table 6.3. Sampling periods, operational parameters and VSS concentrations in the pilot tank	119
Table 6.4. The gene copy number of 16S rDNA bacteria, <i>amoA</i> AOB, <i>Nitrobacter</i> , <i>Nitrospira</i> , <i>amoA</i> AOA and Anammox bacteria in the MBR samples	121
Table 6.5. Nitrogen converting microorganisms ratio in the MBR based on bacterial 16S rRNA gene	122
Table 7.1. Parameters involved in the energy cost	133
Table 7.2. Parameters involved in the ultimate sludge disposal (dry product cost from 1% to 99% dry solids, DS)	133
Table 7.3. Proportional values of important operation parameters (with sludge drying). (Option 1: full-scale BNR plant; Option 2: biomass filtration, flux: $0.42 \text{ m}^3/\text{m}^2/\text{d}$; Option 3: biomass filtration, flux: $0.53 \text{ m}^3/\text{m}^2/\text{d}$)	139
Table 7.4. Proportional values of important operation parameters (without sludge drying). (Option 1: full-scale BNR plant; Option 2: biomass filtration, flux: $0.42 \text{ m}^3/\text{m}^2/\text{d}$; Option 3: biomass filtration, flux: $0.53 \text{ m}^3/\text{m}^2/\text{d}$)	139

LIST OF SYMBOLS / ABBREVIATIONS

A	Filter surface area
amoA	Ammonia monooxygenase
Anammox	Anaerobic ammonia oxidation
AOA	Ammonia oxidizing archaea
AOB	Ammonia oxidizing bacteria
AS	Activated sludge
b	Decay rate
BNR	Biological nutrient removal
BOD ₅	5 days biological oxygen demand
C	Volume of solid particles deposited by unit volume of filtrate
C	Substrate concentration (indices I, o, e)
CAS	Conventional activated sludge
CFBR	Cake filtration biological reactors
COD	Chemical oxygen demand
DNA	Deoxyribonucleic acid
DO	Dissolved oxygen
DS	Dry solids
EBPR	Enhanced biological phosphorus removal
EPS	Extracellular polymeric substances
FISH	Fluorescence in situ hybridization
F/M	Food to microorganism ratio
HRT	Hydraulic retention time
k	Cake permeability
k	Multiplicative constant for plugging (Equation 2.23, indices; b, i, s, c)
L	Pore length / Media thickness
—	

m	Wet to dry cake mass ratio
MBR	Membrane bioreactor
MF	Microfiltration
MLSS	Mixed liquor suspended solids
MLVSS	Mixed liquor volatile suspended solids
n	Fouling mechanism exponent
N^*	Number of media pores
NaOCl	Sodium hypochlorite
NF	Nanofiltration
NH_4-N	Ammonium nitrogen
NOB	Nitrite oxidizing bacteria
NO_3-N	Nitrate nitrogen
P	Filtration pressure
p_0	Applied pressure
p_l	Liquid pressure
p_s	Compressive stress
P_{sm}	Cake compressive stress at the cake/medium interface
Q	Flow rate
Q_0	Flow rate at $t = 0$
q_l	Superficial velocity of liquid
r	Pore radius
R	Filter resistance
RAS	Return activated sludge
R_c	Cake resistance
R_g	Biomass growth rate
rRNA	Ribosomal ribonucleic acid
R_m	Medium resistance
RO	Reverse osmosis
R_s	Substrate utilization rate
s	Particle mass fraction of the suspension
SMP	Soluble microbial products

SRT	Sludge retention time
SS	Suspended solids
t	Time
TKN	Total Kjeldahl nitrogen
TMP	Transmembrane pressure
TN	Total nitrogen
TP	Total phosphorus
TS	Total solids
TSS	Total suspended solids
UF	Ultrafiltration
UV	Ultraviolet
V	Cumulative filtrate volume per unit medium surface area
V_f	Total volume permeated through the membrane at time t
VSS	Volatile suspended solids
w	Cake mass per unit medium surface area
WAS	Waste activated sludge
WWTP	Wastewater treatment plant
x	Distance measured away from medium
X	Sludge concentration (indices I, o, e)
X_A	Autotrophic biomass
X_E	Endogenous residue from biomass
X_H	Heterotrophic biomass
X_I	Inert suspended solids
Y_{\max}	Real sludge yield
Y_{obs}	Observed sludge yield
$Y_{\text{obs,B}}$	Observed biomass yield
<i>Greek Letters</i>	
α	Specific cake resistance
α_{av}	Average specific cake resistance

$[\alpha_{av}]_{\rho_s}$	Average specific cake resistance
α .OTE	Oxygen transfer efficiency in process conditions
μ	Liquid viscosity
Δp_c	Pressure drop over the cake
Δp_m	Pressure drop over the medium
ρ	Filtrate density
θ_x	Sludge retention time

1. INTRODUCTION AND SCOPE

Activated sludge technique is a very common process for municipal wastewater treatment. The last and important step of an activated sludge process is separation of microorganisms and treated wastewater. The separation is usually done in final clarifiers. In other words clarification – separation of microorganisms and treated wastewater – is the indicator of the process efficiency, because regardless of disinfection, efficiency of clarification affects all the discharge parameters (organic carbon, nitrogen and phosphorus) and it is highly depended on the mixed liquor suspended solids (MLSS) concentration in the process tanks. According to the experiences on activated sludge process, the desired separation of biomass and treated wastewater can be achieved when process biomass concentration is 3 – 4 g MLSS L⁻¹ and for a safe operation of final clarifier biomass should not exceed 5 g MLSS L⁻¹. However, adverse conditions like sludge bulking, rising, pin point floc formation decrease the sedimentation efficiency.

The advances in membrane technology have lead to the increase of biomass filtration systems. Because separation of treated wastewater phase by filtration does not require specific floc structure or mass and operation of bioreactors at elevated biomass concentrations is possible. Besides, biomass filtration offers high effluent quality and efficient treatment as a result of sufficiently high sludge retention times and, consequently, diverse microorganism content of biomass.

The possibility of operating a bioreactor at high (MLSS) concentrations, which means low sludge growth due to high sludge age, has attracted many researchers and engineers, because the problems of sludge handling have been still standing like the tip of the

iceberg in many biological wastewater treatment plants. However, filter media clogging has been the most important problem of the biomass filtration systems and, steady and sustainable operation of membrane filtration units requires careful management of membrane fouling. Several methods for preventing membrane fouling externally have been implemented. Thus, the membrane material itself has been studied comprehensively in order to develop less or non-fouling membrane surface.

1.1. Sludge Disposal in Activated Sludge Plants

Today in Istanbul, besides the small industrial activated sludge plants, there are over 66 publicly owned municipal wastewater treatment plants in operation, which belong to Istanbul Municipality Water and Sewerage Administration. The large treatment plants are: Ambarlı, Ataköy, Paşaköy and Tuzla Wastewater Treatment Plants. Paşaköy plant was designed for 500,000 people equivalent and 67,700 kg SS d⁻¹, 48,600 kg BOD₅ d⁻¹, 9,700 kg TN d⁻¹ and 1,340 kg TP d⁻¹ wastewater load. Currently, existing plant has average wastewater strength of 40,600 kg SS d⁻¹, 29,000 kg BOD₅ d⁻¹, 6,960 kg TN d⁻¹ and 855 kg TP d⁻¹, and 135 ton d⁻¹, 25 % sludge produced and 30 ton d⁻¹, 98 % dry product removed from the plant. Tuzla plant was designed for 1,150,000 people equivalent and 136,925 kg SS d⁻¹, 92,250 kg BOD₅ d⁻¹, 5,000 kg TN d⁻¹ and 800 kg TP d⁻¹ wastewater load. The existing plant receives average wastewater strength of 213,200 kg SS d⁻¹, 101,350 kg BOD₅ d⁻¹, 18,600 kg TN d⁻¹ and 2,950 kg TP d⁻¹, and 280 ton d⁻¹, 25 % sludge produced and 55 ton d⁻¹, 98 % dry product removed from the plant. Ataköy plant was designed for 195,000 kg SS d⁻¹, 117,000 kg BOD₅ d⁻¹, 23,400 kg TN d⁻¹ and 3,120 kg TP d⁻¹ wastewater load. The existing plant receives average wastewater strength of 137,355 kg SS d⁻¹, 144,500 kg BOD₅ d⁻¹, 25,420 kg TN d⁻¹ and 2,990 kg TP d⁻¹ and 87 ton d⁻¹, 95 % dry product removed from the plant. If total population of Istanbul considered as more than 14 million, total disposed biomass amount when whole municipal wastewater of Istanbul treated, would be approximately 10 times of the current sludge amount.

1.2. Problems of Sludge Disposal

In municipal wastewater treatment plants, sludge disposal accounts for approximately 60 % of construction cost and 40 % of operation cost. Thus, sludge treatment units should be well designed and carefully operated and maintained. In order to minimize operational problems, treatment system selection and technical items of the system are important subjects to be considered during design. On the other hand, most important aspects of sludge disposal are odor problem, unforeseen increase of daily, weekly, monthly, semiannual and annual maintenance frequency; considerable manpower is consumed in sludge treatment units and breakdown of these units cause an increase in biomass concentration and directly effect the sedimentation efficiency and decrease the effluent quality.

Nowadays, addition of sludge drying and incineration units to treatment plants can decrease the waste sludge volume up to $\frac{1}{4}$ of the dewatered sludge volume. Accordingly, transportation cost and landfill area requirement will decrease with the same ratio; besides leachate production and leachate treatment cost will decrease. Also, after sludge drying process, treatment plant sludge can be used as fertilizer or as fuel source in several industries (the dry sludge is especially an attractive source for cement factories). But drying or incineration of dewatered sludge (25 – 30% TS) means additional construction, operation and maintenance cost.

1.3. Scope

As it is stated above, in a system like membrane bioreactor (MBR), complete retention of sludge by membrane process makes it possible to maintain high MLSS in bioreactor, which causes long sludge retention time (SRT) and low food-to-microorganism (F/M) ratio. The long SRT also causes less sludge production while low F/M ratio gives a

chance to reduce hydraulic retention time (HRT). The daily sludge disposal cost for 1 ton of dry sludge (TS > 95%) in İstanbul is around 120 TL, which means 43,400 TL for a year. So, as the sludge amount will be decreased before sludge processing units a minimum sludge producing system means considerable energy and chemical (polymer) saving and also operational cost reduction.

Many researchers have stated different solutions to the clogging of filter material in high MLSS systems. Despite the membrane fouling control techniques, cake formation on membrane surface further minimizes the pore size; for example 0.4 μm pore size of a flat-sheet membrane can decrease to 0.1 μm during operation and the producers do not deny the reduction of the pore size to improve the membrane effluent quality. On the other hand, in order to prevent pore blocking, different cleaning systems are used for membranes that can be listed as air scouring, backwashing and chemical cleaning. Continuous air scouring and periodical chemical cleaning are used almost in all systems. However, for a large treatment plant e.g. 100.000 $\text{m}^3 \text{d}^{-1}$ of flow rate, membrane scouring air requirement is 91,350 $\text{Nm}^3 \text{h}^{-1}$ for the above mentioned brand, it may be an additional construction cost of 1 – 4 blowers, and about 18,000 diffusers and about 1,400 kW of operational cost.

The scope of this study was to develop an alternative high biomass filtration system, which includes cake filtration following nitrification and denitrification of municipal wastewater; and unlike membrane processes in the market, this system will promote cake formation. The chosen filter material was a polyester cloth and by the help of cake formation, sludge was retained in the reactor (target MLSS is 15,000 mg L^{-1} or higher) and treated wastewater was filtered out. The main objective of the developed filter system was to bring up a submerged system that achieves separation of treated wastewater (permeate) from activated sludge by filtration that depends on cake filtration principles. Another objective of the study was to bring up a submerged filter system that does not cause fouling problem. The system was a cake filtration system that uses the activated sludge as a ‘filter’; instead of preventing, it

allows the formation of the cake layer, which is believed to cause fouling on the surface and within the pores of filter material. In addition to filtration studies about the cloth filter unit operated in parallel with a submerged microfiltration membrane, the properties of sludge cake was investigated by molecular studies and the sludge production pattern was analyzed to state that the process can reach to equilibrium sludge production conditions without any deterioration of filtration process. Thus, the cost of such a plant operation was compared to that of a conventional biological nutrient removal system.

2. BACKGROUND AND LITERATURE REVIEW

2.1. Introduction

The activated sludge process for biological nutrient removal systems in municipal wastewater treatment basically consists of three processes in series, in which the desired reactions are carried out in a mixture of wastewater and biomass, resulting in a clean effluent. The first step consists of pretreatment (screening and grit removal) to remove coarse materials and other undesired substances. Usually this is followed by primary treatment (primary sedimentation), in order to remove the settleable solids (mainly carbon) in wastewater. Subsequently, the influent is mixed with the biomass and treated under anaerobic or aerobic and/or anoxic conditions. The treated wastewater is separated from the biomass, usually in a clarifier tank, where the biomass is partially returned to the reactor to continue biodegradation and partially wasted.

One of the major features of the activated-sludge process is the formation of floc particles, ranging from 50-200 μm . These floc particles contain different kinds of microorganisms that are held together by extracellular polymeric substances (EPS) and/or soluble microbial products (SMP), and can be removed by gravity settling. The activated sludge flocs contain a wide range of species of bacteria and protozoa, which are responsible for the conversion of organic material and nutrients. Depending on the type of organism and reactor conditions, different types of conversions can take place. Most important and common of all is aerobic oxidation (oxic), in which oxygen is the electron acceptor while organic carbon and ammonium nitrogen are electron donors for carbon removal and nitrification respectively. The other reaction type is the denitrification process (anoxic oxidation) in which nitrate nitrogen is the electron acceptor and organic carbon is the electron donor. In some plants, aerobic and anoxic oxidations are coupled with enhanced biological phosphorus

removal. All reactions are performed as part of the life cycle of the respective microorganism. For each reaction type the bacteria require a carbon source, an electron donor and an electron acceptor, which together yield an end product and form so called excess sludge that determines the sludge age of the system.

The integration of biomass filtration into an activated sludge process has been widely used in the field of wastewater treatment, due to their important advantages like high effluent quality, good retention of all microorganisms and viruses, maintenance of high biomass concentration [1]. Throughout the last two decades, rapidly developing new systems, materials and decreasing media costs have been another important driving force for the widespread application of membrane bioreactors (MBRs) [2]. Most commercial biomass filtration units have been applied as either hollow fiber or flat sheet submerged membrane modules, which have been in operation for over 15 years, and they have proven to be both reliable and simple to operate [3, 4].

2.2. Filtration Principles

Filtration is one of the oldest unit operations that involves the mechanical separation of a disperse phase (particle/fluid mixture) from a continuous fluid phase. The fluid passes through a porous barrier, which is termed as the filter medium, and particles that are larger than the pore size of the medium accumulate to form a filter cake on the upstream side of the medium. Filters also may be described by the hydraulic arrangement employed to pass water through the medium [5]. The driving force for this process, which forces permeate through the filter, is the pressure difference across the filter medium and the cake.

Filters are classified according to the driving force used in the process: gravity or pressure filters. Gravity filters are open to the atmosphere, and flow through the medium is

achieved by gravity. Pressure filters utilize a pressure pump to maintain the driving force and filter the fluid through the medium. The two systems are merely two ways to provide a hydraulic gradient across the filter [5].

The filtration processes, according to their flow characteristics, can be formed as follows [6]:

- Constant pressure filtration
- Constant rate filtration
- Variable rate - variable pressure filtration
- Stepped pressure filtration

The method in which the applied pressure over the filter is held constant so that the rate of filtration decreases continuously from the beginning towards the end of filtration is called constant pressure filtration. In constant rate filtration, the applied pressure over the filter system is adjusted to achieve a constant filtration rate at the downstream. In contrast to these types of operations, industrial filtrations involving centrifugal pumps are accomplished under variable pressure – variable rate conditions [7]. Stepped pressure filtration is carried out for experimental purposes, it is possible to manually increase pressure during a filtration and simulate various pumping conditions [7].

Filtration can be further classified according to the particle deposition mechanism: separation by capturing of particles inside the porous filter medium is termed depth filtration and separation at the filter medium's surface is termed surface filtration. When particles deposit on to already deposited particles the resulting particle agglomerate is termed filter cake and the corresponding filtration mechanism is cake filtration. Cake filtration is preceded by surface filtration [8].

2.3. Cake Filtration

Cake filtration is a solid-liquid separation process that can be described basically as passing of a solid-liquid suspension through a porous medium while solids in the suspension retained on the surface of the filter medium form a cake with porous structure, which acts as another filter medium, as filtration proceeds. The more solid-liquid suspension is filtered the cake becomes the actual filter medium that positively affects the filtration process. Thus, cake formation is a critical step for obtaining the desired results from a cake filter. On the other hand, as the cake thickness increases, the pressure resistance across the cake also increases. The cake build-up is quite noticeable, often up to 3.5 cm thick and generally after a filtering cycle, the cake is removed from the filter medium and discarded [9].

Since Ruth [10] carried out the classical theoretical analysis of cake filtration in the 1930s many researchers have been working on filtration models and techniques. The mechanism of flow within the cake and filter medium, and the external conditions imposed on them are the basis for modelling a filtration process [6]. The analyses of cake filtration have been made stating the fluid flow through the cake and medium under an applied pressure gradient. Earlier cake filtration studies have been done by chemical engineers and the process has been widely used in the chemical and process industry. Thus, the development of cake filtration technology was left mainly to equipment manufacturers, which tended to be small-scale operations [11]. The contribution of cake filtration mechanism in water filtration, especially in wastewater treatment, has gained interest for various membrane filtration systems.

2.3.1. Sludge Cake Formation

Microorganisms can attach and colonize on any surface material, by the vertical transport of fluid through the media. [12]. Within minutes of contact the first microorganisms will adhere to the surface and the formation of cake is strongly influenced by the concentration of cells in water phase. It was shown that dead cells of microorganisms adhere at the same rate to the surface as living cells because these cells already carry the sticky material, extracellular polymeric substances (EPS): polysaccharides, proteins, glycoprotein, lipoproteins and other molecules of microbial origin which mediates adhesion as well as cohesion [12]. EPS forms a slime matrix that keeps the biofilm or the cake together. The adsorption of biopolymers on the membrane were found to modify its surface property and led to easier biomass attachment and tighter sludge cake deposition, which resulted in a progressive sludge cake growth and serious membrane fouling [13]. Sludge cake is kept together by weak physio-chemical interactions which are hydrogen bonds, electrostatic interactions and van der Waals interactions and the energy provided by these interactions ranges between 0.1 – 10 percent of that covalent C – C bond depending on respective formations of the macromolecules, water content, pH, ionic strength, temperature and other parameters [12, 14].

The extend of biofilm accumulation will depend on different factors such as nutrient concentration, type and availability, shear forces, mechanical stability of the biofilm matrix, as influenced by: oxidizing agents, biodispersants, mechanical stress, temperature, type of microorganisms, physiological activity, structure and physical strength of EPS [12].

2.3.2. Pressure Drop through the Filter Cake

Once a cake is built up on the surface of a filter medium, the flow resistance is not constant and a different approach is needed to determine the behavior of filter cakes, which is considered as the complexity of cake filtration [15]. Cake formation increases pressure drop across the filter and reduces the flow of filtrate. The development of cake formation models began with the Darcy's Law that describes the water flow through porous sand media. According to conventional cake filtration theory, the flow rate of liquid is proportional to the pressure gradient and for steady laminar flow through homogeneous and incompressible porous media:

$$q_l = \frac{k}{\mu} \frac{dp_l}{dx} \quad (2.1)$$

q_l : Superficial velocity of liquid (m s^{-1})

p_l : Liquid pressure (Pa)

x : Distance measured away from medium (m)

k : cake permeability (m^2)

μ : Liquid viscosity (Pa.s)

Filter cakes in general are compressible [16]. Applied pressure on compressible cakes leads to particle deformation and rearrangement that can end up with either plastic deformation or cake swelling after pressure release. It was demonstrated that activated sludge forms highly compressible cakes even at low pressures [17, 18]. So, for a compressible cake, Darcy's equation may become as [19]:

$$q_l = -\frac{k dp_s}{\mu dx} \quad (2.2)$$

p_s : Compressive stress (Pa)

The liquid and particle velocities, q_l and q_s , are in the opposite direction of x and within the coordinate system are inherently negative. One major assumption of the conventional Thus, a variety of pore liquid pressure and compressive stress, p_l and p_s , relationships can be established. For one-dimensional cake filtration, the pressure terms are dominant and the relationship between the pressure terms can be simplified as [20];

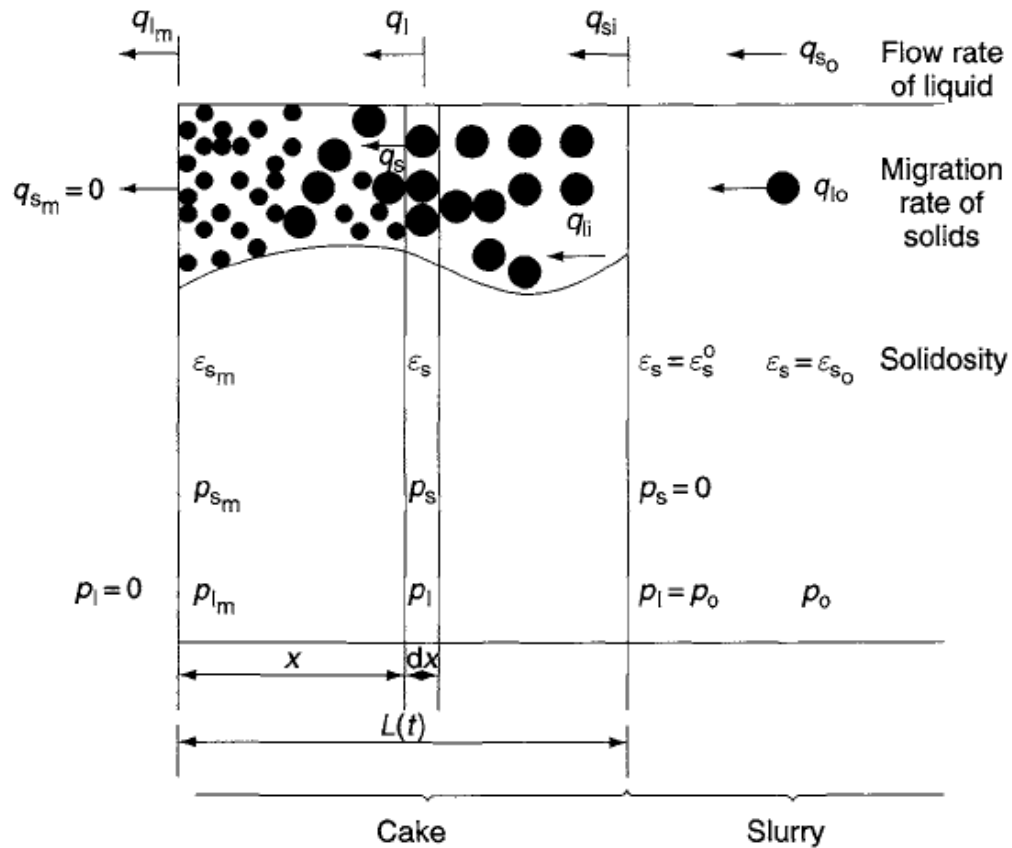


Figure 2.1. Schematic diagram of cake formation and growth [16].

$$\frac{dp_l}{dp_s} = f' \quad (2.3)$$

The simplest case for $p_l - p_s$ relationship proposed by Tien and coworkers [20] is;

$$dp_l + dp_s = 0 \quad (2.4)$$

where $f' = -1$.

In cake filtration process, at the very initial short period, filtration runs without cake formation, afterwards cake formation takes place. Once a cake builds on medium during the filtration of a suspension, the cake itself takes a significant proportion of the total pressure drop. This leads to a gradual drop in the flowrate and cumulative filtrate volume slows down with time. Hence, the filtrate flowrate at constant driving pressure becomes a function of time [19]. The filtered liquid passes through two resistances in series: that of the cake and that of the medium. The overall pressure drop at any time is the sum of the pressure drops over the medium and cake [21]. At the cake/suspension interface $x = 0$, p_l is equal to p_o , the applied (or operating) pressure, at the downstream side of the medium, p_l may be assumed to be zero and p_{lm} is the pressure at the boundary between cake and medium. If the pressure drop over the cake and the medium are Δp_c and Δp_m ;

$$\Delta p = p_o - 0 = (p_l - p_{lm}) + (p_{lm} - 0) = \Delta p_c + \Delta p_m \quad (2.5)$$

According to the expression with two resistances in series, Equation 2.1 can be written as;

$$q_l = \frac{1}{\mu} \frac{\Delta p}{(R_m + R_c)} \quad (2.6)$$

where, the resistance replaces the x/k .

R_m : Medium resistance (m^{-2})

R_c : Cake resistance (m^{-2})

The resistance of the cake may be assumed to be proportional to the amount of cake deposited on the filter medium.

$$R_c = [\alpha_{av}]_{P_{s_m}} \cdot w \quad (2.7)$$

$[\alpha_{av}]_{P_{s_m}}$: Average specific cake resistance ($m \text{ kg}^{-1}$)

(P_{s_m} , cake compressive stress at the cake/medium interface, Pa)

w : cake mass per unit medium surface area ($kg \text{ m}^{-2}$)

Introducing the average specific cake resistance into Equation (2.6) gives;

$$q_l = \frac{1}{\mu} \frac{\Delta p_m + \Delta p_c}{\left(R_m + [\alpha_{av}]_{P_{s_m}} \cdot w \right)} \quad (2.8)$$

which can be also written as;

$$q_l = \frac{1}{\mu} \frac{P_o}{\left(R_m + [\alpha_{av}]_{P_{s_m}} \cdot w \right)} \quad (2.9)$$

The Equation (2.9) is the basic equation of the conventional cake filtration theory that means the instantaneous filtration rate (q_t) is directly proportional to the pressure applied (p_o) and inversely proportional to the flow resistance of the cake and the medium [16].

For incompressible cakes, the specific cake resistance (α , m kg^{-1}) should be constant. Because the cakes formed during filtration processes are generally compressible, an average specific cake resistance should be defined for related stages of filtration. Ruth [10] defines the average specific cake resistance;

$$\alpha_{av} = \frac{\Delta P_c}{\int_0^{\Delta P_c} \frac{1}{\alpha} dP_s} \quad (2.10)$$

The performance of cake filtration may be seen from the volume of filtrate collected and the solid particles recovered per unit medium surface area (V and w respectively) as functions of time [10].

$$q_t = \frac{dV}{dt} \quad (2.11)$$

The relationship between V and w can be expressed as follows;

$$w = \frac{V \rho s}{1 - \overline{ms}} \quad (2.12)$$

V : cumulative filtrate volume per unit medium surface area (m)

s : particle mass fraction of the suspension (-)

\overline{m} : wet to dry cake mass ratio (-)

ρ : filtrate density (kg m^{-3})

t : time (s)

Substituting the above expressions into Equation 2.9 gives;

$$q_l = \frac{dV}{dt} = \frac{1}{\mu} \frac{p_o}{\left\{ R_m + [\alpha_{av}]_{\Delta P_c} \cdot \frac{V \rho_s}{1 - m_s} \right\}} \quad (2.13)$$

Equations 2.9 and 2.13 are equivalent and the difference of Equation 2.13 is, it has one dependent variable, the cumulative filtrate volume V , if wet to dry cake mass ratio can be treated as a constant [16].

2.3.3. Filtration Experiments and Expressing the Performance

In a large scale continuous filtration system, main control parameters are applied pressure, pressure drop, concentration drop of the slurry and the performance indicators are: filtrate flowrate and the rate of cake formation. The flowrate is a simple monitoring tool, which can be even measured by the ‘bucket and stopwatch’ method, and used for filtration analysis as the basic variable in the form of cumulative filtrate volume.

In constant pressure filtration, the applied pressure, p_o , is constant; so, the only variables are V and t . Rearranging Equation 2.13 gives;

$$p_o = \mu \rho_s (1 - \overline{m_s})^{-1} [\alpha_{av}]_{\Delta P_c} V \frac{dV}{dt} + \mu R_m \frac{dV}{dt} \quad (2.14)$$

Integration of Equation 2.14 between the limits (0, 0) and (t, V) and the assumption that R_m remains constant gives;

$$p_o t = \mu \rho_s \overline{(1 - \bar{m}s)^{-1} [\alpha_{av}]_{P_{s_m}}} \frac{V^2}{2} + \mu R_m V \quad (2.15)$$

Equation 2.15 expresses the main feature of the conventional cake filtration theory that is widely used in design calculations and data interpretation and is known as the ‘parabolic law’ of constant pressure filtration if the quantity $\overline{(1 - \bar{m}s)^{-1} [\alpha_{av}]_{P_{s_m}}}$ can be treated as constant. The expression $[\alpha_{av}]_{P_{s_m}}$ is a function of ΔP_c and P_{s_m} [16]. In course of filtration, flow through a cake causes particle rearrangement and collapse of pores, hence filter cake structure changes and usually average properties are defined. Hence, the average specific cake resistance over compressive stress ranging from 0 to P_{s_m} , which is the value at cake / medium interface, can be expressed as;

$$(\alpha_{av})_{P_{s_m}} = \frac{\Delta P_c / P_{s_m}}{\left[\int_0^{P_{s_m}} \frac{1}{2} (-f') dP_s \right] / P_{s_m}} \quad (2.16)$$

If α_{av} and \bar{m} evaluated at $\Delta P_c \approx p_0$ and Equation 2.13 is rewritten with the assumption of the medium resistance to be equivalent to that of a fictitious cake layer corresponding to a cumulative filtrate volume of V_m [16];

$$q_l = \frac{dV}{dt} = \frac{p_o}{\mu[\alpha_{av}]_{P_{s_m}(p_o)} \frac{\rho s}{1-\bar{m}s}} (V + V_m) \quad (2.17)$$

and

$$V_m = \frac{1-\bar{m}s}{\rho s (\alpha_{av})_{P_{s_m}(p_o)}} R_m \quad (2.18)$$

Integrating Equation 2.17 gives;

$$(V + V_m)^2 = A(t + t_m) \quad (2.19)$$

where,

$$A = \frac{2 p_o (1-\bar{m}s)}{\mu[\alpha_{av}]_{\Delta P_c = p_o} \rho s} \quad (2.20)$$

and

$$t_m = \frac{V_m^2}{A} = \frac{\mu[\alpha_{av}]_{\Delta P_c = p_o} \rho s}{2 p_o (1-\bar{m}s)} V_m^2 \quad (2.21)$$

Equation 2.19 may be written as;

$$\frac{t}{V} = \frac{V}{A} + \frac{2V_m}{A} \quad (2.22)$$

According to Equation 2.22, for constant pressure filtration the plot of t/V vs. V yields a straight line with a slope of,

$$\left(p_o / 2 \right) \mu \rho_s \left[\alpha_{av} \right]_{\Delta P_c = p_o} \left[\left(1 - \overline{ms} \right)_{\Delta P_c = p_o} \right]^{-1}$$

and an intercept of,

$$\mu \frac{R_m}{p_o}$$

Thus, with significant cake thickness, negligible media resistance and ΔP_c approaching to p_o , the quantities of R_m , \overline{m} , $[\alpha_{av}]$ approach their respective constant values [22]. So, a linear relationship between t/V vs. V may be established.

Teoh and coworkers [22] has summarized four methods for the determination of filtration data:

1. Method based on the linear plot of t/V vs. V of constant pressure filtration data,
2. Method based on cake filtration data obtained with operating pressure increasing stepwise,
3. Method based on the measurements of cake internal properties,
4. Method based on the knowledge of the instantaneous filtration rate.

As it is summarized above, the first method is a simple and commonly used procedure for determining $[\alpha_{av}]_{\Delta P_c = p_o}$, the specific cake resistance. Thus, the interpretation of constant pressure filtration data is commonly based on the so-called parabolic law of the conventional filtration theory. The basic assumptions of the theory are: the pressure drop across the cake is essentially the same as the applied pressure (the medium resistance is negligible), the wet to

dry cake mass ratio is constant and the particle velocity within the cake is small as compared with the filtrate velocity [23]. Furthermore, the initial stage of filtration and cake formation are generally analyzed separately [24].

2.4. Filtration Mechanisms

Many models have been proposed in order to deeply understand the filtration mechanisms that actually explain when and why the fouling occurs. Filtration always leads to an increase in the resistance to flow. In the case of a dead-end filtration process, cake formation on the media, which increases the resistance, might be expected to be roughly proportional to the declining permeate volume. For cross-flow processes, this deposition continues until the scouring forces of the fluid passing over the media balance the adhesive forces binding the cake to the media, resulting steady state conditions [2].

Four different kinds of blocking models were first proposed by Hermans and Bredee [25]: complete blocking, intermediate blocking, standard blocking and cake filtration. Grace [26] developed the models and Hermia [27] derived a common equation that applied to all four fouling mechanisms for constant pressure filtration.

$$\frac{d^2 t}{dV_f^2} = k \left(\frac{dt}{dV_f} \right)^n \quad (2.23)$$

V_f : Total volume permeated through the membrane at time t (mL)

k : Multiplicative constant for plugging

n : Fouling mechanism exponent

t : Filtration time (s)

2.4.1. Complete Blocking Filtration Law

In this model, it is assumed that each particle reaching the media pores participates in the blocking phenomenon by pore sealing, which leads to the assumption that particles are not superimposed one upon the other [27]. Darcy's law given in Equation 2.1 is also expressed as;

$$Q = \frac{PA}{\mu R} \quad (2.24)$$

For initial flowrate through filter and unclogged media the equation becomes;

$$Q_0 = \frac{PA_0}{\mu R} \quad (2.25)$$

Q : Flow rate (h^{-1})

Q_0 : Flow rate at $t = 0$ (h^{-1})

A : Filter surface area (m^2)

μ : Filtrate Newtonian dynamic viscosity (Ns m^{-2})

P : Filtration pressure (N m^{-2})

R : Filter resistance (m^{-1})

At time t ;

$$Q = \frac{PA_t}{\mu R} \quad (2.26)$$

If the volume of filtrate, V_f has been filtered and blocked a portion of filter surface area equal to σV_f ;

$$A_t \cong A_0 - \sigma V_f \quad (2.27)$$

For a constant pressure filtration;

$$Q = \frac{P(A_0 - \sigma V_f)}{\mu R} \quad (2.28)$$

Introducing Equation 2.25 into 2.28 gives;

$$Q = Q_0 - \frac{P\sigma V_f}{\mu R} \quad (2.29)$$

If $\frac{P\sigma}{\mu R}$ is defined as the plugging constant for complete blocking, k_b (s^{-1}), the equation can be put in the following form, which gives a linear relationship between V_f and Q ;

$$k_b V_f = Q_0 - Q \quad (2.30)$$

Integrating Equation (2.30) with respect to time yields;

$$Q = \frac{dV_f}{dt} = Q_0 - k_b V_f \quad (2.31)$$

$$\frac{dV_f}{(Q_0 - k_b V_f)} = dt \quad (2.32)$$

$$\frac{1}{k_b} \ln(Q_0 - k_b V_f) I_0^{V_f} = t I_0^t \quad (2.33)$$

gives,

$$Q = Q_0 e^{-k_b t} \quad (2.34)$$

which is the $Q = f(t)$ relationship, while

$$k_b V_f = Q(1 - e^{-k_b t}) \quad (2.35)$$

For a constant pressure filtration, the resistance coefficient can be defined as the rate of variation with respect to filtrate volume of instantaneous resistance to filtration which can be measured by the inverse of flow rate [27]:

$$k_b = \frac{d}{dV_f} \left(\frac{1}{Q} \right) = \frac{d^2 t}{dV_f^2} \quad (2.36)$$

Introducing Equation 2.30 into 2.36 gives;

$$\frac{d^2 t}{dV_f^2} = \frac{d}{dV_f} \left(\frac{1}{Q_0 - k_b V_f} \right) \quad (2.37)$$

The derivative gives;

$$\frac{d^2 t}{dV_f^2} = k_b (Q_0 - k_b V_f)^{-2} \quad (2.38)$$

$$\frac{d^2 t}{dV_f^2} = \frac{k_b}{Q^2} \quad (2.39)$$

which can be written as;

$$\frac{d^2 t}{dV_f^2} = k_b \left(\frac{dt}{dV_f} \right)^2 \quad (2.40)$$

Fouling mechanism exponent for complete blocking is 2. This equation can be considered as the characteristic form of the complete blocking filtration law under constant pressure [27].

2.4.2. Intermediate Blocking Filtration Law

This blocking law is based on the assumption that every solid particle contacted with an open pore seals it. But in this case, the model is adopted in such a way that particles are allowed to settle on other particles, which can also mean that each particle does necessarily block a pore. So, the law evaluates the probability of a particle to block a pore [27].

If A_0 is the initial active filter surface area and V^* is a small prefilter volume containing particles at time Δt , the projected area on the filter, Σ is:

$$\Sigma = \sigma V^* \approx \sigma V_f \quad (2.41)$$

The active surface area and the volume of filtrate will be reduced to:

$$(A_0 - \Sigma)$$

and,

$$V_f(A_0 - \Sigma) / A_0$$

The unblocked surface area at time t , A_t is equal to that at time $t - \Delta t$, $A_{t-\Delta t}$ that states the new blocked area, which is proportional to both the free surface at time $t - \Delta t$ and filtrate volume passing through this free surface [27].

For time lags to tend towards a limit dt :

$$A_{t+dt} = A_t - \sigma(Q_t dt) \left(\frac{A_t}{A_0} \right) \quad (2.42)$$

$$A_{t+dt} - A_t = dA \quad (2.43)$$

Introducing Equation 2.24 gives;

$$dA = -\sigma \frac{PA}{\mu R} dt \frac{A}{A_0} \quad (2.44)$$

Integrating $\int_{A_0}^A \frac{dA}{A^2} = -\frac{\sigma P}{\mu R A_0} \int_0^t dt$ gives;

$$A = \frac{A_0}{\left(1 + \frac{\sigma P}{\mu R} t \right)} \quad (2.45)$$

and Equation 2.45 can also be written as;

$$Q = \frac{Q_0}{\left(1 + \frac{\sigma P}{\mu R} t\right)} \quad (2.46)$$

If the equation is rearranged;

$$\frac{1}{Q} = \frac{1}{Q_0} + \frac{\sigma P}{\mu R Q_0} t \quad (2.47)$$

If $\frac{\sigma P}{\mu R Q_0}$ is defined as the plugging constant for intermediate blocking, k_i (m^{-3}), the equation can be put in the following form,

$$\frac{1}{Q} - \frac{1}{Q_0} = k_i t \quad (2.48)$$

Rearranging the equation gives;

$$k_i t Q_0 = \frac{(Q_0 - Q)}{Q} \quad (2.49)$$

Integrating $k_i dV_f = \frac{-dQ}{Q}$ yields the following $Q = f(V_f)$ relationship:

$$Q = Q_0 e^{-k_i V_f} \quad (2.50)$$

Rearranging the Equation 2.50 in order to obtain $V_f = f(t)$ relationship gives;

$$\frac{1}{Q} = k_i t + \frac{1}{Q_0} \quad (2.51)$$

For $Q = dV_f/dt$, integrating $Q_0 \frac{dt}{(k_i Q_0 t + 1)} = dV_f$ yields;

$$k_i V_f = \ln(k_i Q_0 t + 1) \quad (2.52)$$

The resistance coefficient for intermediate blocking filtration is;

$$\frac{d^2 t}{dV_f^2} = \frac{d}{dV_f} \frac{1}{Q} \quad (2.53)$$

Introducing Equation 2.50 into Equation 2.53 gives;

$$\frac{d^2 t}{dV_f^2} = \frac{d}{dV_f} \left(\frac{1}{Q_0} e^{k_i V_f} \right) \quad (2.54)$$

The derivative gives;

$$\frac{d^2 t}{dV_f^2} = \frac{k_i}{Q_0} e^{k_i V_f} = \frac{k_i}{Q} \quad (2.55)$$

which can be written as;

$$\frac{d^2 t}{dV_f^2} = k_i \frac{dt}{dV_f} \quad (2.56)$$

So, Equation 2.56 can be considered as the characteristic form of the intermediate blocking filtration law for constant pressure [27]. Fouling mechanism exponent for intermediate blocking is 1.

2.4.3. Standard Blocking Filtration Law

Hermia [27] assumed that pore volume decreases proportionally to filtrate volume by particle deposit on the pore walls. The decrease of pore volume will be equal to the decrease of pore section with the assumption of constant pore diameter and length.

$$N^* (-2\pi r dr) L = C dV_f \quad (2.57)$$

N^* : Number of media pores (-)

L : Pore length / Media thickness (m)

C : Volume of solid particles deposited by unit volume of filtrate (-)

r : Pore radius (m)

Integrating the mass balance Equation 2.57 on solid particles gives;

$$N^* \pi (r_0^2 - r^2) L = C V_f \quad (2.58)$$

Initial flow rate in standard blocking model is found Poiseuille's equation, which gives [28];

$$Q_0 = N^* \left(\frac{\pi r_0^4 P}{8 \mu L} \right) \quad (2.59)$$

Poiseuille's law defines the pressure drop in a fluid flowing through a long cylindrical pipe with radius r and length L . In case of a laminar flow the volume of flow rate, which is given by the pressure difference, ΔP , divided by the viscous resistance, R , depends

linearly on the viscosity of the fluid, μ and the length of the cylinder but on the fourth power of radius.

$$\text{Volume of flow rate} = \frac{\Delta P}{R} = \frac{\pi \Delta P r^4}{8\mu L} \quad (2.60)$$

If it is assumed that there are a number of circular lamina of fluid (with radius r' = 0 to r) and having a velocity determined only by their radial distance from the center of the cylinder; flow through each lamina (velocity x area), $Q(r')$, is given by [28]:

$$Q(r') dr = \frac{1}{4\mu} \frac{\Delta P}{L} (r^2 - r'^2) 2\pi r' dr = \frac{\pi}{2\mu} \frac{\Delta P}{L} (r' r^2 - r'^3) dr \quad (2.61)$$

Integrating over r' from 0 to r gives;

$$Q = \frac{\pi}{2\mu} \frac{\Delta P}{L} \int_0^r (r' r^2 - r'^3) dr = \frac{\Delta P \pi r^4}{8\mu L} \quad (2.62)$$

Hence, for N^* number of pores, the initial flow rate of standard blocking filtration law can be expressed by Equation (2.62). The equation states that for a constant pressure filtration, the decrease in the filtrate volume passing through the media is proportional with the decreasing pore radius as a result of pore constriction. Thus,

$$\frac{Q}{Q_0} = \frac{r^4}{r_0^4} \quad (2.63)$$

and,

$$N^* \pi L r^2 = N^* \pi L r_0^2 - C V_f \quad (2.64)$$

Hermia [27] derived following equation;

$$Q = Q_0 \left(1 - \frac{k_s V_f}{2} \right)^2 \quad (2.65)$$

where, plugging constant, k_s for standard blocking (m^{-3}) is equal to;

$$k_s = \frac{2C}{\pi L N^* r_0^2} \quad (2.66)$$

Integrating Equation 2.65 gives the $V_f = f(t)$ relationship;

$$\frac{k_s t}{2} = \frac{t}{V_f} - \frac{1}{Q_0} \quad (2.67)$$

The $Q = f(t)$ can also be derived from Equation 2.65;

$$Q = \frac{Q_0}{\left(1 + \frac{k_s Q_0 t}{2} \right)^2} \quad (2.68)$$

Inserting Equation 2.65 into Equation 2.23 gives;

$$\frac{d^2 t}{dV_f^2} = \frac{d}{dV_f} \left[\frac{1}{Q_0 \left(1 - 0.5 k_s V_f \right)^2} \right] \quad (2.69)$$

The resistance coefficient for standard blocking filtration is;

$$\frac{d^2t}{dV_f^2} = k_s Q_0^{1/2} \left(\frac{1}{Q} \right)^{3/2} \quad (2.70)$$

If the resistance coefficient is simplified;

$$k'_s = k_s Q_0^{1/2} \quad (2.71)$$

and Equation 2.70 becomes;

$$\frac{d^2t}{dV_f^2} = k'_s \left(\frac{dt}{dV} \right)^{3/2} \quad (2.72)$$

Equation 2.72 represents the characteristic form of the standard blocking filtration law for constant pressure [27]. Fouling mechanism exponent for standard blocking is 1.5.

2.4.4. Cake Filtration Law

The cake filtration theory may also be expressed with the common equation that describes the filtration mechanisms (Equation 2.23). According to the resistance in series rule, the total resistance at time t , R_t (m^{-1}) is the sum of filter media resistance, R_0 (m^{-1}) and the cake resistance R_c (m^{-1}) [27]:

$$R_t = R_0 + \alpha W / A \quad (2.73)$$

Equation 2.24 at time t can be written as;

$$Q = \frac{PA}{\mu R_t} \quad (2.75)$$

Equation 2.12, which results from a mass balance on cake, can be written as;

$$W = cV_f = \frac{V_f \rho_s}{1 - m_s} \quad (2.75)$$

where W (kg) is the cake mass accumulated on media and c (kg m^{-3}) is the mass of dry cake solids per unit volume of filtrate. Inserting Equation 2.75 into Equation 2.73 and rearranging the equation gives;

$$R_t = R_0 \left[1 + \frac{\alpha V_f \rho_s}{(1 - m_s) A R_0} \right] \quad (2.76)$$

and Ruth's constant, k_R , can be derived from the equation. Ruth's filtration equation is:

$$\frac{dV_f}{Adt} = \frac{P}{\mu \left[\alpha \left(\frac{W}{A} \right) + R_m \right]} \quad (2.77)$$

The equation states that differential or instantaneous rate of filtration per unit area (dV_f/Adt) is given as the ratio of a driving force, pressure P , to the product viscosity μ and sum of cake resistance $\alpha (W/A)$ and filter medium resistance R_m [29]. Equation 2.77 can be rearranged and expressed as with the medium resistance neglected;

$$V_f dV_f = \frac{A^2 P}{\mu \alpha c} dt \quad (2.78)$$

Integrating and rearranging the equation gives;

$$\left(\frac{V_f}{A}\right)^2 = \frac{2P}{\mu \alpha c} t = \frac{2P(1-\bar{m}s)}{\mu \alpha \rho s} t \quad (2.79)$$

Thus, Ruth's constant can be written as;

$$k_R = \frac{2P(1-\bar{m}s)A^2}{\mu \alpha \rho s} \quad (2.80)$$

Equation 2.79 becomes;

$$V_f = k_R t \quad (2.81)$$

It is possible to define;

$$\frac{2}{k_R} = \frac{\mu \alpha \rho s}{A^2 P(1-\bar{m}s)} = \frac{\alpha \rho s}{AR_0 Q_0(1-\bar{m}s)} \quad (2.82)$$

and plugging constant for cake filtration, k_c ($s \text{ m}^{-6}$), can be written as;

$$k_c = \frac{2}{k_R} \quad (2.83)$$

Then, Equation 2.76 becomes;

$$R_t = R_0(1 + k_c Q_0 V_f) \quad (2.84)$$

so, Equation 2.75 becomes;

$$Q = \frac{PA}{\mu R_0(1 + k_c Q_0 V_f)} \quad (2.85)$$

and,

$$Q = \frac{Q_0}{(1 + k_c Q_0 V_f)} \quad (2.86)$$

Rearranging the equation gives;

$$k_c V_f = \frac{1}{Q} - \frac{1}{Q_0} \quad (2.87)$$

Integrating the equation to give $V_f = f(t)$ relationship [27];

$$\frac{dt}{dV_f} = \frac{1}{Q_0} + k_c V_f \quad (2.88)$$

$$\frac{k_c V_f}{2} = \frac{t}{V_f} - \frac{1}{Q_0} \quad (2.89)$$

and, $Q = f(t)$ can be written as [27];

$$Q = \frac{Q_0}{(1 + 2k_c Q_0^2 t)^{1/2}} \quad (2.90)$$

Inserting Equation 2.88 into Equation 2.23 gives;

$$\frac{d^2 t}{dV_f^2} = \frac{d}{dV_f} \left[\frac{1 + k_c Q_0 V_f}{Q_0} \right] \quad (2.91)$$

The resistance coefficient for cake filtration is;

$$\frac{d^2 t}{dV_f^2} = k_c \quad (2.92)$$

The Equation 2.92 represents the characteristic form of the cake filtration law for constant pressure [27]. Fouling mechanism exponent for blocking in cake filtration is 1.0.

2.5. Membrane Bioreactors

Membrane bioreactor (MBR) technology is advancing rapidly around the world for both research and commercial applications. A membrane system can be defined as two essentially uniform and homogeneous fluid phases between which matter and energy can be exchanged at rates governed by the properties of a third phase or group of phases that separates them [30]. The third phase is called the membrane and is simply a perm-selective material that resists transport [2, 30].

The term membrane bioreactor refers to a system developed for wastewater treatment that combines a biological reactor and a membrane module. MBRs offer several advantages, including high biodegradation efficiency, high MLSS concentrations in the process tanks, excellent effluent quality, low sludge production and compactness [31]. As a

result, MBR is an attractive option for the treatment and reuse of industrial and municipal wastewaters.

A membrane bioreactor, consists of an activated sludge (AS) reactor and a microfiltration/ultrafiltration membrane, which simply replaces final clarifier, typically has high bioreactor MLSS concentration and nominal pore sizes ranging from 0.1 to 0.4 μm , has the potential to fundamentally advance biological treatment processes. Membrane separates on the basis of molecular (or particle) size, according to the pore size of the membrane, the filtration process can be classified as microfiltration (MF), ultrafiltration (UF), nanofiltration (NF) or reverse osmosis (RO) [32]. MF membranes are capable of rejecting bacteria, cysts, and suspended solids. In addition to these materials UF membranes also remove viruses, protein, and some natural organic matter.

Table 2.1. Membrane filtration types.

Membrane process	Pressure (bar)	Pore size (nm)
Microfiltration	0.1 – 2	100 – 1000
Ultrafiltration	0.1 – 2	10 – 100
Nanofiltration	4 – 20	1 – 10
Reverse osmosis	10 – 30	0.1 – 1

The advantages of high MLSS operation and biomass filtration include:

- Tertiary filtration processes or UV disinfection can be eliminated, thereby reduces plant footprint.

- Unlike secondary clarifiers, the quality of solids separation is not dependent on the MLSS concentration or characteristics and there is no reliance upon achieving good sludge settleability. Because elevated mixed liquor concentrations are possible, the aeration basin volume can be reduced, which further reduces the plant footprint.
- MBR can be designed with long sludge age, hence sludge production is considerably lower than conventional systems.
- Membranes can produce an effluent quality suitable for reuse applications. Indicative output quality of microfiltration/ultrafiltration systems include $SS < 1 \text{ mg L}^{-1}$, turbidity $< 0.2 \text{ NTU}$ and up to 4 log removal of virus (depending on the membrane nominal pore size). In addition, MF/UF provides a barrier to certain chlorine resistant pathogens such as *Cryptosporidium* and *Giardia* [33].

The disadvantages of membrane technologies:

- There has been increasing operation experience in the last decade, however there is limited information on large scale applications (MBR has been mostly preferred in rather small-scale plants).
- Despite the decreasing material cost, high construction cost is still higher than conventional systems and, more information is needed on full-scale operation and maintenance cost.
- Lack of experienced operators (especially in Turkey).
- Operation and maintenance problems; in general the problems are well known but still there is the need for cost effective improvements.
- Regulations of effluent quality is not stringent everywhere.

2.5.1. Technology Implementation

The new and more stringent legislations, which affect both sewage treatment and industrial effluent discharge, to prevent and remedy water scarcity impacts (Figure 2.2)

have led to the progress of membrane manufacturing technology. Hence, membrane filtration (microfiltration or ultrafiltration) has replaced tertiary treatment steps and parallel to this, membrane filtration has been used for solid/liquid separation in biological treatment processes. Legislation is the primary driving force in Northern Europe and parts of the United States and Canada, while in other parts of the world, China, India, Australia and the Middle East, water stress is the dominant issue [34].

The researchers from the Department of Environmental Engineering, Rensselaer Polytechnic Institute, Troy, New York, and Dorr-Oliver, Inc., Connecticut in the U.S conducted first investigations into membranes for wastewater treatment [35]. The idea of replacing the final clarifiers of the conventional activated sludge (CAS) process was attractive, but it was difficult to justify the use of such a process because of the high cost of membranes, low economic value of the product (tertiary effluent) and the potential rapid loss of performance due to fouling. The first generation MBRs only found applications in niche areas with special needs like isolated trailer parks or ski resorts. The breakthrough for the MBR, came in 1989 by submerging the membranes in the reactor itself and withdrawing the treated water through membranes [34]. In Europe, the first full-scale MBR plant for treatment of municipal wastewater, which is a combination of common bioreactors and membrane filtration units for biomass retention, was constructed in Porlock, UK (commissioned in 1998, 3800 p.e.). Since early 2000s, MBRs have become increasingly popular for wastewater treatment. In 2002, one MBR line was commissioned in Brescia, Italy, with an initial flow of $38,000 \text{ m}^3 \text{ d}^{-1}$ that was later increased to $42,000 \text{ m}^3 \text{ d}^{-1}$. In 2004, the Nordkanal MBR plant (in Kaarst, Germany) was commissioned with a design maximum daily flow of $45,000 \text{ m}^3 \text{ d}^{-1}$ to serve a population of 80,000 p.e. [36].

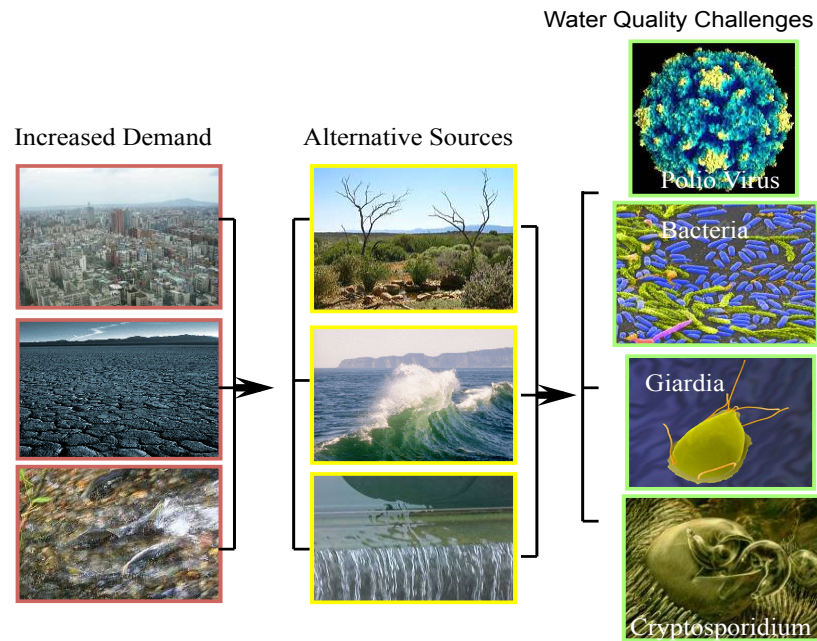


Figure 2.2. Drivers of membrane technology implementation [38].

2.5.2. Membrane Materials

Membrane materials have been manufactured in different characteristics including fouling resistance, hydrophobicity, hydrophilicity, mechanical strength or chemical tolerance. Material properties influence the exclusion characteristic of a membrane. A membrane with a particular surface charge may achieve enhanced removal of particulate or microbial contaminants of the opposite surface charge due to electrostatic attraction [37]. On the other hand, the separation characteristic of a membrane is defined by nominal weight cut-off (NMWCO) ability provided by the pore size and distribution of the membrane.

The vast majority of membrane materials are polymeric based; other forms of membranes include ceramic or metallic materials. Typical polymeric membranes are manufactured using phase-inversion techniques like solvent evaporation or temperature

change. Common membrane materials are, polysulfone (PS), polyethersulfone (PES), polyacrylonitrile (PAN), polypropylene (PP), polyvinylidene fluoride (PVDF), polyethylene (PE). Basically, the materials can be classified as hydrophilic and hydrophobic that is related to the surface tension of membranes. Hydrophilic membranes adsorb water while hydrophobic membranes have little or no tendency to adsorb water. Hydrophilic materials can be wetted forming a water film or coating on their surface because of their surface chemistry [34]. Mechanical strength is another consideration, because a membrane with greater strength can withstand larger transmembrane pressure (TMP) levels allowing for greater operational flexibility [37]. Chemical, thermal, and hydraulic resistances of ceramic and stainless steel materials are greater than any other membrane material. However, these membrane modules are not preferred for MBR applications due to their high cost. On the other hand, replacement cost of the modules is much less than polymeric membranes because they are hardly damaged.

2.5.3. Membrane Configurations

Flat sheet or hollow fiber forms are common manufacturing configurations of membrane materials. Membrane modules are categorized as:

- Flat sheet /plate and frame
- Hollow fiber
- Multi tubular
- Capillary tube
- Pleated filter cartridge
- Spiral wound

There are two types of membrane bioreactor configurations with membranes placed either outside (side-stream) or inside (submerged) the bioreactor. For the external configuration, the biomass is filtered under pressure in a membrane module, whereas for the

submerged configuration, vacuum-driven filtration is carried out in the aeration tank. In submerged configuration (Figure 2.3), the energy consumption required for filtration is significantly lower for two main reasons: no recycle pump is needed since aeration generates a tangential liquid flow in the vicinity of the membranes, and the operating conditions are much milder than in an external MBR system because of the lower values of TMP and tangential velocities [39, 40].

2.5.4. Membrane Fouling

The majority of membrane material and process research and development are dedicated to its fouling problems. Membrane fouling is basically the accumulation of suspended or dissolved materials on the surface and/or in the pores of membrane materials

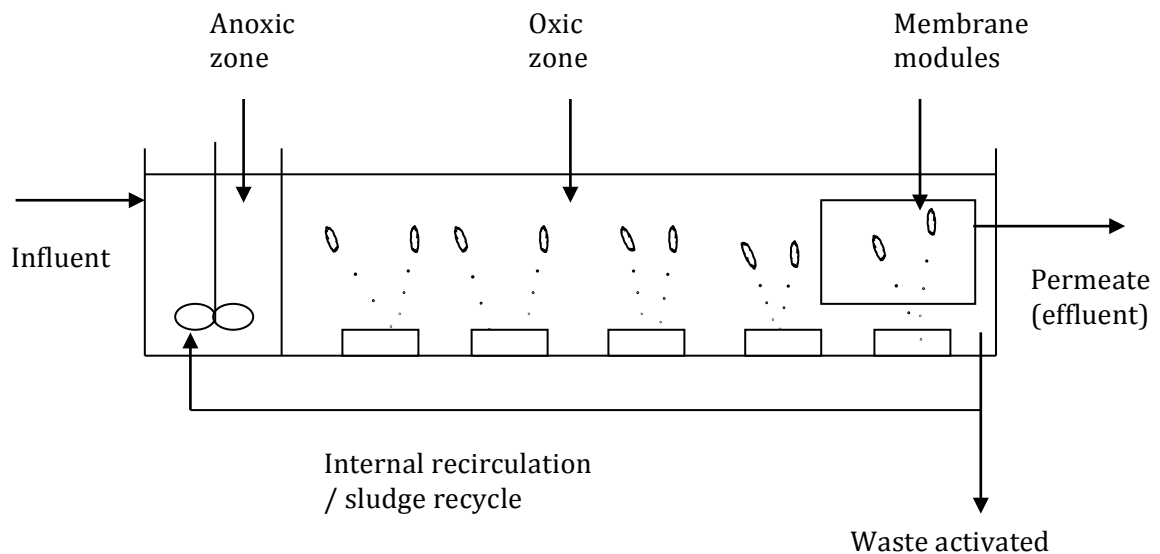


Figure 2.3. Nitrification/denitrification MBR plant scheme.

that causes a decline in membrane flux or permeability with time. Thus, fouling is stated as the filterability, which is related to volume of treated water, and reversibility of the fouling layer, which is related to regaining the membrane performance after it was fouled. Filterability defines the short-term flux changes and long-term flux filtration performance is affected by both filterability and reversibility [41].

Furthermore, Braak and coworkers [42] summarized that fouling mechanisms may arise usually in three ways:

- A fast but short rise in trans membrane pressure (TMP): conditioning fouling. Strong interactions, among which adsorption between the membrane surface and colloids, including extracellular polymeric substances (EPS), soluble microbial products (SMP), cause initial fouling and pore blockage.
- A long period during which TMP increases slightly: slow, steady fouling. The particles settle on the membrane surface and form the cake layer.
- A very strong rise of TMP: TMP jump. During the previous step permeability is not much affected but fouling is not uniform. Some areas suffer stronger fouling because of flux heterogeneities along the membranes.

It has been demonstrated that a critical flux exists, below which the membrane fouling can be neglected and thus membrane cleaning is not required [43]. Hence it is important to choose an adequate permeate flux or TMP. Once the critical flux is exceeded, an exponential increase in TMP is expected due to rapid cake formation on the membrane. However, some research has shown that significant irreversible fouling will occur during long periods of sub-critical flux [44].

The common compounds that cause membrane fouling can be categorized as: macro-scale and micro-scale foulants [45]. Macro-scale foulants include wastewater originated leaves, hair etc. and can easily be removed by pretreatment e.g. microscreening.

Micro-scale foulants may be summarized as [45]:

- (a) Particulate / colloidal foulants
- (b) Chemical reactions
- (c) Organic foulants
- (d) Inorganic foulants
- (e) Biological foulants

Inorganic foulants such as metal hydroxides and other scalants are a major concern for nanofiltration and reverse osmosis. Thus, organic materials form bonds with the membrane surface. Major organic foulants are known as humic materials and microbial originated EPS (carbohydrate or protein) and SMP. Also, chemical reactions with the polymeric media may cause rarely but highly irreversible fouling. In addition, bacteria and protozoa that easily adhere onto the membrane surface are considered as major blocking tools.

2.5.5. MBR Operation

MBR operating conditions directly affect the fouling tendency of activated sludge. Thus, the permeate flux is the most important operating parameter governing membrane fouling [46]. As permeate velocity increases, drag forces acting on particles will also increase, consequently bringing more particles to the membrane surface. Doubling the permeate flux has been found to more than double the fouling rate due to an linear increase in the forward transport of particles to the membrane surface and subsequent compaction of the deposited fouling layer [47]. Fouling rate is a critical design and operation parameter for MBR applications. To prevent fouling, membranes do not operate continuously; at specified intervals (e.g. minutes or hours) in the operation cycle, permeate production is stopped and a backwash or membrane relaxation is performed to improve the membrane permeability. Generally, shear at the membrane surface is provided by coarse bubble aeration and a tangential flow of liquid is created to mechanically scour some of the accumulated foulants.

However, some metabolic products and wastewater originated organic or inorganic solids, colloidal materials and macromolecules may still remain and accumulate on the membrane surface or inside the pores that can lead to declining membrane flux over time [48, 49]. Inorganic compounds such as struvite, which lead to inorganic fouling, are more likely to deposit on the membranes in anaerobic systems [48]. At much longer periods in an operating cycle like weeks or months, membranes are chemically cleaned to remove accumulated materials and restore flux. The chemical cleaning typically carried out by soaking membrane in cleaning solutions of e.g. sodium hypochlorite (NaOCl) for a several hours. Rapid loss of flux over time increases the cleaning frequency, consequently increases operating and maintenance (O&M) cost, decreases membrane lifetime. Those types of fouling, which can be removed by relaxation or chemical cleaning, is considered as reversible fouling, however, the residual unrecoverable membrane flux is considered as irreversible fouling.

Long sludge retention times (SRT) and the possibility of increasing mixed liquor suspended solids (MLSS) are considered as benefits of MBR operation. Uncoupling of hydraulic and solids residence times (HRT and SRT), yielding an additional degree of freedom for process control and establishment of slowly growing microorganisms with particular degradation features – reduced excess sludge production due to the enhanced utilization of maintenance energy demands at high SRTs – intensify overall process operation [36].

Membrane aeration is the biggest contribution to operating costs. In submerged MBR applications, aeration is the act of circulating air that provides both oxygen for aerobic metabolic processes and increases the cross flow velocity to scour the fouling layer from the media. Many fundamentals of the interaction between hydrodynamics of the multiphase flow in MBRs and fouling have been studied but experimental results still not satisfactory for design and operation. Hence, applied scouring air rates are normally based on previous experiences and manufacturers' recommendations, which may lead to higher oxygen consumption in operation.

2.5.6. Bio-treatment in MBR

MBRs are capable of biological nutrient removal including oxic carbon removal, nitrification, denitrification and biological phosphorus removal like any other conventional activated sludge system. The MBR process achieves degradation of high COD (>95%) with a wide variety of carbon sources and virtually complete TSS removal when treating domestic wastewater. This yields treated wastewater of high quality and is particularly important, as water quality regulations have become increasingly stringent. The use of membrane filtration following biological treatment makes it possible to operate the bioreactor at high MLSS concentrations like 10 - 20 g_{MLSS} L⁻¹. Some researchers reported even higher biomass concentrations up to 50 g_{MLSS} L⁻¹ [50, 51]. Consequently, a wide range of sludge retention time (SRT) and hydraulic retention time (HRT) values can be successfully applied. Thus, it is possible to use a short HRT and a long SRT at the same time. HRT becomes less important and the system can work at high organic loading rates being insensitive to HRT with efficient organics removal [52]. The increased SRT values of the MBR process can also result in better degradation of (COD removal > 90%) refractory or difficult to degrade compounds such as herbicides, high molecular weight compounds, oily wastes and explosives [53, 54,55].

The oxidation of wastewater in an MBR results in sludge production in the form of waste activated sludge (WAS) like any activated sludge system. However, MBRs are reported to yield lower sludge production compared to conventional systems [56, 57]. SRT is an important factor affecting the performance of bioreactors, so SRT can have significant influence upon biomass properties in an MBR system. Because, at high MLSS concentrations, cell maintenance mostly replaces the cell growth on biodegradable organics. Moreover, due to the accumulation of slowly growing microorganisms better nutrient removal is possible. On the other hand, increased biomass concentrations accompanied by increased extracellular polymeric substance (EPS) and soluble microbial product (SMP) concentrations (as proteins and carbohydrates) and a shift toward smaller particles, give rise to a deterioration of sludge

properties like viscosity and dewaterability that play an important role in the overall operation economics due to their influence on filtration and sludge management [58].

Attention has been given to the relationship between MLSS concentration and membrane fouling. Increasing MLSS concentration has been considered to intensify the membrane fouling. However, literature reports about the influence of MLSS on MBR operation are generally contradictory. Several authors report an increase on fouling with increasing MLSS concentrations. Wu and Huang [59] showed that MLSS higher than 10 g L^{-1} had a significant effect on membrane filterability due to increased viscosity of the mixed liquor, and MLSS concentration lower than 10 g L^{-1} had almost no effect. Similar results reported by Lousada-Ferreira and coworkers [60]. However, Ng and coworkers [61] found that the concentrations of total organic carbon, proteins, and carbohydrates in the mixed liquor supernatant increased with decreasing SRTs of 3, 5, 10 and 20 d. In this study, the longest SRT was 20 d, while in real practice the target SRT might be much longer.

Biological nutrient removal (BNR) in an MBR system is carried out like any other conventional activated sludge system through manipulations of its biological process. The most commonly applied configuration of total nitrogen (TN) removal is pre-denitrification followed by nitrification. Besides, many researchers have reported complete and stable nitrification with higher rates than CAS [62]. Teck and coworkers [63] reported the specific nitrification rate as $1.71 \text{ mg}_N \text{ g}_{MLVSS}^{-1} \text{ h}^{-1}$ at final stable phase of their reactor. In addition, MBRs have been combined with all common processes for nitrogen removal: simultaneous, intermittent, and alternating nitrification/denitrification, and Anammox [36]. Generally, denitrification has been reported to be problematic when dissolved oxygen (DO) is high in an MBR, mainly because of constant scouring air need; but an anoxic condition can be achieved in the reactor through intermittent aeration [64]. However, the growth of denitrifying microorganisms, hence simultaneous nitrification and denitrification can be stimulated under high DO concentrations, which rest upon the high MLSS concentration and micro anoxic/anaerobic zones formed within flocs [65].

Because MBRs are usually operated at elevated sludge ages, chemical P-removal is commonly suggested when P-elimination is required. But, it has been shown that enhanced biological phosphorus removal (EBPR) is also possible in BNR systems with membrane separation. Ramphao and coworkers [66] stated that in multi-zone BNR systems with membranes in the aerobic reactor and fixed volumes for the anaerobic, anoxic, and aerobic zones, the mass fractions can be controlled (within a range) with the internal recycle ratios. This zone mass fraction flexibility is a significant advantage in MBRs over conventional BNR systems, because it allows for changing of the mass fractions to optimize biological N and P removal in conformity with influent wastewater characteristics and the effluent N and P concentrations required.

As it is stated above, stable and efficient nitrification can be achieved in MBRs. High MLSS operating principle and consequently high SRT provides quiet sufficient environment for slow growing nitrifiers. Nitrification is a two-step process that consists of aerobic ammonium oxidation and nitrite and nitrate oxidation. The dominant group of bacteria in an MBR system has been shown to be β -subclass Proteobacteria including some currently characterized nitrogen converters such as *Nitrosomonas* and *Nitrospira* [67]. The groups of microorganism that catalyze these processes are aerobic ammonia-oxidizing bacteria or archaea (AOB, AOA), which convert ammonium to nitrite, and nitrite-oxidizing bacteria (NOB), which oxidize nitrite to nitrate. These organisms both use oxygen as a terminal electron acceptor. However, the discovery of anaerobic ammonium-oxidizing (Anammox) bacteria has changed the traditional thought of ammonium oxidation to be a strictly aerobic process [68].

In addition, elevated nitrification efficiency can provide more sustainable membrane flux due to soluble microbial products (SMP) elimination [69, 70]. Drews and coworkers [71] stated the inhibition of nitrification increased SMP rejection, which indicates that SMP were too large pass through the media and were likely to form cake layer. However, grazing of protozoa on nitrifiers cause decrease of nitrification activity. Higher concentrations

of protozoa, particularly flagellates and free ciliates, have been reported for MBRs compared with a conventional activated sludge operating at the same SRT [2, 56]. The decrease of nitrifying activity may be due to the change in nature of the activated sludge with increasing SRT, which can result in inert material accumulation and competition of biomass. Endogenous respiration is a commonly used term representing all forms of biomass loss and energy requirements not associated with growth by considering related respiration under aerobic conditions: decay, maintenance, endogenous respiration, lyses, predation, and death [40]. Besides providing the growth slow growing bacteria, high SRT and high MLSS concentration can encourage endogenous respiration of a microbial community in MBR and reduce the viability of population, especially nitrogen converters as they comprise a small portion in the total biomass. Thus, optimal biomass concentration should be determined and the biomass content should be well understood for a successful operation of MBR, including sustainable filtration flux, efficient biotreatment, sludge production and operating expenses.

3. THE PILOT UNIT - CAKE FILTRATION BIOLOGICAL REACTOR (CFBR) AND MEMBRANE BIOLOGICAL REACTOR (MBR)

The Paşaköy Advanced Biological Wastewater Treatment Plant (Figure 3.1) is a biological nutrient removal (BNR) system, consisting of anaerobic, anoxic and aerobic zones, with a capacity of $200,000 \text{ m}^3 \text{ d}^{-1}$. Influent wastewater source is of domestic origin from households near Paşaköy region and contains high levels of nitrogen and suspended solids, which are typical for Istanbul. The treated wastewater is channeled into the Riva Stream through a tunnel and the stream flows into the Black Sea. The aeration tanks consist of a series of four oxidation ditches in which anoxic and aerobic zones are created with 10 hours of hydraulic retention time. Organic carbon oxidation and nitrification occur in the same reactor and the reactors are operated at an average solid retention time of 20 days. Depending on the influent conditions, it has been operated as A2O (anaerobic/anoxic/aerobic) or Johannesburg processes (anoxic for return activated sludge/anaerobic/anoxic/aerobic), where carbon, nitrogen and phosphorus were removed biologically. In 2009, the parallel Stage II of the treatment plant was put into operation as a tertiary biological treatment plant with the same flowrate and operating conditions as those of Stage I. In addition to the removal of carbon, nitrogen and phosphorus in the Stage II plant, a rapid sand filtration unit and a UV disinfection system were constructed following the secondary clarifiers. The removal of waste activated sludge consists of direct dewatering and sludge drying units. In addition, cogeneration unit has been mounted in order to supply electric and thermal energy demand for sludge drying.

A pilot scale membrane bioreactor (MBR) and a cloth filter unit (CFBR) with a capacity of $100 \text{ m}^3 \text{ d}^{-1}$ (one per thousand of the dry weather flowrate of 2nd stage of the full-scale plant) were constructed in the Paşaköy WWTP to compare the performance of each system under field conditions (Figure 3.2). The pilot plant was constructed (Figure 3.3) as a nitrification-denitrification plant with internal recirculation and pre-anoxic zones. A plan view of the plant and its location in the WWTP is given in Figure 3.4.



Figure 3.1. General overview of the Paşaköy WWTP.



Figure 3.2. General overview of fine screens, grit chamber, Parshall flume and the pilot plant (A: Membrane permeate line B: Cloth filter permeate line).



Figure 3.3. Atelier and on-site construction of the pilot unit.

The pilot unit is located near the aerated grit chambers of the Paşaköy WWTP, and raw water that feeds the pilot plant is pumped from the effluent channel of the grit chambers to the anoxic zone. The wastewater passes through 50 mm coarse screens, 10 mm fine screens, and through the aerated grit chambers before entering the 3 mm drum screen of the pilot plant.

The treatment sequence in the pilot plant consisted of three consecutive zones. The first zone was fully anoxic, the second was a time controlled anoxic/oxic zone and the third was fully oxic. The second and third zones were equipped with fine and coarse bubble diffusers respectively. The semipermeable membranes of the MBR and CBFR, which separated the treated wastewater and the biomass, were located in the third chamber.

The nitrate-rich sludge was re-circulated internally by a pump from the third zone to the first zone, at a pumping rate of approximately four times of the influent flow rate. However, the pre-anoxic zone provided denitrification of the nitrates generated in the two oxic (nitrification) zones by utilising the influent biodegradable organic carbon as carbon source. The second zone was a continuation of the anoxic zone as well as it was

the first oxic zone; oxic conditions were achieved by aerating the tank 10 to 45 minutes in an hour, depending on the influent load variations. Aeration of the tank was achieved by fine bubble EPDM diffusers (second zone) and coarse bubble diffuser pipes (third zone) installed at the bottom of the tank (Figure 3.5). Two rotary-lobe blowers provided air to the diffusers (Figure 3.6). Coarse bubble diffusers were used to scour the membrane and the cloth filter surface. The flowrate of the air used for scouring was $55 \text{ m}^3 \text{ h}^{-1}$ per 100 m^2 of filter area. Scouring air provided a parallel flow of mixed liquor to membrane surface, and solid deposition continued until the scouring force of the air balances the adhesive forces, binding the cake to the membrane.

The membranes were constructed as two parallel flat sheet microfiltration modules consisting of 300 sheets (Table 3.1). Each module has 150 membrane cartridges each of which has 0.8 m^2 effective filtration area, showing a total surface area of 120 m^2 per module. The cloth filter system consisted of a 200 cm long 2" diameter HDPE pipe, which had 314 holes with 0.3" diameters (Figure 3.7). The filter cloth, which had a surface area equivalent to that of one side of the membrane sheets, was wrapped and sealed around the 2 m long tube (2" diameter HDPE pipe) The specifications of the fabric was determined by İTÜ Textile Engineering Laboratory (Table 3.2, Figure 3.8). Construction cost of CFBR was approximately 10 percent of the pilot MBR unit.

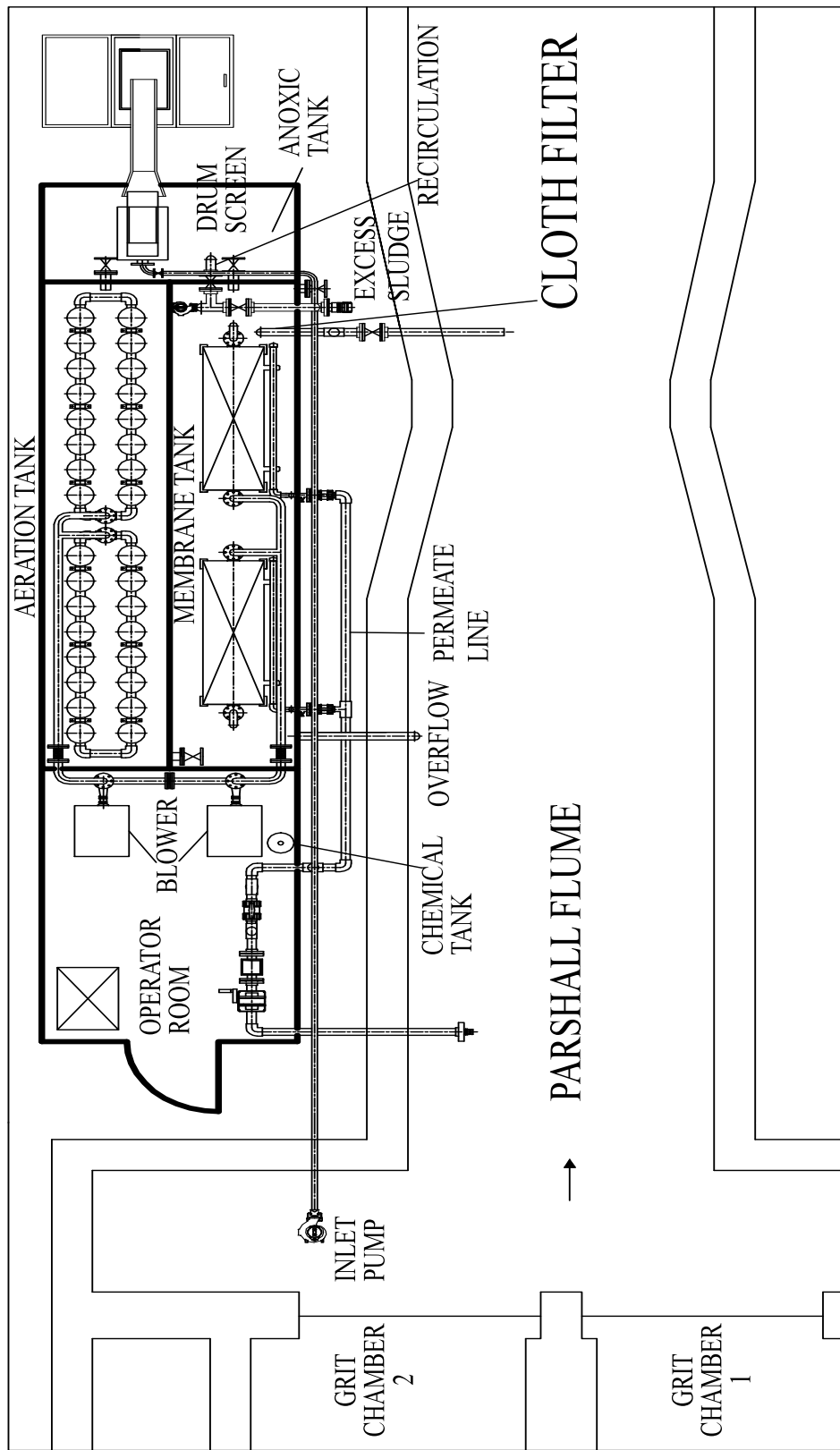


Figure 3.4. General overview of the membrane bioreactor and the cloth filter. (The cloth filter is located within the reactor close to the membrane plates).



Figure 3.5. Coarse bubble diffusers (left) and diffuser piping (right).



Figure 3.6. Control room: power panel, data logger, blowers and permeate instruments (left); permeate line in detail (right).

Table 3.1. Membrane Specifications.

Membrane type	Flat sheet
Total membrane surface area	240 m ²
Maximum pore size	0.4 µm
Maximum transmembrane pressure	1,000 mmWC
Membrane surface chemistry	Hydrophilic
Membrane material	Chlorinated polyethylene

Table 3.2. Cloth Filter Specifications.

Cloth Material	100% polyester
Total surface area of cloth	0.36 m ²
Total surface area of filtration	0.015 m ²
Pore size	15 - 40 µm
Surface chemistry	Hydrophobic
Weft strength	1,300 N
Warp resistance	1,207 N

Permeates of both systems were discharged by gravity, using the 2 metres of water head over the two permeate pipes; thus, applied pressure for filtration was constant (Figure 3.2). The effluent of both systems was discharged into the Parshall flume channel of the treatment plant. Both the MBR and CFBR were operated continuously (24 hours/day); however membrane modules were relaxed three times a day (in three shifts) for 3-5 minutes. Total process volume was 56 m³, which consists of 14 m³ of anoxic zone, 21 m³ of fine bubble aeration zone and 21 m³ of coarse bubble aeration zone.



Figure 3.7. Construction steps of the cloth filter unit.

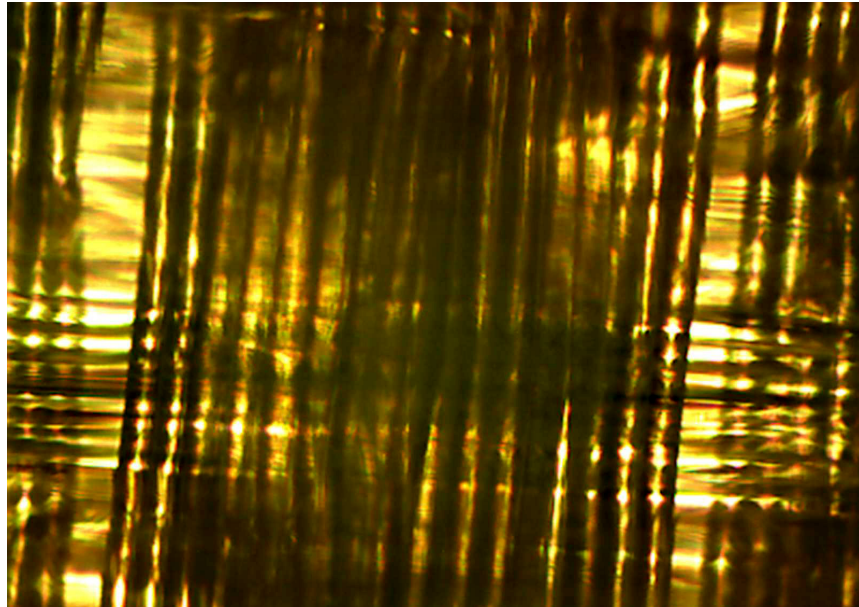


Figure 3.8. Microstructure of the cloth filter.

Online operational control tools were redox meters, oxygen meters, level sensors and pressure indicators on both permeate lines and the aeration tanks. The unit was operated automatically and was monitored using a SCADA system. Measurements were transferred online to a computer by a data logger. All of the measured data was collected for analyses.

Before start up of the pilot unit and the actual operation, the filters were tested in clean water (Figure 3.9, top). Following inspections and preparation were performed before starting the clean water test. The air supply piping connections, the permeate piping connection, and level of each filter unit were re-checked; also, sands and debris in the tanks were completely cleaned. Then, the pilot unit was filled with tap water up to the level specified for a normal operation and the chemical injection valve was opened in order to allow the air trapped in membrane cartridges to escape.

After the tanks were filled with clean water, the aeration blowers were started to make sure that they operate normally and provide even and uniform aeration in

the tanks. Permeate valves were opened and the permeate flow rate, pressure, and water temperature were measured. The system was shut down and emptied for sludge seeding and actual operation.

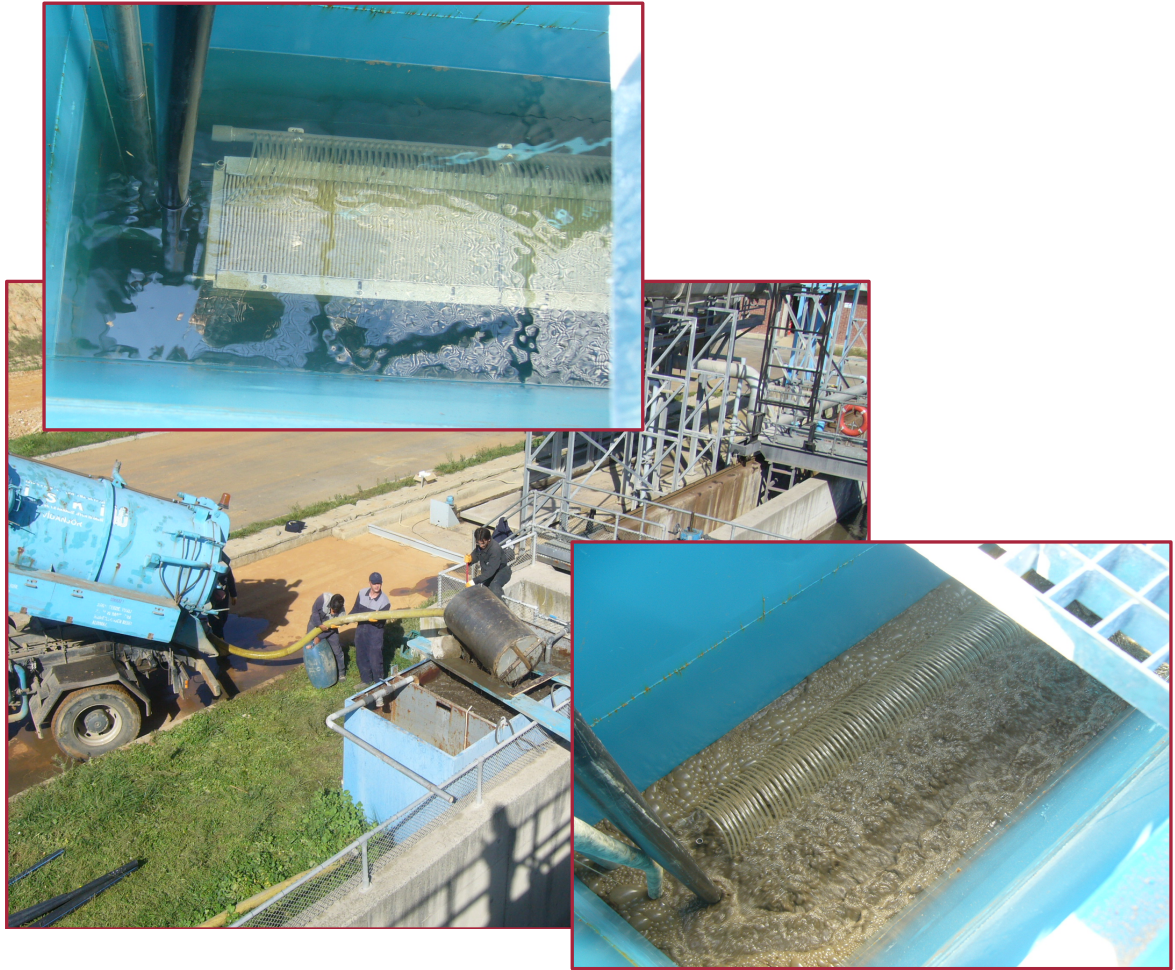


Figure 3.9. Clean water test and sludge seeding.

Direct membrane filtration of raw wastewater usually causes membrane fouling. Therefore, sludge seeding is recommended before beginning the actual operation in order to treat the wastewater biologically. Thus, the more the sludge is seeded, the more stable the initial condition becomes. The seed sludge was taken from the return activated

sludge (RAS) lines of the full-scale plant. The RAS sludge was pre-screened through 3 mm pore-sized portable screen and put into a separate tank from which it was pumped to the pilot unit (Figure 3.9) until the sludge concentration in the tanks was around 3,000 mg MLSS L⁻¹.

4. EVALUATION OF CAKE FILTRATION BIOLOGICAL REACTORS (CFBR) VERSUS MEMBRANE BIOLOGICAL REACTORS (MBR) IN A PILOT SCALE PLANT

4.1. Introduction

When the treated wastewater and biomass are separated by filtration, very large quantities of mixed liquor contact with the filter material. Ideally the filter material allows the passage of the fluid through its pores while retaining all suspended solid particles originally present in the fluid. Microorganism cells tend to adhere to surfaces; this is considered to be a survival strategy. Regardless of the surface material and hydrophobicity or hydrophilicity in a membrane system, adhesion to a membrane surface is facilitated by the water flow through the membrane. So, some organisms will settle on the surface of the membrane material, and they will multiply and form a sludge cake that is considered to be membrane biofouling during operation [12]. Biofouling is an operational term applied when the effects of biofilms exceed a certain threshold or tolerance level, and filtration always leads to increase in flow resistance, which consequently decreases flux.

Cake layer formation is the key factor limiting the flux when operating a membrane bioreactor. The formed cake layer on the media can act as a secondary membrane that determines filtration properties of the system, so the membrane material itself may no longer be necessary. Thus, the membrane material may be replaced by a low cost material, which does not provide excessive media resistance; coarse filters act as a support over which a cake layer can be formed. Such systems, which solids rejection will be provided by a cake layer defined in literature as self-forming dynamic membrane [72]. Moghaddam and coworkers [73] operated a non-woven coarse pore filtration activated sludge process under high mixed liquor suspended solids (MLSS) concentration in aerobic

and anoxic/aerobic conditions. Jeison and coworkers [74] studied with two types of materials to act as a support for dynamic membrane formation in an anaerobic system; a non-woven material which is used as a spacer material to cast membranes and polyester mesh fabrics of different pore sizes in the range 1-150 μm . Kiso and coworkers [75] operated an aerobic bioreactor equipped with a 100 μm mesh, at fluxes over 20 $\text{L m}^{-2} \text{h}^{-1}$. However, many other researchers have recently researched on self-forming dynamic membrane formation over coarse filters and showed that such membranes can be operated successfully under aerobic and anaerobic conditions [76 – 83].

The goal of the study presented in the chapter was to develop an alternative to a membrane filtration system that could separate and concentrate the MLSS in an activated sludge system. The membrane was replaced by a simple cloth filter, which allows the accumulation of self-forming dynamic membrane layer on the filter surface. The MLSS formed a cake on the filter cloth with a pore size that was much smaller than the cloth fabric. The chosen filter material was a thin polyester cloth, which is actually used for textile purposes, and by the help of cake formation, the mixed liquor is retained in the reactor to form a target MLSS concentration of 15,000 mg L^{-1} or higher. It was previously found that bacteria could develop immobilised colonies on cotton cloth; however, this is a relatively slow process that requires up to several days. More recent studies have led to the conclusion that hydrophobic interaction is a predominant force involved in bacterial adhesion to solid surfaces [84]. Because bacteria are immobilised on the macro-porous surface of fibres, immobilised bacteria should have free access to nutrients [85]. The effective pore size of the sludge cake that forms on the membrane surface was reported to be 0.01 microns, smaller than the pore size of the membrane used in this research (0.4 μm). The cloth filter reactor was called Cake Filter Biological Reactor (CFBR). Moreover, the aim of this research was to compare a CFBR and an MBR system, through analysing the filtration characteristics and the fouling mechanisms.

4.2. Materials and Methods

4.2.1. Theoretical Section

The membrane filtration theory and conventional cake filtration theory is based on the local properties in the filter cake, and assumes a one-dimensional Darcian flow in the filter cake (see Chapter 2). Cake filtration is considered to be an important method for solid and liquid separation and is widely used in the chemical and process industry. Indeed, investigations of cake filtration have received considerable attention in the past. The development of conventional theory can be summarized in two steps: 1. Combining the mass balance equation and the momentum balance equation (Darcy's law) for the liquid phase in the cake to form the governing equation with both porosity and liquid pressure as the dependent variables and 2. Assuming that only point contacts exist between particles [10, 86]:

The basic equations of the cake filtration theory used in filtration analyses of this study, which are described detailly in Chapter 2, may be listed as follows:

$$q_l = \frac{dV}{dt} = \frac{p_0}{\mu \left\{ [\alpha_{av}]_{\Delta p_c} \frac{V \rho_s}{1 - m_s} + R_m \right\}} \quad (4.1)$$

The above expression states that instantaneous filtration rate (q_l) is directly proportional to the applied pressure p_0 and inversely proportional to the flow resistance [16]. For constant applied pressure filtration, equation (4.1) may be written as:

$$\mu s \rho (1 - \bar{m}_s)^{-1} [\alpha_{av}]_{\Delta p_c} V \frac{dV}{dt} + \mu R_m \frac{dV}{dt} = p_0 \quad (4.2)$$

Integrating with initial condition $V = 0$, $t = 0$ and R_m assumed to be constant:

$$\mu s \rho \left(1 - \overline{ms}\right)^{-1} \left[\alpha_{av}\right]_{\Delta p_{s_m}} \frac{V^2}{2} + \mu R_m V = p_0 t \quad (4.3)$$

For cross-flow filtration, by modifying the conventional filtration theory to account for the presence of particle depolarisation in cake formation, instantaneous filtration velocity is [16]:

$$q_{l_m} = q_l = \frac{p_0}{\mu s \rho (\alpha_{av})_{p_{s_m}} \int_0^t \frac{\beta q_{l_m} dt}{1 - s \left[(\overline{m} - 1) \beta + 1 \right]} + \mu R_m} \quad (4.4)$$

For the fraction of cake removal or fraction of particle flux being deposited, $\beta = 1$, the above expression reduces to Equation (4.1). In an ideal case, the surface shear resulting from the cross-flow prevents the accumulation of particles on the membrane surface. However, there is always cake formation on the membrane surface, and as this cake grows its hydraulic resistance increases, and the filtration flux at a constant applied pressure declines. Consequently, accumulation of particles on the membrane surface for unit volume of filtrate decreases. This causes the decline of filtration flux to slow and, in some cases, causes a steady or pseudo-steady flux [87].

From the conventional constant pressure filtration equation, a plot of t/V versus V is expected to yield a linear relationship for the entire filtration data (see Chapter 2). The linearity of t/V vs. V plot is observed only when the value of V (or time) or the cake thickness is sufficiently large. The initial part of the data contributes to the non-parabolic behavior of the entire range of filtration data [88]. Flux decline in cross-flow filtration is considered to be due to two distinct independent mechanisms: pore plugging and cake deposition. The initial rapid flux decline is mainly due to pore plugging by particle adsorption on the membrane wall or pore constriction, and the latter slow flux decline is due to cake deposition on the membrane surface [89]. In usual cases, when filtering

suspensions containing more than a few percent of solids, blocking of particles inside or on the top of the membrane occurs, leading to a reduction in filtration flux [90].

The four filtration models describe the fouling mechanisms during a filtration run can be summarized as [26, 92]:

- Complete blocking: plugging of pore entrances and the prevention of any flow through pores as a result of the reduced open flow area.
- Standard blocking: particles accumulate inside the membrane on the pore walls. Since the pores are constricted, the membrane permeability is reduced.
- Intermediate: plugging of pore entrances by a fraction of particles and a deposition of the rest on top of them.
- Cake filtration: particles accumulate at the surface in a permeable cake of increasing thickness that adds a hydraulic resistance to filtration.

For a constant pressure filtration, the common frame of following power-law relationship were derived by the assumption of separate mechanisms (Table 4.1) [25, 27]:

$$\frac{d^2t}{dV_f^2} = k \left[\frac{dt}{dV_f} \right]^n \quad (4.5)$$

The standard blocking and conventional cake filtration theory on flux decline has been shown be the best suited to membrane filtration [2, 93, 94]. Grenier and coworkers [90] conducted the fouling analysis in two steps and identified two prevailing mechanisms namely surface blocking and cake filtration. Ho and Sung [89] concluded that the initial rapid flux decline was in good agreement with standard blocking filtration law, while the latter gentle flux decline is attributable to the cake filtration law. On the other hand, Xu and Chellam [95] stated that the initial stages of flux decline prior to the secretion of new

extracellular polymeric substances (EPS) was quantitatively described by the intermediate blocking law before transitioning to cake filtration at later times.

Table 4.1. Filtration models and fouling mechanisms.

<i>Filtration model</i>	<i>n</i>	<i>Derived form [27]</i>	<i>Fouling mechanism</i>
Complete blocking	2	$Q = Q_0 - k_b \cdot V_f$	Pore blocking
Standard blocking	1.5	$t/V_f = k_s/2 \cdot t + 1/Q_0$	Pore constriction
Intermediate blocking	1	$1/Q = k_i \cdot t + 1/Q_0$	Pore blocking and surface deposit formation
Cake filtration	0	$t/V_f = k_c/2 \cdot V_f + 1/Q_0$	Surface deposit formation

4.2.2. Experimental Section

The filtration was performed in the pilot unit as described in Chapter 3. The cloth filter and the membranes were operated continuously (24 hours/day) in parallel at all times. The pressure and cumulative mass of filtered water were monitored both through the data acquisition system of the full-scale plant and the data-logger of the pilot plant. Thus, the data recorded by the data logger and carried weekly to a computer. The clean filter resistances of both filter systems were calculated by measuring pressure difference at four different fluxes.

Filtration ability of the selected cloth material was tested initially in a laboratory filter set-up. Laboratory scale filtration experiments for cloth media were conducted in a filtration cell. The cell had a height of 9.5 cm and an inner diameter of 10.1 cm. Test suspension entered the cell through the upper port and permeate left the cell through lower orifice. The results of the laboratory set-up showed that, a cake layer immediately builds up on the cloth filter and in less than 5 minutes, the cloth filter – cake

system can hold almost the entire biomass subjected to be filtered through the cloth filter, just like the membranes in the pilot plant. Because the cloth filter and the cake accumulated (Figure 4.1), stabilized as a filter system in a negligible period of time compared to the whole pilot plant operation period, the bioreactor performance of both CFBR and MBR was considered as identical and they were constructed in the same bioreactor zone. But their filtration behaviours, characteristics and mechanisms would be different, as presented in this chapter.

In order to assure the biological activity and the treatment performance, the following parameters were monitored throughout the experiments: pH, salinity, COD, TKN, $\text{NH}_4^+\text{-N}$, $\text{NO}_3^-\text{-N}$, SS, VSS, total coliform, and faecal coliform. The operational parameters, MLSS, MLVSS and filterability, were also measured during the operation. Standard Methods for the Examination of Water and Wastewater were used for all analyses [96]. The filterability was measured as volume (mL) of permeate in the first 5 minutes; total coliform and faecal coliform were measured by Sartorius laboratory kits.

4.3. Results and Discussion

4.3.1. Bioreactor Performance

Operation of the pilot plant was stable with respect to COD and ammonium nitrogen ($\text{NH}_4^+\text{-N}$) removals. The annual average raw water and effluent quality for the CFBR is given in Table 4.2. The average COD and $\text{NH}_4\text{-N}$ removal rates were 96 % and 99 % respectively. Despite the excellent ammonium nitrogen removal, the nitrate nitrogen ($\text{NO}_3^-\text{-N}$) removal efficiency fluctuated; approximately 70 % nitrate nitrogen removal was achieved. Air scouring was performed constantly at the flow rate advised by the membrane manufacturer. Because the amount of scour air was kept constant and was not controlled, dissolved oxygen could be transferred to the anoxic zone causing fluctuations in the effluent $\text{NO}_3^-\text{-N}$ values. The target MLSS of the system was around 15,000 mg L⁻¹.

Because the aim of this study was to compare the performance of the MBR and the CFBR, more emphasis was given to the effluent quality achieved from the cloth filter and the membrane.



Figure 4.1. Stabilised cake layer on the cloth filter.

Suspended solids concentrations in permeate of both the membrane and the cloth filter were less than 10 mg L^{-1} , which is the guaranteed maximum SS discharge limit of membrane modules. However, both CFBR and MBR systems produced effluent with 0 pcs./100 mL faecal coliform, except for the few occasions mainly because of the loosening

of the cloth from the hook-up points on the perforated pipe – cloth filter system. In such incidences the peak values of faecal coliform reached 1,000 to 8,000 pcs./100 mL.

Table 4.2. The Raw Water and Effluent Quality for CFBR.

Parameter	Raw Water (mg L ⁻¹)	Effluent of CFBR (mg L ⁻¹)
Chemical Oxygen Demand (COD)	465	35
Total Kjeldahl Nitrogen (TKN)	51	< 0.5
Ammonia Nitrogen (NH ₄ -N)	42	< 0.5
Suspended Solids (SS)	280	< 10

4.3.2. Filtration Analyses in Laboratory and SS Removal Efficiency of the Cloth Filter

Before the start up of the pilot scale cloth filter system, clean polyester filter material was tested in a similar laboratory set-up. Initial grab samples showed that the cloth material without cake growth could hold only 75 % of suspended solids. This removal efficiency would result in 4,000 mg L⁻¹ MLSS concentration in the effluent of a reactor operating at 16,000 mg L⁻¹ MLSS concentration. However, as the cloth material begins to form a cake on its surface, suspended solids concentration in the filtrate can be reduced to values less than 10 mg L⁻¹ in less than 5 minutes.

As shown in Figures 4.2, SS results of the pilot scale unit were lower than desired SS discharge limit. The first limit in the figure represents the SS discharge standard from final clarifiers in the Paşaköy plant and the second limit represents the guaranteed maximum SS discharge limit of the membrane modules. The pilot plant tests were continued for one year and there were two separate runs done without changing cloth.

Deterioration of the effluent SS values towards the end of the run periods is believed to be due to loosening of the filter cloth from the pipe at the attachment locations after a long operation period. However, the SS results (Figure 4.3) in the laboratory set-up were lower than 4 mg/L at all samples, which show that the cloth – cake filter system is capable of obtaining lower SS values in the permeate under idealised mechanical conditions.

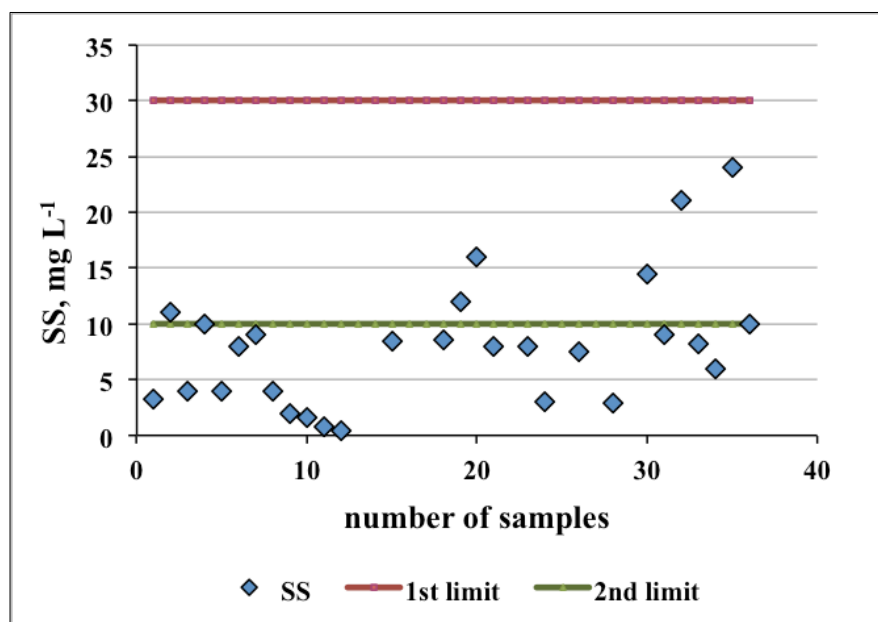


Figure 4.2. Permeate SS results of pilot scale cloth filter.

Figure 4.4 represents the laboratory filtration test results. Activated sludge concentrations of both pilot plant sludge (MBR/CBFR) and return activated sludge (RAS) concentrations were 16,491 mg L⁻¹ and 16,578 mg L⁻¹ respectively. Both sludges showed similar behaviour during the filtration tests. According to conventional cake filtration theory for constant pressure filtration, equation (3) gives time (t) as a second order polynomial of cumulative filtration volume per unit area (V); or there is a linear relationship between t/V and V that is commonly known as the parabolic law of constant pressure filtration [16, 23]. Linearity deviations were previously believed to take place because of greater medium resistance, sudden decrease of filtration area (filtration rate)

and interior medium clogging [97, 98]. However, linearity deviations of laboratory scale experimental results were due to the sudden decrease of filtration rate at after three minutes of filtration. Also, as mentioned before, a sharp decrease in filtrate MLSS concentration due to effective cake formation corresponded to these decreases of filtration rate. Similarly, filtration experiments were conducted in the lab-scale unit with different concentrations of pilot plant sludge (Figure 4.5). The plot of cumulative filtration volume (V) vs. time (t) for filtration of different MLSS concentrations was best fitted to second order polynomial regression ($R^2 > 0.98$). Variations of MLSS concentration affected the total filtrate volume. On the other hand, a linear relationship between the reciprocal of the filtration rate (t/V) and the cumulative volume was not observed (Figure 4.5).

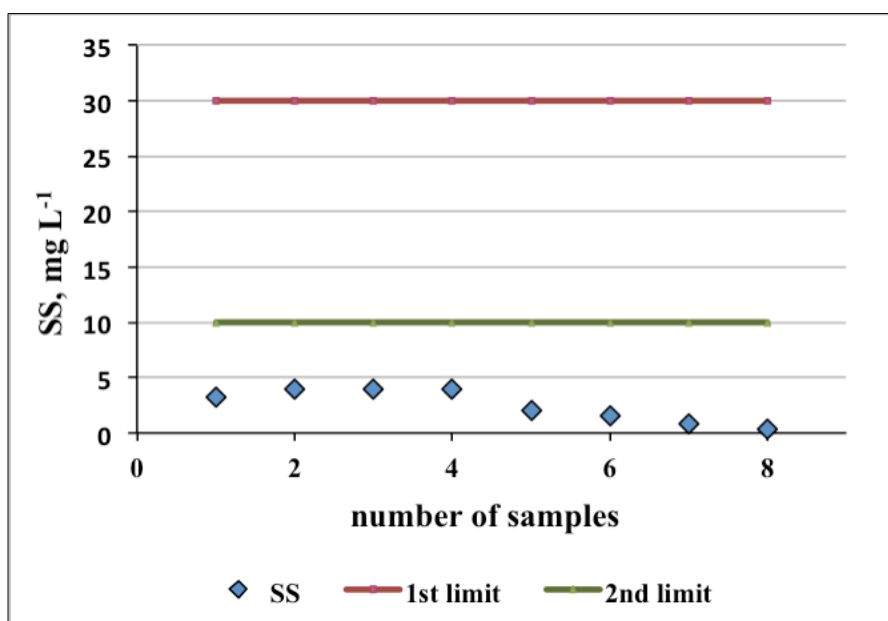


Figure 4.3. Permeate SS results of laboratory scale cloth filter.

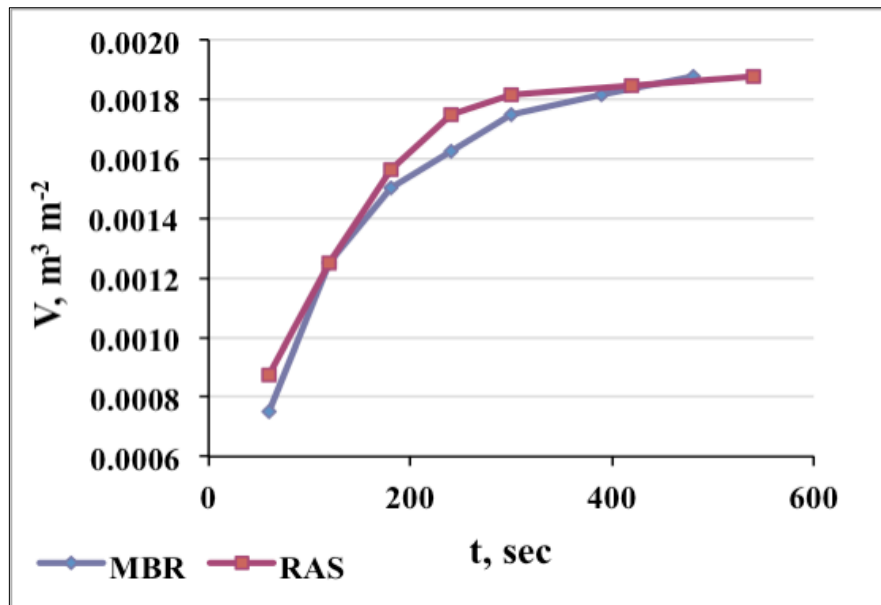


Figure 4.4. (a) Experimental data of constant-pressure filtration used in the laboratory study at $p_o = 800$ Pa. The 1.6% activated sludge samples from return activated sludge (RAS) of the full-scale plant and the pilot plant were filtered and the medium was composed of two layers of polyester filter. Plot of V vs. t .

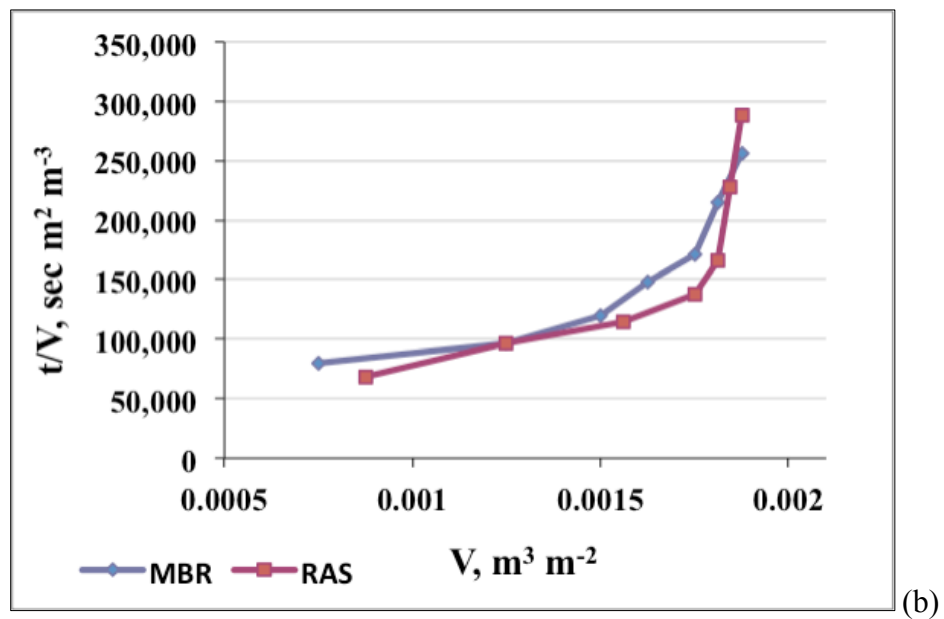


Figure 4.4. (b) Plot of t/V vs. V .

Several factors can be recounted to explain the deviation from linearity, including medium clogging because of the penetration of particles into the medium. Similar to our results, Teoh and coworkers [22] stated no linearity between t/V vs. V initially and the extend of non-linearity increased with the increase of the medium resistance. Tiller and Cooper [99] showed that, the average specific cake resistance at the initial period is somewhat smaller than that of the latter period; in the conventional filtration concept it is assumed constant during the entire filtration process. However, the non-linear behaviour of t/V vs. V diminishes by the progressive cake formation on the medium and consequently the cake resistance becomes dominant. At the beginning of a constant pressure filtration, pressure drop across the cake equals to zero ($\Delta p_c = 0$) and as Δp_c approaches asymptotically to operating pressure p_o , the medium resistance becomes insignificant. In our experiments, as the pressure drop across the cake increased, the linearity of t/V vs. V established in the latter period. Similar behaviour of the cloth filter medium and the cake formed by the biomass in the pilot scale experiments is given in the following sections.

In practice, the filtration behaviour is too complex to be expressed by one single filtration model. In order to identify the prevailing filtration mechanism, the entire filtration period was evaluated as initial and latter period of filtration, because an initial time is taken by the cake to grow to a certain thickness until the pressure drop across the cake and the septum becomes equal. Filtration behaviour and fouling mechanisms were analysed according to the filtration models given in Table 4.1. The transition point of the deviation from linearity (t/V vs. V) was considered to be around four minutes of filtration in the lab-scale unit. Hence, initial period of filtration was plotted separately. Figure 4.6. shows plots of experimental data obtained from a set of experiment for complete blocking (a), intermediate blocking (b), and standard blocking (c) at the initial filtration period; Figure 4.6. (d) shows a plot of filtrate volume (V) versus filtration time/filtrate volume (t/V) for the cake filtration model at the latter filtration period. In the lab-scale unit, standard blocking model plots of both MBR/CFBR and RAS sludge were fitted better ($R^2 > 0.98$) than complete blocking and intermediate blocking models with the measured data for the initial period of filtration. However, the latter period of filtration was best fitted to the cake filtration model ($R^2 \cong 1.0$).

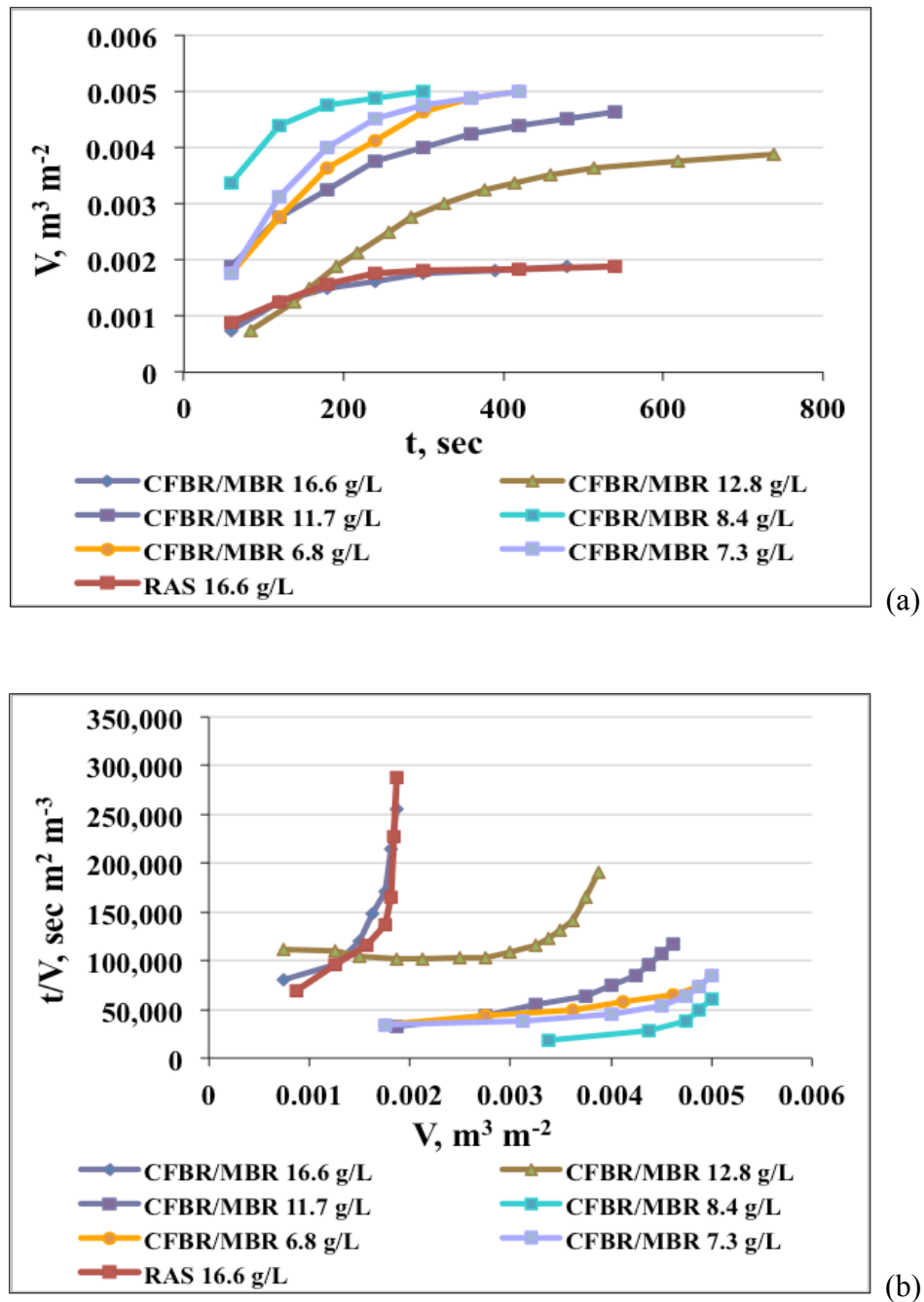


Figure 4.5. Plot of V vs. t (a) and t/V vs. V (b). Experimental data of constant-pressure filtration used in the laboratory study at $p_o = 800$ Pa. Different concentrations of activated sludge samples from the pilot plant and 1.6% return activated sludge (RAS) of the full-scale plant were filtered in the lab-scale unit and the medium was composed of two layers of polyester filter.

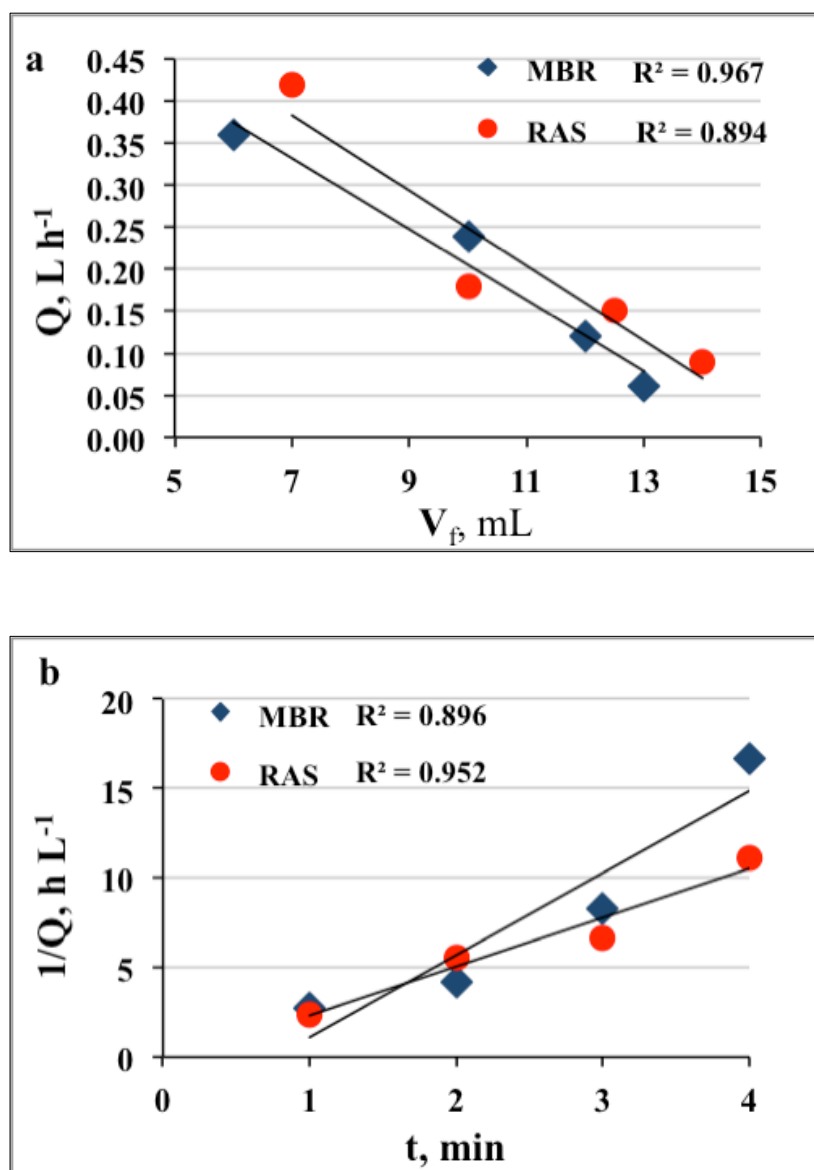


Figure 4.6. Flux decline rate for MBR/CFBR and RAS sludge filtration: (a) complete blocking model, (b) intermediate blocking model.

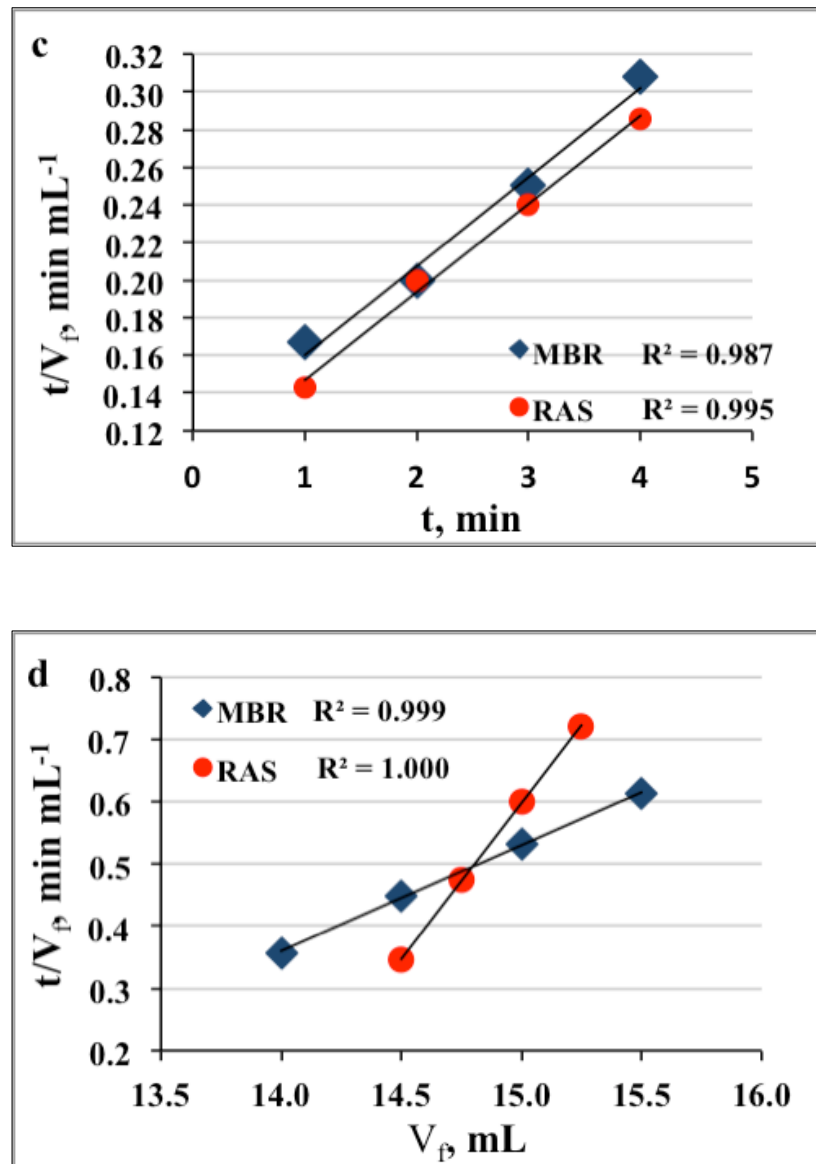


Figure 4.6 (continued) (c) standard blocking model, and (d) cake filtration.

4.3.3. Filtration Analyses in the Pilot MBR/CFBR

Two different cloth filter and three different membrane runs were conducted in the pilot plant on site. The cloth filter and membrane experiments were halted because of maintenance requirements. The membrane experiments had to be stopped twice during the first and the second runs to chemically clean the membranes (Figure 4.7). The end of third

run was the maintenance period. This period was not taken into consideration for the cloth filter because its operation was almost stable, so the cloth filter performance analyses were done considering the pressure difference (Δp) and CFBR process to be two different runs. As a result of the sharp change in the tendency of the pressure difference, CFBR was stopped for observation and maintenance, but cloth filter was not changed. Thus, the filtration process was defined in two runs.

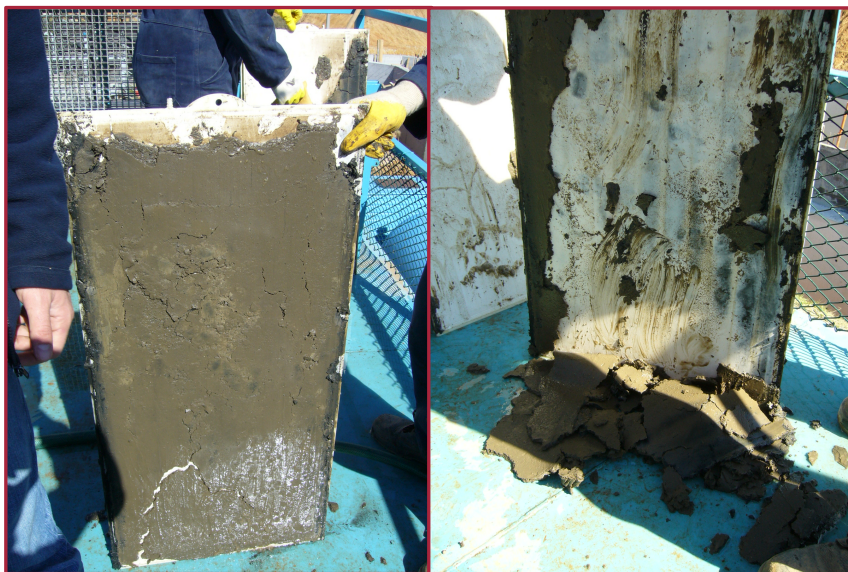


Figure 4.7. Fouled membrane cartridges in the first run.

4.3.3.1. Trans-Membrane Pressures (TMP) and Flux Variations

In order to monitor variations of TMP and membrane flux, and detect the blocking points throughout each filtration run, the data obtained by pressure transducers and flow meters, which were mounted on permeate lines, was recorded automatically (with a sampling frequency of once per every 5 seconds) using the data logger. The data collected was then used to analyse the fouling mechanisms. Because the bioreactor operated 24 hours a day, filtration through the membranes and the cloth filter was carried out continuously and simultaneously, except the relaxation periods of the membranes (3 –

5 minutes in three shifts per day). The increase of the trans-membrane pressure and flux variations are shown in Figure 4.8 and Figure 4.9 respectively.

The design operation flux of membranes was $17.5 \text{ L h}^{-1} \text{ m}^{-2}$. Previous studies using the same pilot plant showed that the maximum allowed trans-membrane pressure of the membranes should be around 25 kPa, and any further increase in pressure accelerates the need for chemical cleaning. Also, further increases of trans-membrane pressure and decreases of flux will lead to irreversible fouling.

Filtration (first run) began at around 6 kPa cake resistance (adjusted due to CFBR) and increased gradually from $6 \text{ L h}^{-1} \text{ m}^{-2}$ to the target flux; the increase of flux retarded because of trans-membrane pressure peaks, however, the flux could be controlled to adjust for desired values. The second run began at 18 kPa TMP, and TMP reached a predetermined limit value (25 kPa) earlier. Third run began again at around 6 kPa cake resistance and flux was sustainable around $9 \text{ L h}^{-1} \text{ m}^{-2}$ almost the whole run. Consequently, variations of TMP were lower. Trans-membrane pressure peaks observed during the first and the second run were recovered by increased membrane relaxation period (20-30 min.) and sludge wastage.

Fouling mechanisms (complete blocking, intermediate blocking, standard blocking and cake filtration) were analysed for 59 days of operation; due to the stable cake resistance, first 8 days were considered as initial filtration period. Standard blocking and cake filtration models fit better than the other two models with the measured data for both initial filtration ($R^2 > 0.98$) and the latter period ($R^2 > 0.95$). Figure 4.10 and 4.11 show plots of experimental data obtained from the operation of the MBR unit for complete blocking (a), intermediate blocking (b), standard blocking (c), and cake filtration (d) models at the initial and latter periods of filtration respectively. Since the pore size of membranes much smaller than the cloth, the cake formation effected the filtration from the very beginning. However, unlike the cloth filter and the CFBR unit, standard blocking model fits well for longer durations of filtration, which shows pore constriction continued

at the latter period. Consequently, the cake resistance increased and flux declined slightly during the entire filtration, which ended up with a chemical cleaning.

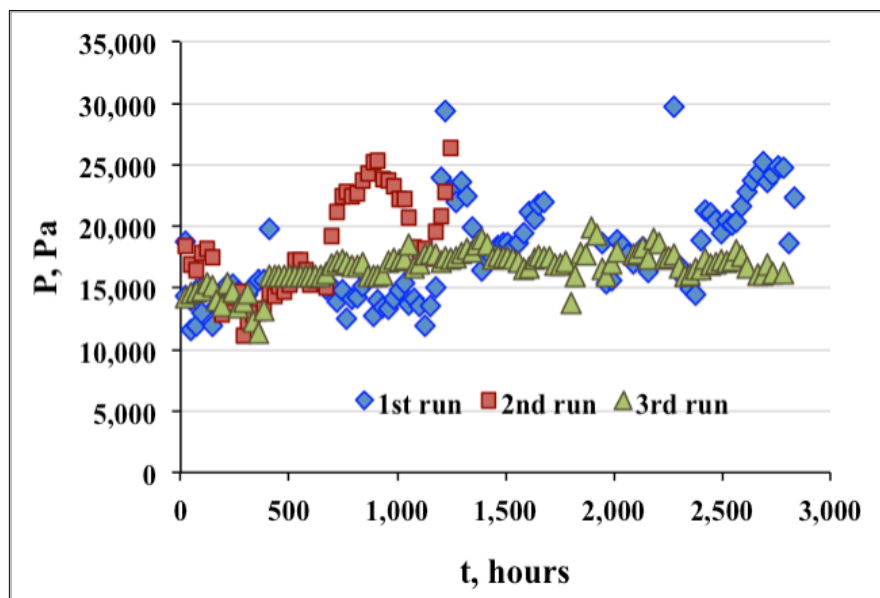


Figure 4.8. Change of the trans-membrane pressure (Pa) of the membranes with respect to operation time (hours).

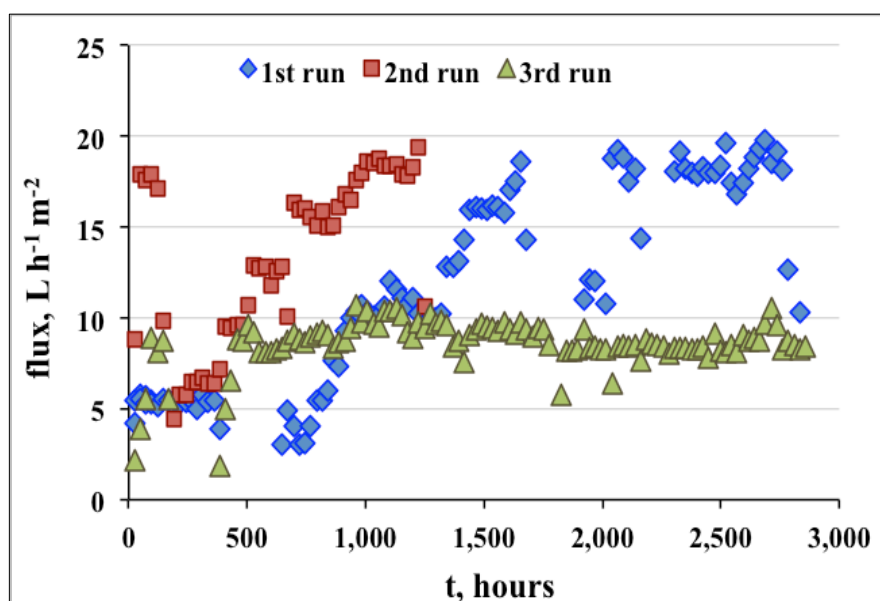


Figure 4.9. Change of the flux ($\text{L h}^{-1} \text{m}^{-2}$) membranes with respect to time (hours).

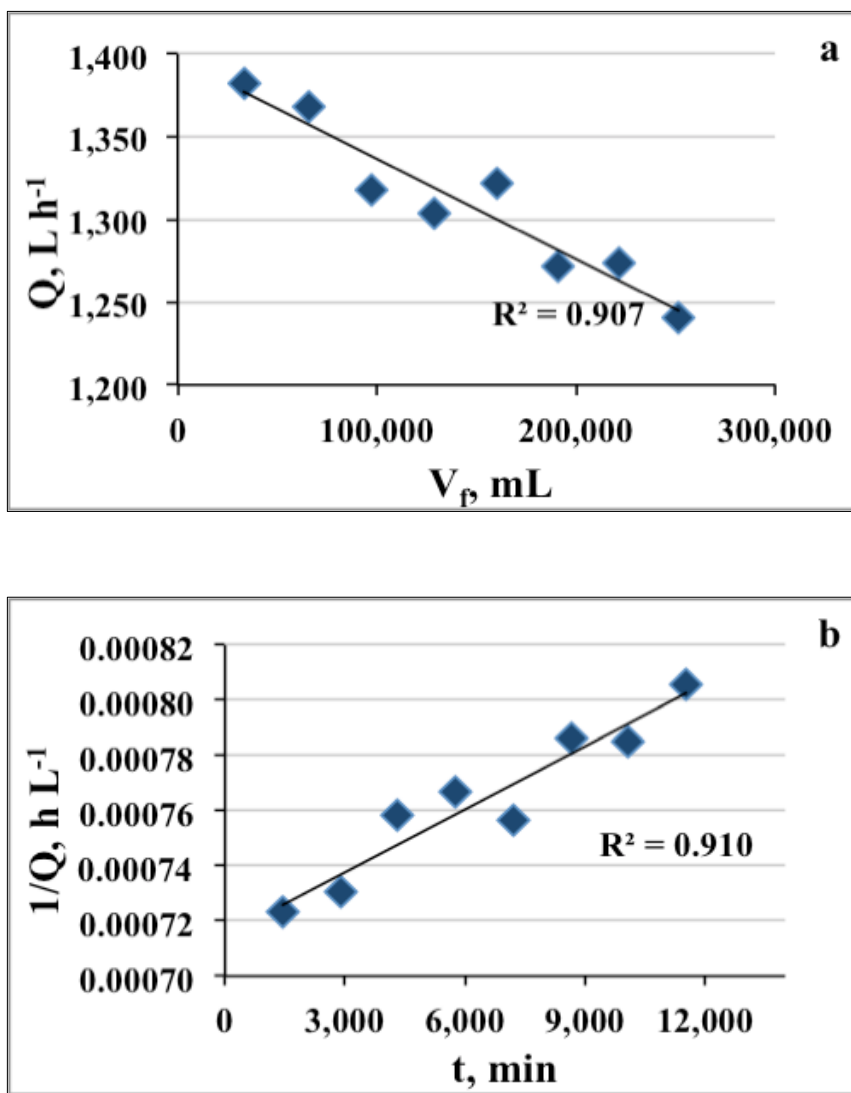


Figure 4.10. Flux decline rate for MBR at the initial filtration: (a) complete blocking model, (b) intermediate blocking model,

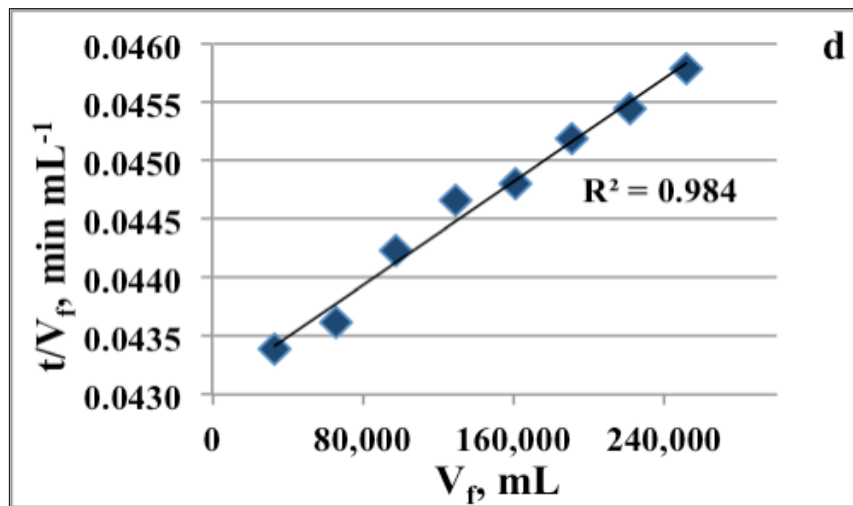
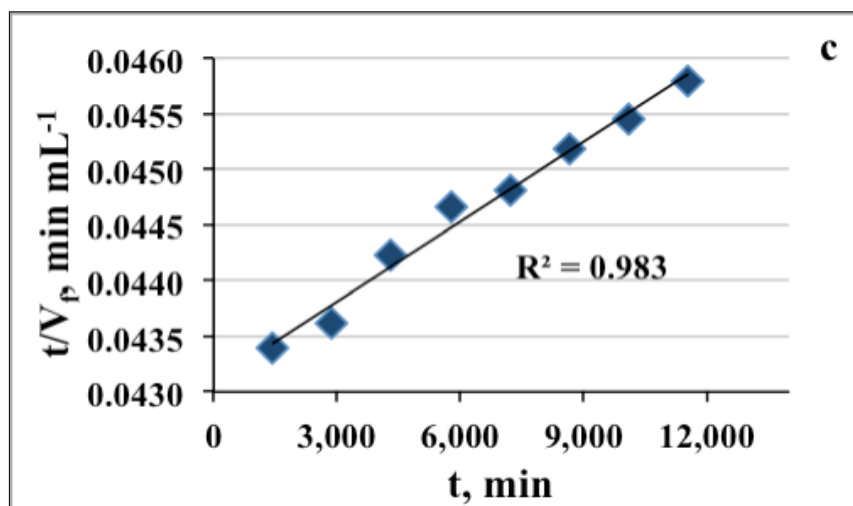


Figure 4.10 (continued) (c) standard blocking model, and (d) cake filtration.

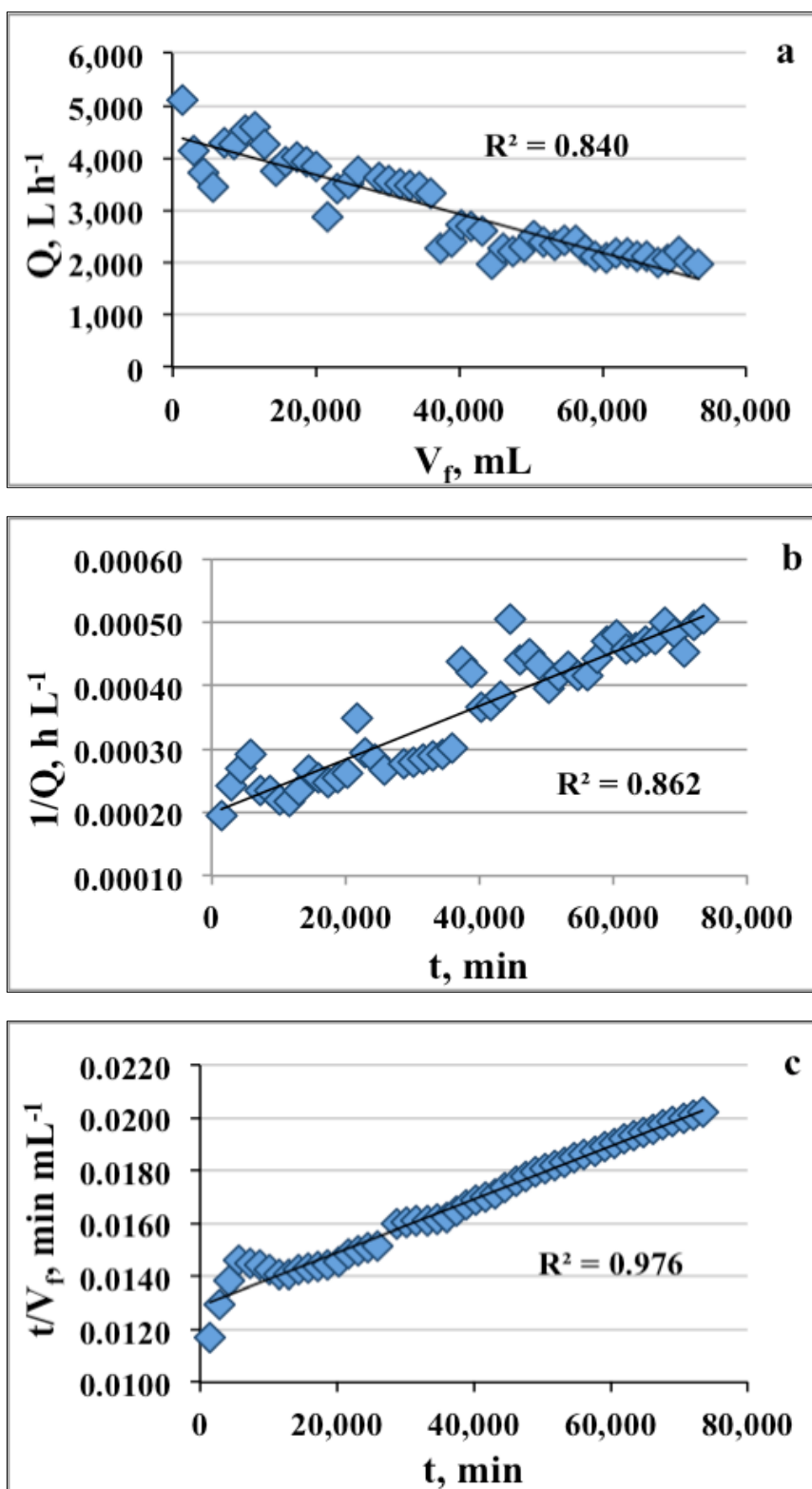


Figure 4.11. Flux decline rate for MBR at the latter filtration: (a) complete blocking model, (b) intermediate blocking model, (c) standard blocking model,

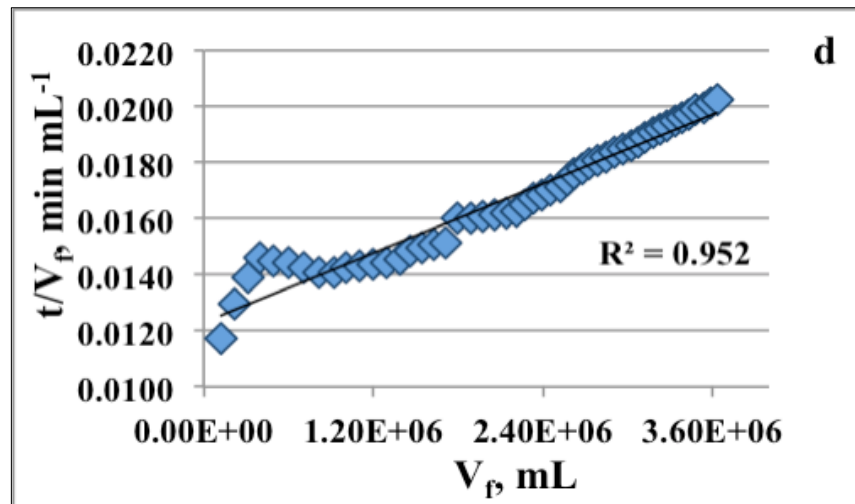


Figure 4.11 (continued) (d) cake filtration.

4.3.3.2. Pressure Drop across Cloth Filter and Flux Variations

Using the data logger, the pressure and flux data of the cloth filter was also recorded automatically as it was described in Section 4.3.3.1. Initial flux of the clean cloth filter was quite high. It was $1,517.5 \text{ L h}^{-1} \text{ m}^{-2}$, and start up cake resistance was around 6 kPa. The flux dropped sharply during the first run, and, at the end of first run, the flux was $110 \text{ L h}^{-1} \text{ m}^{-2}$. During the second run, the flux declined further from $60 \text{ L h}^{-1} \text{ m}^{-2}$ to $48 \text{ L h}^{-1} \text{ m}^{-2}$ and for the last 4,000 hours it was stable at $48 \text{ L h}^{-1} \text{ m}^{-2}$. The cumulative filtration volumes per unit area depending on the decline of flux with run time for the cloth filter are given in Figure 4.12. Cumulative filtration volume (V) vs. time (t) results of the CFBR for two different runs evaluated separately and the results best fit to second order polynomial regression ($R^2 = 0.995$ for first run and $R^2 = 0.989$ for second run); however, the linear relationship between the reciprocal of filtration rate (t/V) and the cumulative volume was observed individually.

As mentioned above, filtration through the cloth filter continued without any cleaning. So, the cumulative filtration volume (V) vs. time (t) and t/V vs. V results of

two runs were plotted in series (Figure 4.13). The linearity deviation can be clearly observed from the figure, and the tendency of cumulative filtration volume changed sharply. As shown in Figure 4.14, the pressure difference (Δp) (and pressure drop across the cake) increased steadily for about 2,300 hours until it reached a stable Δp value, which was close to the operating pressure, at the termination of the run. Also at around 2,300 hours of operation time, the slope of the cumulative filtration volume per unit area curve decreased dramatically.

In comparison to laboratory cell results, the deviation represented by the sharp decrease of flux, was not considered to be related to the sudden decrease of filtration area, but it was regarded as the end of a period of medium clogging. Depending on the first permeate SS concentration (3.2 mg L^{-1}), initial effective cake formation within the media (sudden reduction of filtration area) occurred way before the first sampling period. However, the reduction of effective filtration area as a result of medium clogging continued during the first run, which led to the drop of filtration rate, and the pore constriction completed by the end of the period.

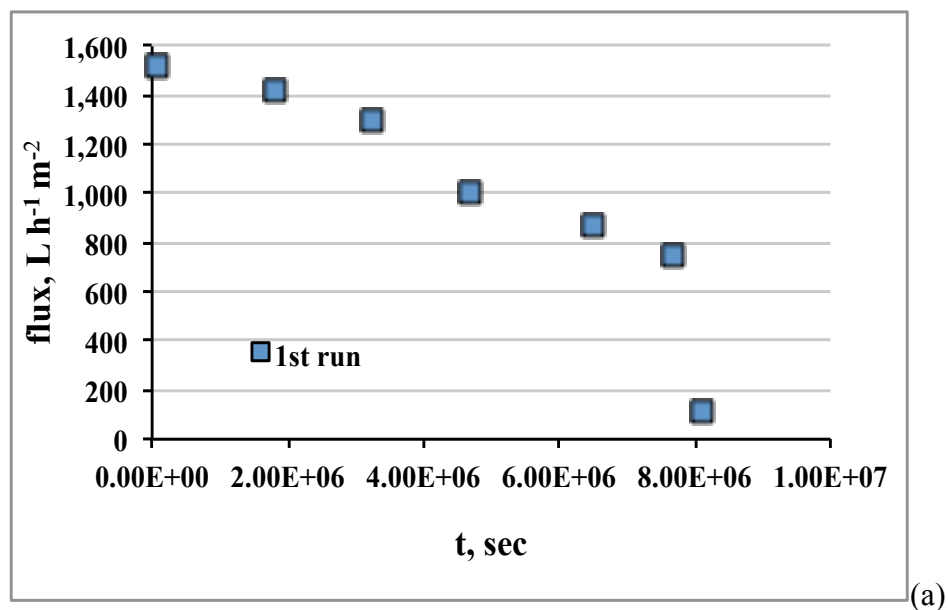


Figure 4.12. Plot of flux ($\text{L h}^{-1} \text{ m}^{-2}$) decline vs. t and V vs. t for the first and second runs of the CFBR.

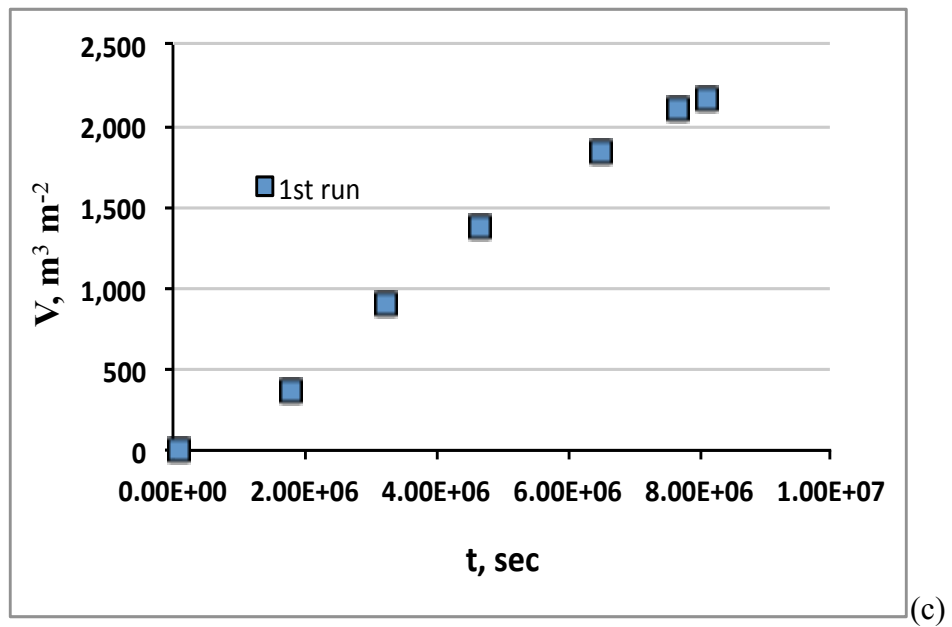
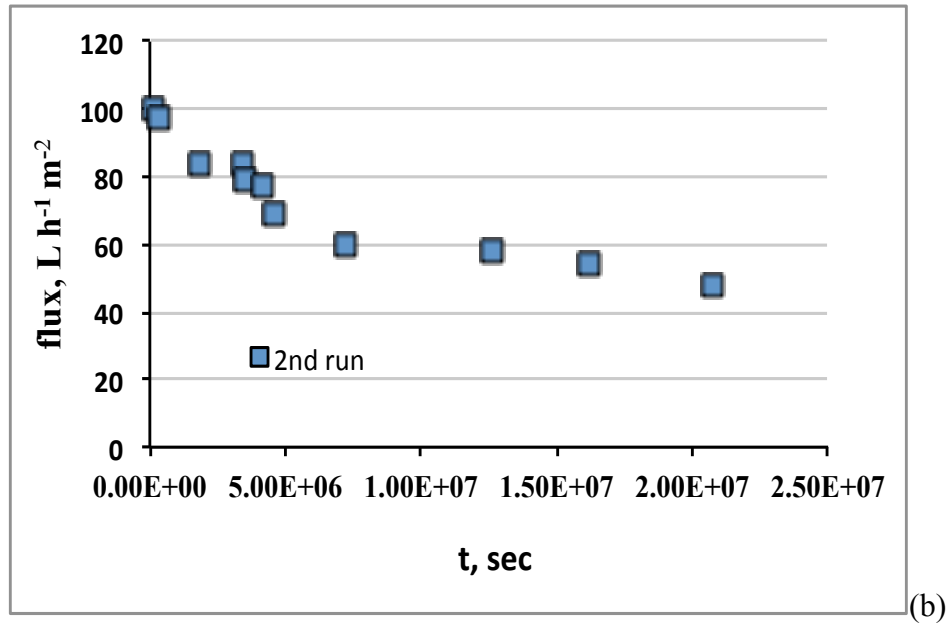


Figure 4.12 (continued) Plot of flux (L h⁻¹ m⁻²) decline vs. t and V vs. t for the first and second runs of the CFBR.

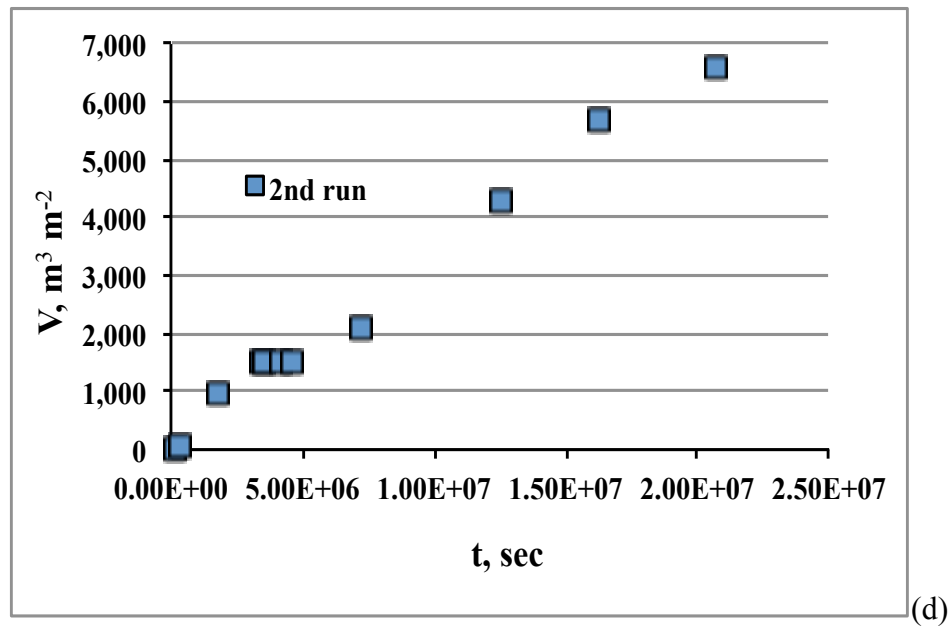


Figure 4.12 (continued) Plot of flux ($\text{L h}^{-1} \text{m}^{-2}$) decline vs. t and V vs. t for the first and second runs of the CFBR.

The system stabilised in the second run due to the sufficient cake growth on the media. Thus, the plot of t/V vs. V can be represented by two linear segments, which show the change of this filtration behaviour. Therefore, the transition point in the plot of V vs. t and t/V vs. V , or a sharp departure from linearity, was considered to be a change in filtration characteristics, and filtration proceeded around critical flux.

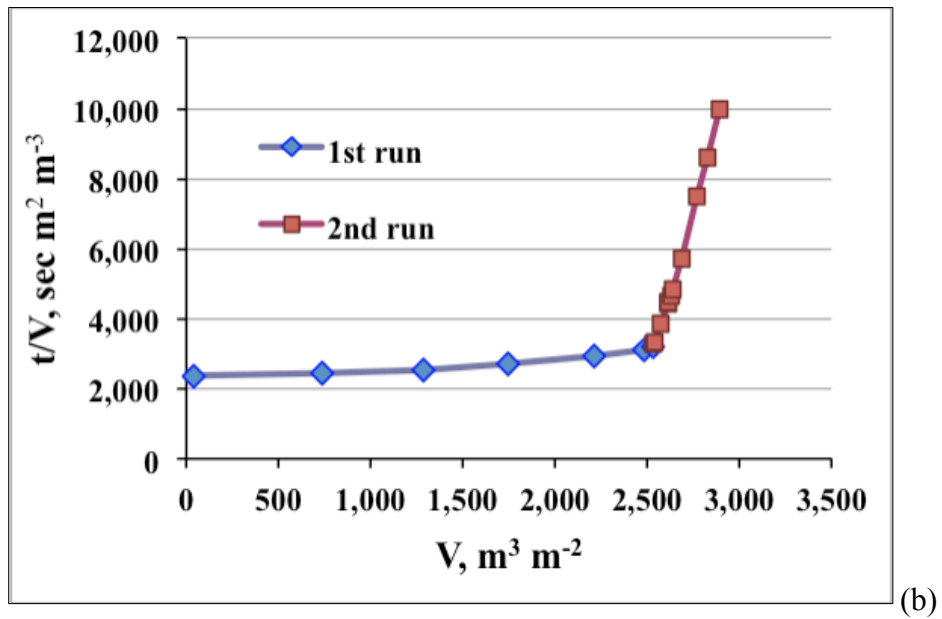
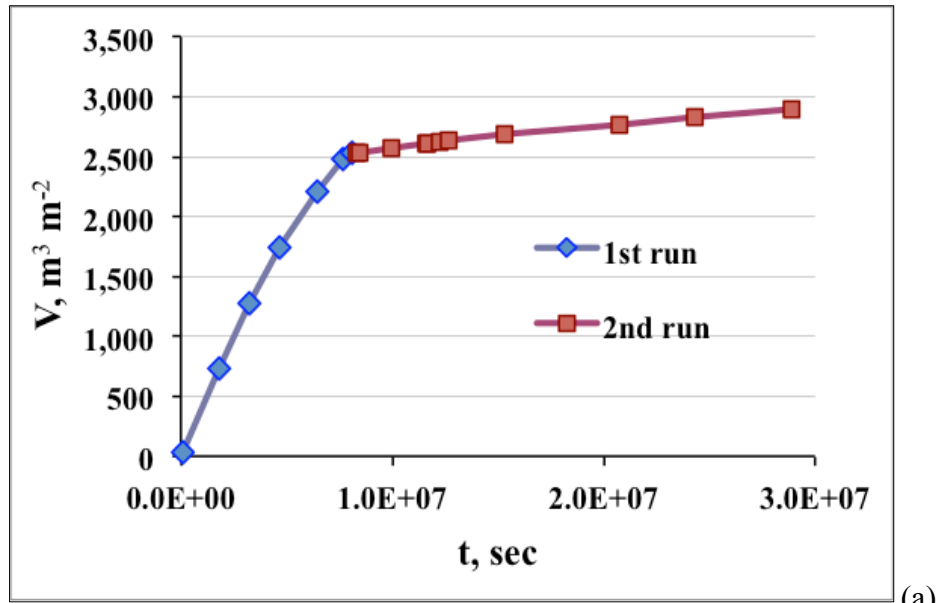


Figure 4.13. Plot of V vs. t (a) and t/V vs. V (b). Experimental data of the CFBR at $p_o = 20$ kPa.

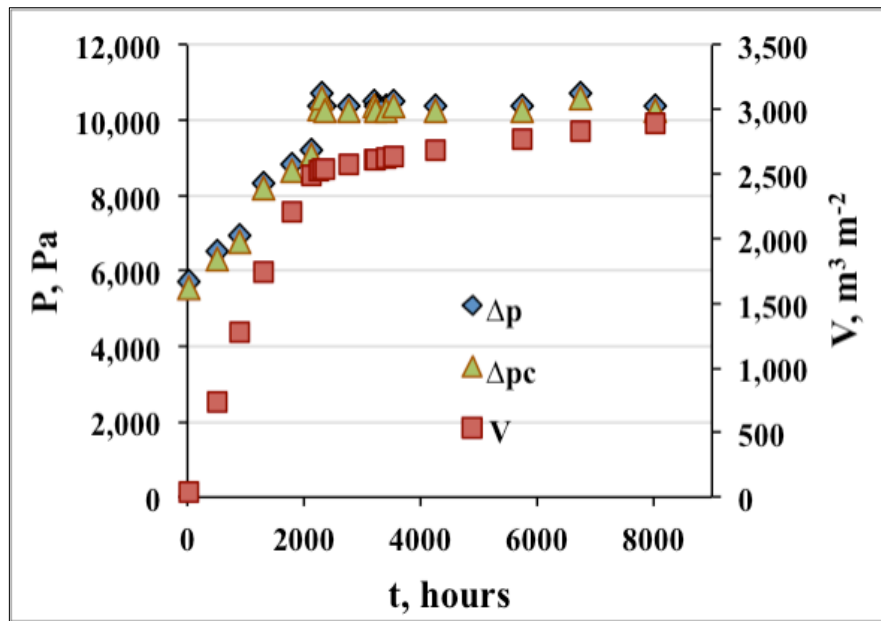


Figure 4.14. Pressure difference (Δp , Pa) of filtration, cake resistance (Δp_c , Pa) on cloth and cumulative filtration volume (V , $\text{m}^3 \text{m}^{-2}$) vs. time (hours). Experimental data of the CFBR at $p_o = 20 \text{ kPa}$.

The transition point of the deviation from linearity (t/V vs. V) was considered as the end of pore constriction and the occurrence of sufficient cake growth on the cloth filter, consequently the beginning of real cake filtration period. Hence, first run and second run were evaluated as the initial and latter filtration period respectively. Figure 4.15 shows plots of experimental data obtained from the operation of the CFBR unit, for complete blocking (a), intermediate blocking (b), and standard blocking (c) at the initial filtration period; Figure 4.15 (d) shows a plot of filtrate volume (V) versus filtration time/filtrate volume (t/V) for the cake filtration model at the latter filtration period. The filtration behaviours were compatible with that of the lab-scale unit. Standard blocking model plots of CFBR, which suggests pore constriction of medium, were fitted better ($R^2 > 0.95$) than complete blocking and intermediate blocking models with the measured data for the initial period of filtration; the latter period of filtration was best fitted to the cake filtration model ($R^2 > 0.99$).

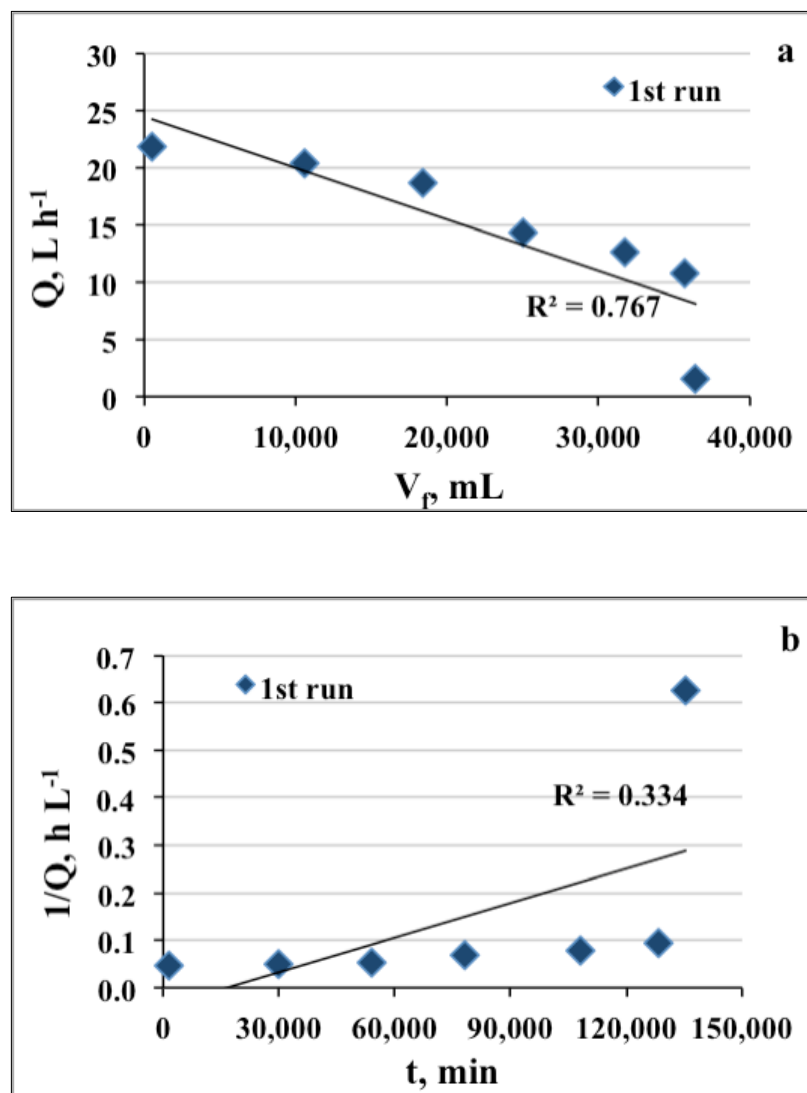


Figure 4.15. Flux decline rate for CFBR: (a) complete blocking model, (b) intermediate blocking model

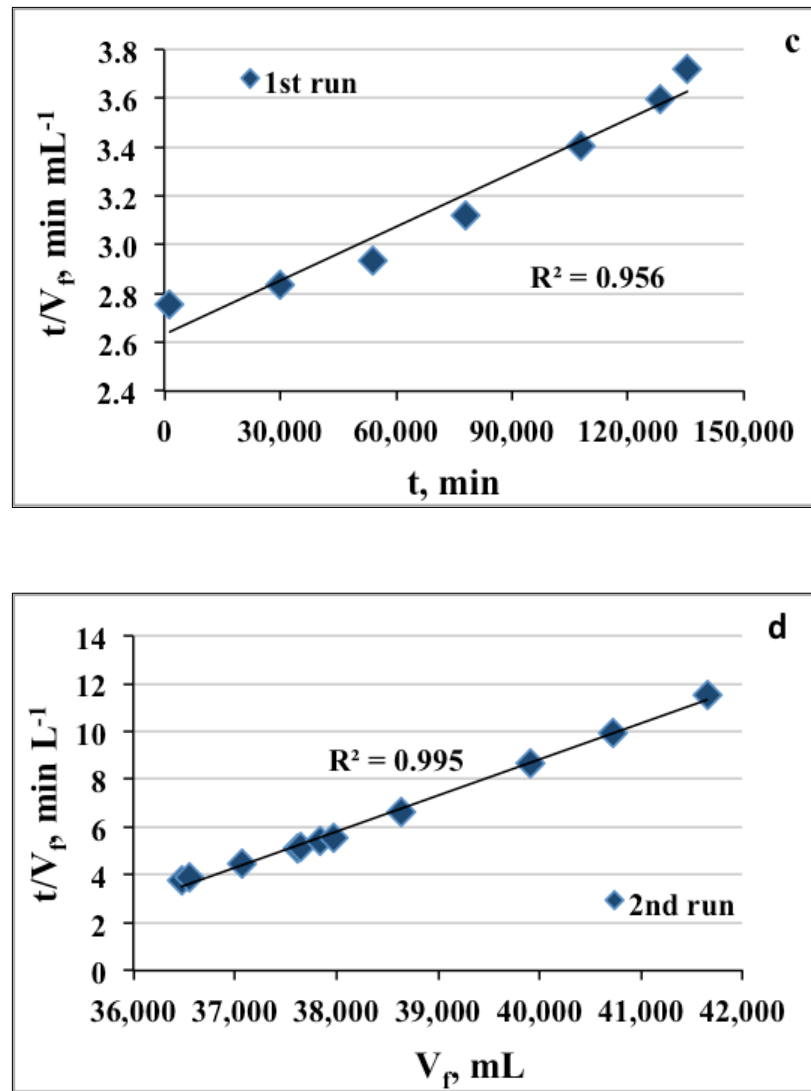


Figure 4.15 (continued) (c) standard blocking model, (d) cake filtration.

5. SLUDGE PRODUCTION AND DEGRADATION AT HIGH BIOMASS SYSTEMS WITH COMPLETE SLUDGE RETENTION

5.1. Introduction

The inclusion of a membrane for solid-liquid separation in activated sludge provides a significant increase of MLSS concentration in the bioreactor and lowers the sludge production. Hence, MBR systems can be run at very high sludge ages (SRT). However, the application of high MLSS concentrations in membrane bioreactors (MBRs) has been usually limited by problems of membrane fouling during filtration of the activated sludge, which decreases the sustainable filtration flux.

Total suspended solid (TSS) concentration and excess sludge production are clearly of great importance in wastewater treatment plants (WWTPs) [100]. The purpose of sludge disposal is to remove inert and excess biological solids in order to prevent accumulation of these solids within the system. Reducing sludge production will reduce required wastage rate that means less sludge disposal cost [57]. So, a realistic prediction of the concentration of active components like heterotrophic, autotrophic biomass and phosphorus accumulating organisms is crucial.

Cronje and coworkers [101] classified the mixed liquor organic (volatile) suspended solids in a bioreactor as: (a) ordinary heterotrophic organism active biomass, (b) endogenous residue and (c) inert material for non-nitrifying aerobic activated sludge systems; (d) autotrophic organism active biomass for nitrifying aerobic and anoxic/aerobic activated sludge systems; additionally, (e) phosphate accumulating organism active biomass and (f) this

organism group's endogenous residue if biological excess phosphorus removal (BEPR) is included. The inert fraction of the organic content of wastewater is very important because it indicates indirectly the biodegradable organic fraction that is available for microbial growth and electron acceptor utilization. The magnitude of particulate residual products generation has shown to be quite wastewater specific with significant difference for various organic carbon sources, which increases as the wastewater composition changes from simpler to more complex organic compounds [102]. However, some organic compounds that are conventionally considered as inert can become biodegradable at high SRT. Hence, the inert sludge concept in activated sludge may no longer be totally valid for MBR sludge. Some recent studies stated that significant biodegradation of the endogenous residue may occur in activated sludge systems operated at high SRTs. In these studies, extracellular polymeric substances (EPS) associated with the endogenous residue are potentially of great importance in explaining the biodegradability of this component [103].

MBR, as a high MLSS system, has drawn special attention in the research field of zero discharge of activated sludge [104]. The yield coefficients obtained in MBRs remained distinctly lower than those observed in conventional systems, which shows the behaviour of the biomass is quite different from conventional operating conditions. Bacteria can assimilate substrate entirely, which means there is a little tendency to synthesize new biomass. This suggests that the metabolization route tends to be directed toward catabolism [105]. High SRT increases the amount of energy spent on maintenance rather than on growth and also induce bacteria predation, lysis and storage product uptake, cryptic growth, which allows a conversion yield reduction from 0.3 to 0.041 [105]. This type of growth generally referred as lysis-cryptic growth. It is considered in two stages: lysis, the rate-limiting step for overall reduction of sludge production and biodegradation [106]. Dead cells cannot be degraded by bacteria and contribute to inert biomass. However, higher organisms such as protozoa, metazoa and nematodes can utilize both dead cells and living bacteria. However, cell lysis will release cell contents into the medium, thus providing an autochthonous substrate, which contributes to the organic loading. The growth, which subsequently occurs on this substrate,

cannot be distinguished from growth on the original organic substrate and is therefore termed cryptic growth [57, 107]. Yet, at long SRTs the accumulation of dead or inactive microorganisms occurs in a bioreactor, and affects the sludge composition and activity. In accordance with the microscopic investigations of biomass viability, the decrease in fraction of active biomass (ammonia oxidizers, nitrite oxidizers and heterotrophs) was predicted to be 33 % to 14 % when SRT increased from 30 to 100 days [108].

The purpose of the study in this chapter was to investigate the sludge production pattern and its effect on the fate of nitrifiers, and treatment efficiency in a pilot scale biomass filtration system with complete solids retention. Also, to state the process can reach to equilibrium sludge production conditions without any deterioration of filtration process, hence no accumulation of inert material occurs at prolonged sludge ages.

5.2. Materials and Methods

5.2.1. Control Parameters

The pilot plant (Chapter 3) was operated for over two years, generally with some weekly sludge wastage and the sludge age kept around 50 days. However, the results of a particular period (approximately 6 months) were presented here. The period comprises a complete sludge retention time without any sludge wastage and the system was evaluated in terms of both production and degradation of inert sludge and biomass in the tanks. The parameters monitored throughout the experiments of complete sludge retention were (Chapter 4): pH, salinity, COD, TKN, $\text{NH}_4^+\text{-N}$, $\text{NO}_3^-\text{-N}$, SS, VSS, MLSS, MLVSS, filterability, total coliform, and faecal coliform.

5.2.2. Determination of the Sludge Production

During the determination of the sludge production (for about 6 months), biological process was operated by maintaining a constant volumetric loading rate (VLR), which is the amount of daily COD feed per litre of reactor volume. Wastewater strength varied on hourly or daily basis, because the reactor was located on site and fed continuously by incoming wastewater to the full-scale plant. In order to keep a constant VLR, influent wastewater pumping rate varied between $2.5 - 1.7 \text{ m}^3 \text{ h}^{-1}$, which corresponded to an average flux between $0.25 - 0.17 \text{ m}^3 \text{ m}^{-2} \text{ d}^{-1}$ in the membrane permeate and $0.96 - 1.2 \text{ m}^3 \text{ m}^{-2} \text{ d}^{-1}$ cloth filter permeate. Thus, the trans-membrane pressure kept constant around $180 - 200 \text{ mbar}$, which was a predetermined range, during one year of operation, to prevent any temporary or permanent sludge accumulation on the membranes (in the filtration tank), which would effect the bulk biomass concentration or lead to a membrane cleaning. However, in the CFBR experiments, the period began after sufficient amount of cake formed on the cloth filter and operated for 240 days with stable trans-cake pressure of $101 - 104 \text{ mbar}$ (Chapter 4).

Before start up of this period the reactor was emptied, cleaned and refilled with half diluted sludge ($\sim 2,500 \text{ mg}_{\text{MLSS}} \text{ L}^{-1}$) taken from the full-scale plant. Throughout this experimental period, no sludge was intentionally removed except for the sludge samples taken daily for analyses. The amount of sludge samples was negligible (approximately 250 mL) compared to 56 m^3 of reactor volume. So, along with the thin layer of biomass stuck to the reactor, the amount of samples was omitted in sludge yield calculations that was obtained by dividing the amount of sludge accumulated weekly in the bioreactor (anoxic and fine bubble aeration tanks) by the cumulative COD removed in the same period. The parameters used in the mass balance equations for the pilot study are shown in Figure 5.1. At the end of the experimental period, the pilot unit was emptied and checked for any sludge accumulation at the bottom of the tanks and within the membrane cartridges. No sludge accumulation was observed except for the above mentioned thin layer of biomass attached to the walls.

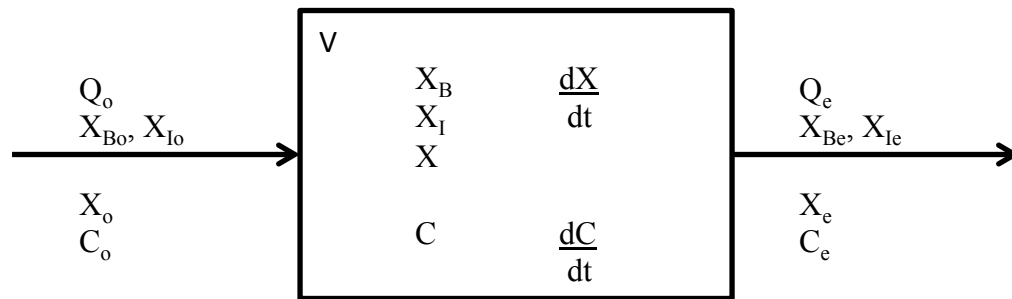


Figure 5.1. Mass balance diagram.

Q : Flowrate, $\text{m}^3 \text{d}^{-1}$

X : Sludge concentration, kg m^{-3}

C : Substrate concentration, $\text{kg}_{\text{COD}} \text{m}^{-3}$

Indices;

B : Biomass, I : Inert sludge, o : Influent, e : Effluent

V : Bioreactor volume, m^3

t : Time, d

Because no sludge removed from the bioreactor, flowrate of the system is;

$$Q = Q_o = Q_e$$

Total particulates within the system;

$$X_o = X_{Bo} + X_{Io} ; \quad X_e = X_{Be} + X_{Ie} ; \quad X = X_B + X_I$$

Performing mass balance on sludge gives:

$$V \frac{dX}{dt} = QX_0 + VR_g - QX_e \quad (5.1)$$

$$\frac{V}{Q} = HRT \quad (5.2)$$

R_g : Biomass growth rate, $\text{kg}_{\text{VSS}} \text{m}^{-3} \text{d}^{-1}$

HRT : Hydraulic retention time, d

Equation (5.1) can be written as;

$$\frac{dX}{dt} = \frac{1}{HRT} (X_0 - X_e) + R_g \quad (5.3)$$

Performing mass balance on substrate gives:

$$V \frac{dC}{dt} = QC_0 + VR_s - QC_e \quad (5.4)$$

R_s : Substrate utilisation rate, $\text{kg}_{\text{COD}} \text{m}^{-3} \text{d}^{-1}$

Equation (5.4) can be written as;

$$\frac{dC}{dt} = \frac{1}{HRT} (C_0 - C_e) + R_s \quad (5.5)$$

After COD removal reached to a steady state;

$$\frac{dC}{dt} = 0 \quad (5.6)$$

The relationship between sludge yield and growth rate can be expressed as;

$$1 / Y_{obs,B} = 1 / Y_{max} + b / (Y_{max}\mu) \quad (5.7)$$

Y_{max} : Real sludge yield, $\text{kg}_{\text{MLVSS}} \text{kg}_{\text{COD}}^{-1}$

b : Decay rate, d^{-1}

μ : Specific growth rate, d^{-1}

Assuming $Y_{obs,B}$ represents the observed yield coefficient of biomass ($\text{kg}_{\text{MLVSS}} \text{kg}_{\text{COD}}^{-1}$) including endogenous respiration, the relation between R_s and R_g can be written as;

$$R_g = - Y_{obs,B} \cdot R_s \quad (5.8)$$

$$\mu = R_g / X_B \quad (5.9)$$

Rearranging equations (5.5) to (5.8) gives;

$$R_g = Y_{obs,B} \frac{1}{HRT} (C_0 - C_e) \quad (5.10)$$

Substituting Equation (5.10) into Equation (5.3) and rearranging the formula;

$$\frac{dX}{dt} = \frac{1}{HRT} [(X_0 - X_e) + Y_{obs,B} (C_0 - C_e)] \quad (5.11)$$

Solving Equation (5.11) yields;

$$X_{t_2} - X_{t_1} = \frac{1}{HRT} [(X_0 - X_e) + Y_{obs,B} (C_0 - C_e)] (t_2 - t_1) \quad (5.12)$$

$t_2 - t_1 = \Delta t$, equals to 1 day in our study and assuming that X_e is negligible, Equation (5.12) gives $Y_{obs,B}$ as;

$$Y_{obs,B} = \frac{(X_{t_2} - X_{t_1})}{(C_0 - C_e)} HRT - \frac{X_0}{(C_0 - C_e)} \quad (5.13)$$

The term $(X_{t_2} - X_{t_1})$ shows the daily yield in MLSS concentration, so if Equation (5.13) is rearranged to give the daily yield in MLSS per removed COD;

$$Y_{obs,B} + \frac{X_0}{(C_0 - C_e)} = \frac{(X_{t_2} - X_{t_1})}{(C_0 - C_e)} HRT \quad (5.14)$$

The left hand side of Equation (5.14) represents an overall sludge yield, Y_{obs} ($\text{kg}_{\text{MLSS}} \text{kg}_{\text{COD}}^{-1}$) that observed during the study:

$$Y_{obs} = \frac{(X_{t_2} - X_{t_1})}{(C_0 - C_e)} HRT \quad (5.15)$$

5.3. Results and Discussion

5.3.1. Evaluation of Sludge Production in the Bioreactor

The study presented here was performed during the third run, when the operating conditions were quite stable. The end of third run was the maintenance and check up period. Filtration (first run) began at around 12 kPa TMP and increased gradually from $6 \text{ L h}^{-1} \text{ m}^{-2}$ to the target flux; the increase of flux retarded because of trans-membrane pressure peaks,

however, the flux could be controlled to adjust for desired values. The second run began at 18 kPa TMP, and TMP reached a predetermined limit value (25 kPa) earlier. Third run began again at around 14 kPa TMP and variations of TMP were lower. Flux was sustainable around $7 - 10 \text{ L h}^{-1} \text{ m}^{-2}$ almost the whole run as a consequence of relaxing the membranes in three shifts instead of once per day.

Sludge yield in the pilot system was determined without excess sludge withdrawal for 305 days till the biomass concentration reached from $2,360 \text{ mg L}^{-1}$ to $23,000 \text{ mg L}^{-1}$ under constant volumetric loading rate ($\text{VLR} = 0.63 \text{ kg}_{\text{COD}} \text{ m}^{-3} \text{ d}^{-1}$). The stability of the MBR flux and the trans-membrane pressure (180 – 200 mbar) could be maintained until $23,000 \text{ mg L}^{-1}$ of MLSS and beyond this value, TMP jump (over 200 mbar) was observed. So, the membranes were chemically backwashed with 900 L of 0.5 % NaClO solution when the MLSS concentration increased to $23,000 \text{ mg L}^{-1}$. On the other hand, once sufficient amount of cake formed on the cloth filter the stability of the cloth filter flux did not related to MLSS concentration. Although the MBR system was operated successfully when the MLSS concentration was $23,000 \text{ mg L}^{-1}$, the results about excess sludge production rate (observed yield coefficient) presented below are between $2,360 \text{ mg L}^{-1}$ and $15,455 \text{ mg L}^{-1}$ (at approximately $22 \text{ }^{\circ}\text{C}$ of wastewater temperature in the tanks), because no significant change was observed in terms of sludge production rate and operation cost after $15,455 \text{ mg L}^{-1}$.

One advantage of the plant is the low sludge production, as it has been stated in the literature. During the operation of the pilot plant in this period of six months, totally 1,260 kg of dry solids were produced (approximately $5,000 \text{ m}^3$ at 25% dry solids (DS) dewatered sludge). In other words, nearly 1.3 tonnes of MLSS was produced from the treatment of $16,250 \text{ m}^3$ of domestic wastewater. Throughout the same period, $24,378,620 \text{ m}^3$ of wastewater was treated in the full-scale plant; 19,895 tonnes of 25% DS sludge processed and 5,000 tonnes of 98% dry sludge was produced. In course of the treatment of same wastewater, 0.078

kg dry matter produced per 1 m³ of permeate in the pilot plant and 0.204 kg dry matter produced per 1 m³ of treated wastewater in the full-scale plant.

In comparison with a conventional biological nutrient removal plant, sludge production decreased by 62 % in the pilot plant. The sludge production per COD removed in the full-scale plant was about 0.65 kg_{SS} kg_{COD}⁻¹ and the MLSS concentration in the tanks was kept around 5,000 mg L⁻¹. The sludge yield per removed COD load in the pilot plant tanks with no sludge withdrawal was analysed and calculated daily (Figure 5.2). The initial (21 days) average sludge yield (MLSS between 2,500 and 5,000 mg L⁻¹) was 0.72 kg_{MLSS} kg_{COD}⁻¹. However, the major decline in the sludge yield was observed until the sludge concentration reaches 7,000 mg L⁻¹ (after 62 days) and the average yield was about 0.25 kg_{MLSS} kg_{COD}⁻¹ when the MLSS concentration was nearly 15,000 mg L⁻¹ (after 140 days). Similar low sludge production values – about 0.25 kg_{SS} kg_{COD}⁻¹ for long sludge residence times – were given in the literature [109, 110, 111]. The theoretical sludge yield coefficient, Y_{\max} and the decay rate, b were calculated by the linear plot of the reciprocals of $Y_{\text{obs,B}}$ and μ that were obtained from Equation (5.8) and (5.9). Y_{\max} and b were calculated as 0.386 kg_{MLVSS}/kg_{COD} and 0.037 d⁻¹ from the intercept and slope of Figure 5.3. respectively. The biomass yield was closer to the higher values given in literature (Table 5.1). The reason for this was considered as higher COD strength of the domestic wastewater including 89 % biodegradable COD.

In order to express the behaviour of sludge in the tank, the whole sludge retention period was shown in 3 parts: a, b and c. The parts ‘a’ (45 days) and ‘b’ (60 days) represents the first 105 days, when the sludge concentration kept increasing in the tank. In part ‘b’ sludge accumulation is considered to be dominated by inert material. The part ‘c’ represents the stabilisation period. Figure 5.4 shows the sludge concentration (mg_{MLSS} L⁻¹ and mg_{MLVSS} L⁻¹) in the bioreactor under constant VLR, which was kept around 0.63 kg_{COD} m⁻³ d⁻¹. The rate of sludge accumulation was higher in the first 105 days of operation (parts ‘a’ and ‘b’) and inert sludge accumulation rate was approximately 2 times higher than biomass

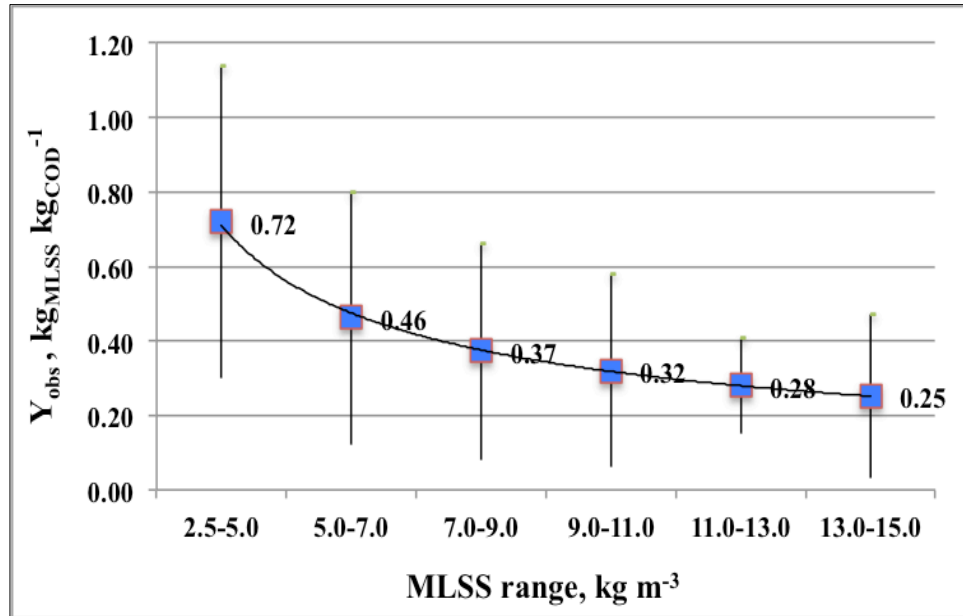


Figure 5.2. Observed sludge yield coefficient (Y_{obs} , $\text{kg}_{\text{MLSS}} \text{kg}_{\text{COD}}^{-1}$) with increasing MLSS concentration in the pilot plant.

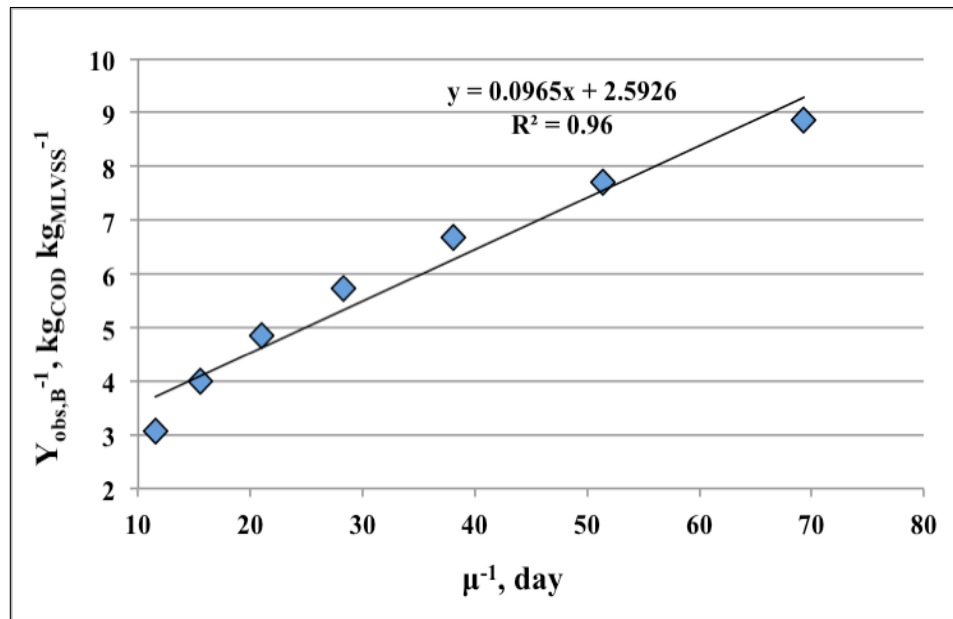


Figure 5.3. The correlation of $Y_{obs,B}^{-1}$ vs. μ^{-1} .

Table 5.1. Some sludge yield (Y_{\max}) and decay rate (b) values given in literature.

	Y_{\max} , kg _{MLVSS} kg _{COD} ⁻¹	b, d ⁻¹	Wastewater source
Huang and coworkers [112]	0.37 – 0.28	0.32 – 0.05	Domestic
Liu and coworkers [113]	0.288	0.023	Synthetic
Sun and coworkers [104]	0.115	0.024	Industrial

accumulation rate. In the latter period (part 'c'), the difference between the two rates was almost 3 % and both MLSS and MLVSS growth showed the similar rate of increase. The net growth in this period slowly declined resulting in stabilisation of average MLSS concentration. Laera and coworkers [114] showed similar behaviour of sludge accumulation with negligible sludge withdrawal. Sun and coworkers [104] stated that, the incoming suspended solids and the inert matter were not accumulated in the bioreactor, possibly due to hydrolysis or enzymatic solubilization producing compounds having molecular size compatible with permeation; thus no sludge accumulation was observed in the longer term. However, different from our results, the MLVSS/MLSS ratio was maintained during the operation at prolonged SRT; in our study the ratio was maintained in the latter period (part 'c'). Figure 5.5 shows that the cumulative influent inert solids load to the bioreactor increased linearly as it was intended to keep constant influent load. Thus, in the first 105 days, the inert sludge amount (kg) retained in the bioreactor, which was determined as the difference between the MLSS and MLVSS in the sludge, increased at a lower rate than cumulative inert material in the feed wastewater. In part 'a' the ratio between these two rates was about 37 %, however, in part 'b' the ratio increased to 61 %. Then in part 'c' the amount of inert material remained constant around 300 kg in the 56 m³ reactor.

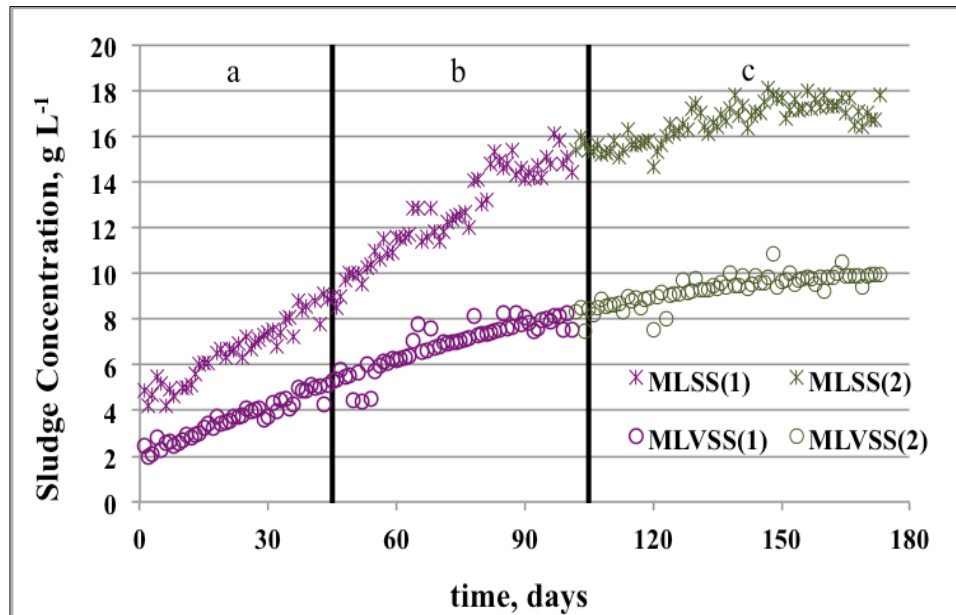


Figure 5.4. Sludge yield in the bioreactor. MLSS (1) and MLVSS (1): MLSS and MLVSS yield in the first 90 days; MLSS (2) and MLVSS (2): MLSS and MLVSS yield in the latter period.

Inerts found in activated sludge systems can be due to inerts in the influent and can also be the result of protozoan activity, which may not degrade the bacterial cell walls fully and leaving behind inert material or can be a result of the two possibilities. The microbial endogenous processes play a significant role in design and operation of activated sludge systems. The energy for growth and maintenance of the microorganisms is obtained from the biochemical oxidation of substrate, so substrate deficient conditions results with endogenous respiration, which can lead to a significant reduction in the overall sludge yield and increase in electron acceptor utilization [115]. Besides endogenous respiration, the decreased biomass yield is typically attributed to concepts like maintenance, death-regeneration, or decay-cryptic growth. The decay mechanism is considered as internal decay, which does not reduce the number of microorganisms but reduces the weight and activity of the biomass due to lack of substrate, and external decay, which is caused by mechanisms like predation and cell lysis leads to significant losses both in number of microorganisms, their mass and activity. Liang

and coworkers [116] showed the example of *Aeolosoma hemprichi* growth, which predated on sludge flocs, resulted by 39 to 65 % sludge reduction without any deterioration of heterotrophic and autotrophic activity. However, the concepts like maintenance, death-regeneration, or decay-cryptic growth cannot easily be distinguished from each other except for the introduction of a fraction of inert material formation during death/lysis in the death-regeneration concept. Basically the different approaches try to link the observed biomass yield ($Y_{obs,B}$) to a maximal growth yield (Y_{max}) and solid retention time (SRT or θ_x) through coefficients for maintenance (m_s), endogenous respiration (k_e), or decay (b) and inert COD formed (f_i) [117].

Maintenance concept:

$$Y_{obs} = Y_{max} \frac{1}{1 + \theta_x m_s Y_{max}} \quad [5.16]$$

Endogenous respiration concept:

$$Y_{obs} = Y_{max} \frac{1}{1 + \theta_x k_e} \quad [5.17]$$

Death - regeneration concept:

$$Y_{obs} = Y_{max} \frac{1}{1 + \theta_x b \left(1 - (1 - f_i) Y_{max} \right)} \quad [5.18]$$

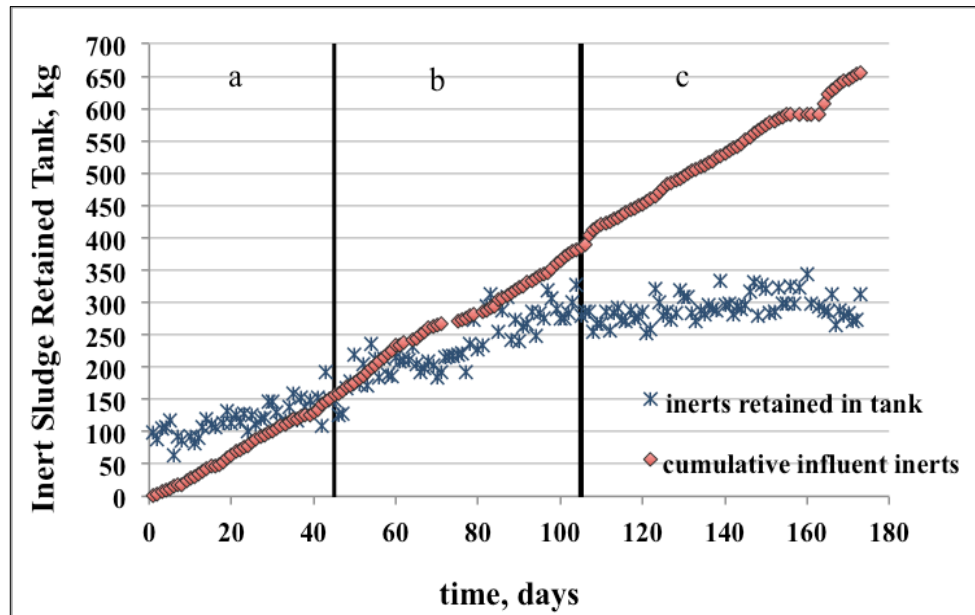


Figure 5.5. Cumulative inorganic material load to the bioreactor and the amount of inorganic sludge accumulated in the bioreactor.

On the other hand, some researchers indicated that most bacteria probably do not die; instead they become dormant when being exposed to starvation conditions [118, 119, 120]. It has been shown that a specific growth hormone like compound, which is made by a fraction of metabolically active cells in a suspension, can readily bring the so-called dead bacteria back to activity. However, in literature, endogenous respiration term usually includes decay, lysis, maintenance, and predation of heterotrophic biomass that results in generation of endogenous residue. Thus, activated sludge suspension is considered as a combination of volatile suspended solids (MLVSS), which is mainly composed of three particulate portions: the active biomass (heterotrophic X_H and autotrophic X_A), the influent non biodegradable organic portion ($X_{I,O}$), the endogenous residue produced from the biomass (X_E) and inorganic suspended solids (X_I) coming from the influent. Thus, the origins, composition and characteristics of X_I (hair, fibre and cellulose) differ greatly from X_E , which is generated as a result of the endogenous respiration of microorganisms in the activated sludge. Recent studies have identified the slow biodegradation of X_E in systems operated at long SRTs [103, 114,

121, 122]; so, the accumulation of inerts inversely depends on the system's SRT, and that they can be degraded by slow growing bacteria, which means that inerts are not ultimately inert [117].

Our results were compatible with the general concept stated above. The graph of cumulative influent inert solids shows the potential accumulation pattern of the wastewater originated inert material that was greater than the rate of real inert material accumulation in the tank at all times. This comparison stated that microorganisms in the pilot tank degraded some portion of inert material. However, the increased rate of inert sludge retention (part 'b') might be as a result of endogenous residue accumulation in the tank. Thus, the general trend of the MLVSS/MLSS ratio and the decrease in the ratio for this particular period expresses the inert sludge retention pattern clearly. The stabilisation of MLVSS and the specific activities in the latter period meant that both portions of inert material could be degraded and no accumulation of 'inert' material occurred in the longer term. Moreover, the organic loading rate (OLR) reached constant values in the latter period (Figure 5.6), which also means that the system reached equilibrium conditions. The removed inert material amount, which is the difference between the incoming inert material and retained inert material in the tank during the process, was given in Figure 5.7. The amount of removal increased steadily in parts 'a' and 'c', however, partially decreased or ceased in part 'b', which shows that more inert material accumulated after 45 days of complete sludge retention.

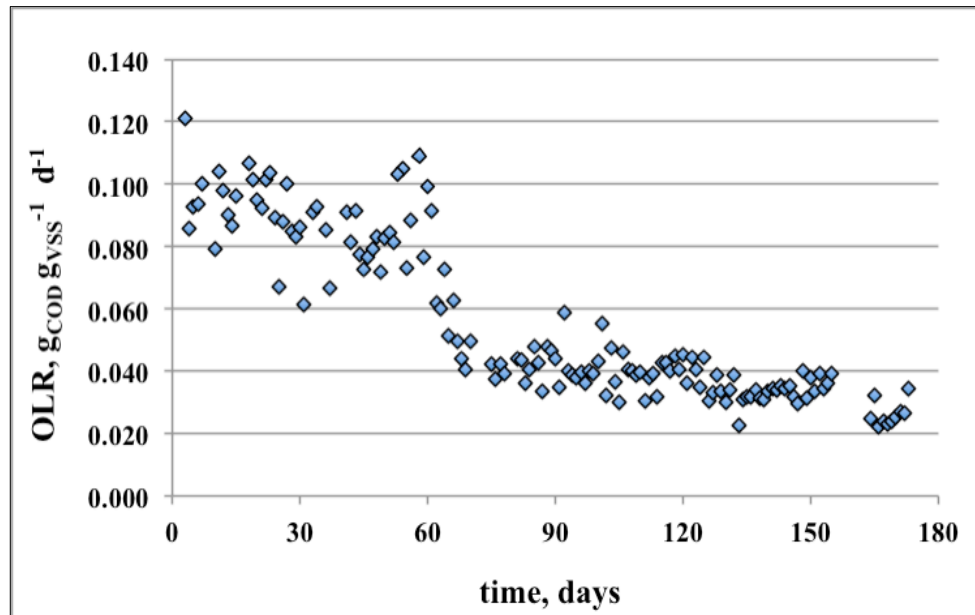


Figure 5.6. Organic loading rate to the reactor.

The mixed liquor volatile suspended solids ratio (MLVSS/MLSS) was 0.50 at the beginning of the study. After one month of complete solids retention (part 'a'), the ratio increased to 0.60 indicating that MLVSS increased faster than inert material, then decreased back to 0.50 indicating higher inert solids production in following 2 months (part 'b'). Finally, the ratio increased again and stabilised around 0.57 during the latter period of 3.5 months (part 'c'). The inerts are found in many activated sludge systems in considerable amounts, as a result of inert material in the influent. The incoming wastewater was screened in two steps (50 mm and 10 mm respectively) and after grit/sand removal, the wastewater was pumped to the pilot tank to be screened through a 3 mm pore sized drum screen in order to prevent inert material entrance to the pilot tank. Because most inerts were eliminated constantly before entering the bioreactor, the change in MLVSS/MLSS ratio was considered to be due to endogenous microbial activity. Constancy of the MLVSS/MLSS ratio together with zero net growth and no discernible accumulation of inert material provide evidence for the absence of excess sludge production under sufficiently long sludge retention times [114, 123, 124].

5.3.2. Effect of Complete Sludge Retention on Nitrogen Converters

Endogenous processes also known to affect the microbial community of activated sludge systems, consequently the capacity, efficiency and stability of treatment systems. Slow growing nitrification bacteria needs longer SRTs than ordinary heterotrophs and their growth rate is used to determine the minimum required sludge retention time of a BNR system. But also, predation due to long SRT could result in overgrazing on nitrifying bacteria and could provoke deterioration of nitrification process [56]. The oxidation of ammonia to nitrite by autotrophic nitrifiers is a key process in the global cycling of nitrogen. The nitrification rate is controlled by the concentration of active autotrophic bacteria (X_A) stabilized in the process, which is imposed by the conversion yield (Y_A), the influent nitrifiable nitrogen, and the decay rate (b_A) [100]. Three groups of microorganisms are known to be responsible for ammonia oxidation: aerobic ammonia-oxidizing bacteria (AOB), aerobic ammonia-oxidizing archaea (AOA), anaerobic ammonium-oxidizing bacteria (Anammox). In the first step of aerobic conversion, oxidation of ammonia to hydroxylamine, is catalyzed by ammonia monooxygenase (AMO); the gene coding for a subunit of this enzyme is *amoA*.

The investigation of the activity and diversity of nitrogen converters in the pilot unit (see Chapter 6 for details) with complete sludge retention showed that gradually increased MLVSS and MLSS concentrations adversely affect the biomass fractions of aerobic ammonia oxidisers in the pilot tank, whereas fraction of nitrite oxidising population did not change significantly. However, complete sludge retention did not affect the Anammox bacteria to the same extent and they showed a more stable growth pattern. The ratio of aerobic and anaerobic ammonia oxidizing bacteria among all microorganisms represented by *amoA* AOB to 16S rRNA and Anammox to 16S rRNA ratios respectively (Figure 5.8). The *amoA* AOB enzyme peaked at day 22, increasing approximately 2.5 times of its initial value. Parallel to the decrease in MLVSS/MLSS ratio (part 'b') the enzyme was also decreased sharply and remained as 33 % of its peak value. Despite the increase in MLVSS concentration, the

detected amount of the enzyme decreased beyond one month of operation and after 92 days of complete solids retention, reached to its minimum equilibrium value, which was almost half of its initial amount in the seed sludge. However, the amount of inert suspended solids increased inversely proportional to the amoA AOB enzyme and came to its maximum value after 3 months of operation. The further degradation of inert solids and stabilisation of MLVSS in the reactor (part 'c') did not affect the amoA AOB enzyme.

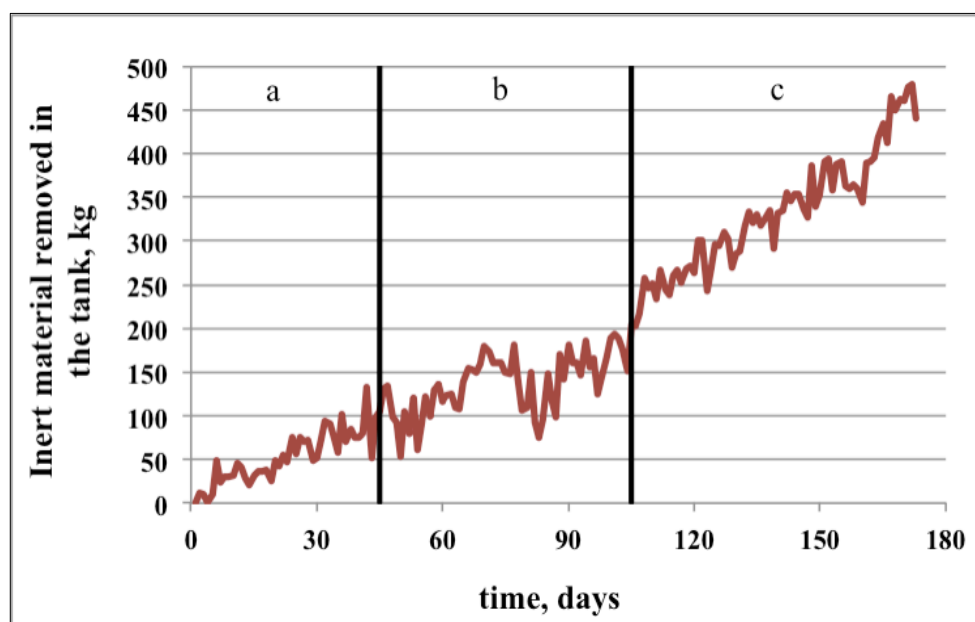


Figure 5.7. Inert material removal in the pilot unit.

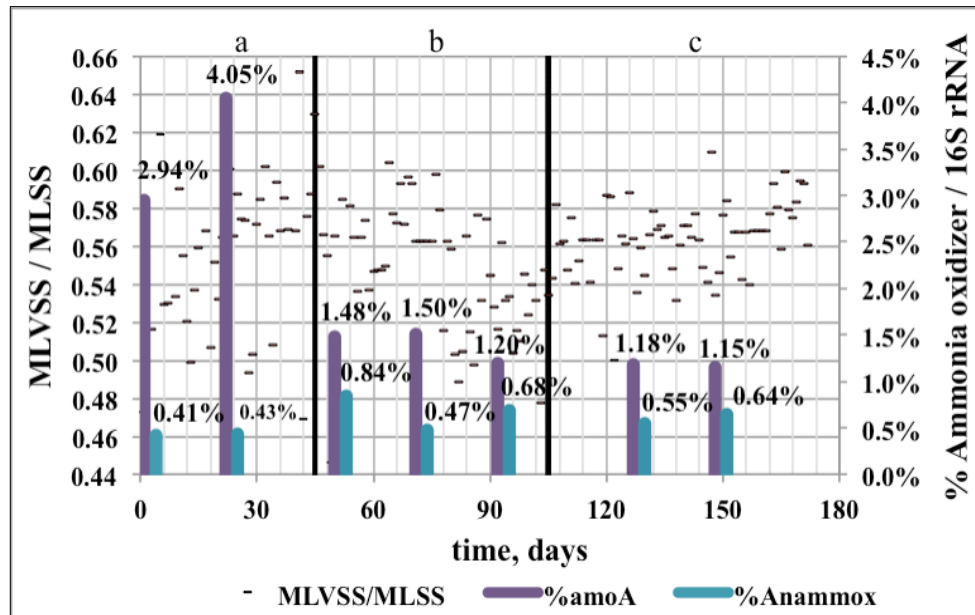


Figure 5.8. Variations of MLVSS/MLSS ratio and the AmoA enzyme (copy numbers/mL extracted MLVSS).

On the other hand, Anammox bacteria did not show the same decreasing pattern. Conversely to the aerobic ammonium oxidizers, Anammox bacteria doubled consecutively at day 22 and day 50 and ended up 36 % higher than its initial amount (Figure 5.8). Anammox bacteria have low growth rates with doubling times about 11 days in both laboratory and full-scale wastewater treatment systems [125]. They have also been stated as strictly anaerobes [126]. However, coexistence of aerobic ammonium oxidizers, nitrite oxidizers and Anammox bacteria has shown by many researchers [127, 128, 129]. At an aerobic-anaerobic interface within a biofilm or a floc, competition can occur between anaerobic Anammox bacteria and aerobic ammonium- and nitrite-oxidizing bacteria; aerobic nitrite (NO_2^-) oxidizers compete with aerobic ammonium oxidizers for oxygen, and Anammox bacteria compete with ammonium oxidizers and nitrite oxidizers for ammonium and nitrite, respectively [130, 131]. Anammox bacteria need both NH_4^+ and NO_2^- as electron donor and electron acceptor respectively, and bicarbonate (HCO_3^-) is the carbon source. Both NO_3^- reduction and aerobic NH_4^+ oxidation might provide NO_2^- to Anammox bacteria. Yet at

elevated concentrations of NH_4^+ , the reduction of NO_2^- to NO_3^- by nitrospira could be inhibited because of increasing free ammonia concentration that provides total nitrogen removal over NO_2^- [132]. Sliemers and coworkers [133] stated the cooperation between aerobic and anaerobic ammonium oxidizers. Zhang and coworkers [134] reported that partial nitrification followed by anammox process can carry out efficiently in a system. Our results confirmed that coexistence of these bacteria could continue under complete sludge retention in the bioreactor (32% non-aerated and 68% aerated zones). Thus, Anammox bacteria were not inhibited by oxic conditions or decreasing sludge production rate and showed rather stable growth pattern.

The amount of all microorganisms represented by 16S rRNA (gene copy numbers/mL extracted MLVSS) (Figure 5.9). The decrease in 16S rRNA correlated with decreasing MLVSS/MLSS ratio. Hence, in part 'b' the declining ratio of MLVSS/MLSS could be dominated by deceleration of growth rate and endogenous activity, rather than accumulation of inert material coming from the influent wastewater. On the whole, the significant decline of the amoA enzyme did not cause an important change in the nitrification efficiency. Thus, Anammox bacteria probably covered the decreased aerobic ammonia oxidation efficiency. The effluent $\text{NH}_4\text{-N}$ concentration was lower than 0.5 mg L^{-1} at all times (99% removal efficiency). However, the effluent concentration was 0.1 mg L^{-1} initially, which was then increased to an average of 0.4 mg L^{-1} and 0.3 mg L^{-1} in part 'b' and part 'c' respectively.

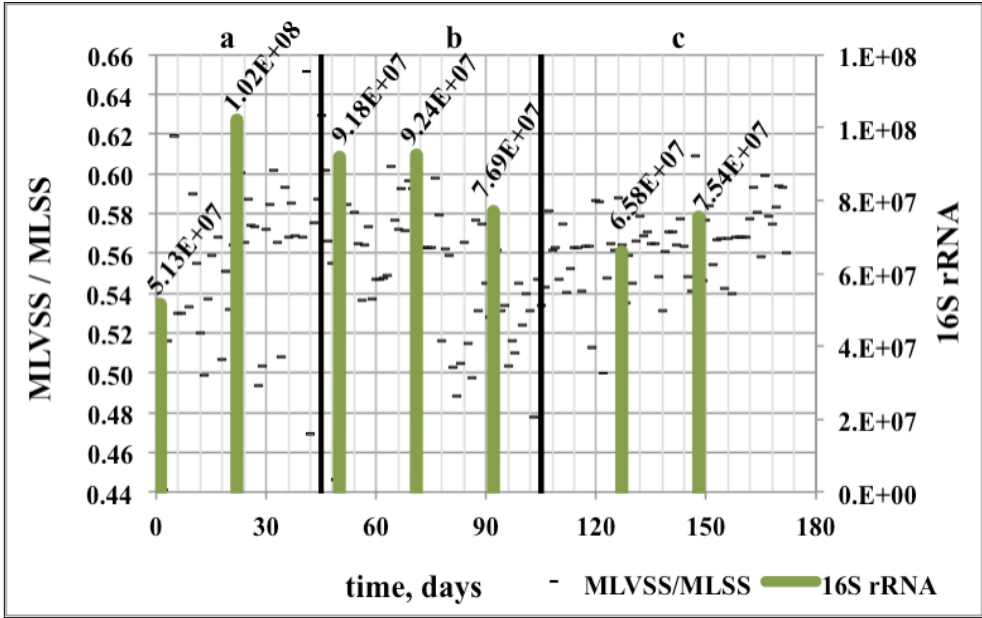


Figure 5.9. Variations of MLVSS/MLSS ratio and 16S rRNA (gene copy numbers/mL extracted MLVSS).

6. INVESTIGATION OF NITROGEN CONVERTERS IN HIGH MLSS FILTRATION SYSTEMS

6.1. Introduction

In biological domestic wastewater treatment plants, growth rate of nitrifiers defines the WWTP design and operating strategies. The nitrogen removal is performed by nitrification - denitrification processes. Nitrification includes the aerobic oxidation of the reduced nitrogen, (i.e., ammonium, to nitrite and nitrate). It is the key process in nitrogen removal and is carried out by two different groups of microorganisms: chemolithoautotrophic ammonia-oxidizing bacteria (AOB) and nitrite oxidizing bacteria (NOB). The key enzyme for AOB is ammonia monooxygenase. The gene coding for a subunit of this enzyme is *amoA*, which has been shown to be a good molecular marker and can serve as a useful target for environmental studies because it reflects the phylogeny of AOB very well [135]. Recently, new players, such as ammonia oxidizing archaea (AOA) and Anammox bacteria have been discovered as a promising alternative to conventional nitrification / denitrification process and these players were suggested to play a significant but previously unrecognized role in the global nitrogen cycle [126, 136, 137]. Activated sludge system is a consortium of variable and mixed-culture microorganisms in an aerobic environment in which different species cooperate or compete with each other. The carbon degrading heterotrophs and nitrifiers are the most dominant microorganisms present in activated sludge simultaneously. Grady and Lim [138] reported that heterotrophic bacteria have maximum growth rates of 5 times and yields of 2 to 3 times of that of autotrophic nitrifying bacteria. The ratio of AOB in all bacterial population should therefore be low in a typical domestic wastewater.

The fraction of nitrifiers in all bacterial culture can be best determined by the help of molecular microbiological tools like real-time PCR technology, which allows quantitative determination of *amoA* and 16SrRNA gene copies [139]. Some researchers indicate that C/N ratio is an important parameter in determining the *amoA*/16S rRNA ratio [140, 141]. The fraction of nitrifiers in a whole bacterial community is expected to increase with decreasing C/N ratio. Sludge age might be playing a role in the relative amount of nitrifiers in a system due to its control on the biomass concentration. However, the positive effect of high sludge age on nitrification rate is still controversial. In literature, there are several studies on the effect of sludge retention time on nitrification efficiency [112, 142 – 145]. Several researchers had also reported that MBR operating at a long SRT could achieve high nitrification efficiency [144, 145]. However, the role of sludge retention time or high VSS concentrations on nitrogen converting microorganism and their fractions has not been extensively investigated using molecular methods. Therefore, the aim of this research is to investigate and monitor the activity and diversity of nitrogen converters, ammonia-oxidizing bacteria (AOB) and nitrite-oxidizing bacteria (NOB), ammonia oxidizing archaea (AOA) and Anammox bacteria in a pilot scale membrane bioreactor (MBR) by using a quantitative real-time PCR method with complete sludge retention.

6.2. Materials and Methods

6.2.1. Sampling from the Pilot Bioreactor

For the identification of the microbial communities, sludge samples were taken with specified periods (days 1, 22, 50, 71, 92, 127, 148) from the oxic zone of pilot tank (Figure 6.1). Sludge samples were concentrated by gravity settling prior to molecular analyses. The samples were processed within 24 hours after their collection and stored in a freezer at $-20\text{ }^{\circ}\text{C}$ after DNA isolation.

6.2.2. DNA Extraction and PCR Amplification

Nucleic acid extraction was performed using the FastDNA SPIN kit (Q-BIOgene) according to the manufacturer's instructions [146]. Quantification of the extracted DNA was performed using Quant-iTTMPicoGreen dsDNA Reagent Kit (Molecular Probes) according to the manufacturer's protocol with a few modifications. Stock PicoGreen dye was diluted to 1/80 instead of 1/200 in 1x TE buffer and 10 μ L of the diluted PicoGreen dye was mixed with 10 μ L of the extracted DNA within the LightCycler glass capillaries. Fluorescence was measured on the LightCycler Instrument (Roche, Mannheim, Germany). For calibration, a serial dilution of lambda DNA standard ranging from 50 to 2000 ng mL⁻¹ was prepared with TE buffer. Each sample was quantitated in triplicate. The template DNA was diluted 10-fold to prevent PCR inhibition.

The PCR amplification was done using a Progene thermocycler (Techne, Cambridge, UK) with the following temperature cycle: denaturation at 95 °C for 5 min, followed by 30 cycles of denaturation at 95 °C for 60 s, annealing at 52 °C for 90 s, elongation at 72 °C for 90 s and post-elongation at 72 °C for 10 min. The reactions were subsequently cooled to 4 °C. PCR products were examined on ethidium bromide-stained agarose gels and were used for cloning analysis. All PCR amplifications were carried out in a total volume of 50 μ L in 500 μ L microtubes that contained 0.5 μ M of each primer, 1.5 U of Taq DNA polymerase (MBI Fermentas), 1 x PCR buffer, 1.5 mM MgCl₂, and 1.25 mM of dNTP and 2 μ L of 10-fold diluted template DNA.

6.2.3. Real-time PCR

Quantitative real-time PCR reactions were carried out using the LightCycler Instrument (Roche, Mannheim, Germany) with the FastStart DNA Master SYBR Green I kit (Roche) following the manufacturer's protocol. After an initial polymerase activation and denaturation step at 95 °C for 10 min, the cycling program was followed by 40

amplification cycles, each comprising denaturation (95 °C for 10 s), annealing (57 °C for 10 s), and extension (72 °C for 45 s). The temperature transition rates were programmed at 20°C s⁻¹. The PCR reaction mixture (20µL) contained 2µL, 10x Mastermix (Roche); 2 µL, 25 mM MgCl₂; 1.25 µM concentrations of forward and reverse primers (Table 6.1), PCR-grade nuclease-free distilled water and 2 µL, 10-fold diluted template DNA.

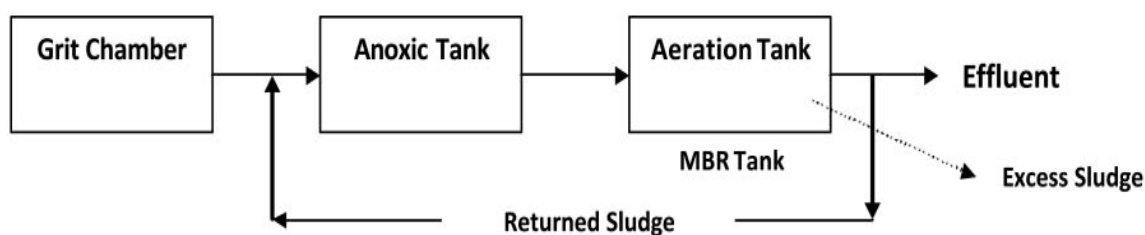


Figure 6.1. A simple box-flow diagram of the pilot unit.

To increase the specificity at the lower annealing temperature, KCl was added to real-time PCR mixtures instead of MgCl₂ with a final concentration of 18 mM, targeting the 16S rRNA gene of *Nitrobacter* [139]. In all applications, negative controls without template DNA were subjected to the same procedure to detect any contamination. Evaluation of real-time PCR data was performed using the LightCycler data analysis software (version 4.0). To verify nonspecific amplification, the reaction products were performed by DNA melting curve analysis, with a temperature transition rate of 0.1 °C s⁻¹ from 65 °C to 95 °C with a continuous monitoring of fluorescence. An external DNA standard curve was constructed using serial dilutions of a known copy number of target genes. The standard curves were obtained using PCR fragments that were excised from a 0.8% agarose gel, purified using a MinElute Gel Extraction Kit (Qiagen) and quantified with the Quant-iT™ PicoGreen dsDNA Reagent Kit [147]. The R² values were always greater than 0.99 for all of the standard curves.

6.2.4. Cloning and Sequencing Analysis

The PCR products of *amoA* and 16S rRNA *Nitrobacter* genes were purified from the gel using QIAquick PCR purification kit (Qiagen). The pDrive vector (Qiagen) was used for cloning. Then, the ligation products were transformed into *EZ Competent Cells* following the manufacturer's guidelines (QIAGEN PCR Cloning^{plus} Kit). White colonies were picked up from each cloned sample. The fragments containing the target were then amplified using the plasmid-specific M13 primer set. Before DNA sequencing, the plasmids of selected transformants were purified using the Fermentas PCR purification kit. DNA sequences were analyzed in Iontek Laboratories (Istanbul, Turkey). Afterwards, a similarity search was performed in the GenBank database using the BLAST search program of the National Center for Biotechnology Information sequence search service [148]. Sequences were analysed using ChromasPro software (Technelysium Pty Ltd., Eden Prairie, MN) and aligned by the multiple alignment Clustal W program. Phylogenetic tree was constructed with the neighbor-joining method using molecular evolutionary genetics analysis package (MEGA version 2.1). The robustness of the phylogeny was tested by bootstrap analysis with 1000 iterations.

6.3. Results and Discussion

Organic loading and TKN loading rates fluctuated between 6.3 – 53.4 kg COD m⁻³ d⁻¹ and 0.83 – 5.50 kg TKN m⁻³ d⁻¹. The influent and effluent wastewater characteristics in the pilot plant during the sampling period were shown in Table 6.2. Experimental results showed that high and stable COD and ammonia removal efficiencies were recorded for this system during the study. MBR requires air scouring to prevent fouling and maintain performance, but during low wastewater flow periods (midnight to 6:00 AM) denitrification efficiency dropped to 60 percent because of high oxygen influence to the anoxic zone. The MLVSS concentrations soon after the start of the reactor began to increase and reached to 10,855 mg L⁻¹ after 148 days of operation (Table 6.3).

At the same time the MLSS concentrations increased from 4,600 mg L⁻¹ to 18,820 mg L⁻¹ and MLVSS/MLSS ratios of the reactor slightly varied between 0.49 and 0.60 without any trend for change.

Table 6.1. Primer sets used in conventional and real-time PCR assays.

<i>Target gene</i>	<i>Primer</i>	<i>Nucleotide sequence (5' –3')</i>	<i>Ref.</i>
Partial 16S rRNA <i>amoA</i> AOB	341f	CCTACGGGAGGCAGCAG	[149]
	907r	CCGTCAATTCCTTTRAGTTT	[150]
	<i>amoA</i> -1F	GGGGTTTCTACTGGTGGT	[151]
	<i>amoA</i> -2R	CCCCTCKGSAAAGCCTTCTTC	[151]
16S rRNA <i>Nitrobacter sp.</i>	FGPS872	TTTTTTGAGATTTGCTAG	[152]
	FGPS 1269	CTAAAACTCAAAGGAATTGA	[152]
16S rRNA <i>Nitrospira sp</i>	NSR 1113F	CCTGCTTTCAGTTGCTACCG	[153]
	NSR 1264R	GTTTGCAGCGCTTTGTACCG	[153]
<i>amoA</i> AOA	Arch- <i>amoA</i> F	STAATGGTCTGGCTTAGACG	[137]
	Arch- <i>amoA</i> R	GCGGCCATCCATCTGTATGT	[137]
16S rRNA Anammox	Pla46F	GGATTAGGCATGCAAGTC	[154]
	AMX667R	ACCAGAAGTTCCACTCTC	[155]

Despite the high removal efficiencies, one of the most problematic aspects of an MBR with complete sludge retention was the extensive membrane fouling, which is considered to be caused by the formation of extracellular polymeric substances (EPS). EPS formation is almost unavoidable at high SRT operation. The advantages of working with high MLVSS in biological systems are well discussed in the literature. High biomass concentration is usually associated with high sludge retention times. Higher SRT allows the retention of slow growing microorganisms, like nitrifying bacteria and hence, improves

nitrification [156]. In recent years, a new trend in high biomass system operation has been working with lower solid retention times (around 10–20 days) and higher MLSS concentrations by lowering HRT. This approach results in stable operation, complete nitrification and reduced bio-solids production [157 – 159]. Cicek and coworkers [159] found that biomass production rate and biomass viability generally increased with decreasing SRT.

At lower SRTs (2 days), nitrification was noticeably affected by the sludge age supposedly due to the wash out of nitrifying microorganisms. On the other hand, Han and coworkers [143] investigated the influence of sludge retention time on membrane fouling and bioactivities in membrane bioreactor system at higher sludge ages. They found that regardless of SRT change, COD removal efficiency was high and stable throughout the experiment. However, they also found that biological activity, especially specific nitrification rate (SNR), slightly decreased with the increase of SRT from 50 to 70 days. Additionally, findings of this study showed that prolonged SRT (100 days) gives rise to

Table 6.2. Average influent and effluent wastewater characteristics in the pilot tank.

<i>Parameters</i>	<i>Influent</i>	<i>Effluent</i>
BOD ₅ (mg L ⁻¹)	249	6
COD (mg L ⁻¹)	465	35
SS (mg L ⁻¹)	280	<10
TKN (mg L ⁻¹)	51.2	0.5
Ammonia-nitrogen (mg L ⁻¹)	41.8	0.3
NO _x (mg L ⁻¹)	<0.5	15.3
TP (mg L ⁻¹)	7.2	5.1
pH	7.5	7.2
Conductivity (μS cm ⁻¹)	1028	954

deterioration effects on SNR. Although total nitrification rate slightly increased, SNR decreased significantly. The authors pointed out that the decrease of the specific nitrification rate at longer SRT might be due to the lower oxygen transfer and deficient substrate. However, the percentage of nitrifier community in the biomass directly affects the SNR. To evaluate the impact of SRT on nitrifier population in an MBR, it is necessary to quantify nitrogen converters and their fraction in mixed liquor.

Table 6.3. Sampling periods, operational parameters and VSS concentrations in the pilot tank.

Samples	VSS (mg L ⁻¹)	TKN load (kg m ⁻³ d ⁻¹)	TKN Removal Efficiency (%)	Extracted DNA (ng µL ⁻¹)	SNR (mgN gVSS ⁻¹ d ⁻¹)
Day 1	2,454	0.83	99.67	288.2	3.36
Day 22	3,750	3.22	99.66	501.9	8.56
Day 50	4,425	3.76	99.86	306.7	8.48
Day 71	6,995	2.80	99.87	393.3	4.00
Day 92	6,500	3.01	99.72	296.4	4.61
Day 127	9,716	2.42	95.08	255.6	2.37
Day 148	10,855	3.00	99.33	374.2	2.75

All sludge samples were concentrated by gravity settling prior to molecular analyses. Therefore, approximately the same amount of MLVSS was taken for DNA isolation. According to quantitative real-time PCR results, the total 16S rRNA gene copy

numbers varied from 6.58×10^7 to 1.02×10^8 copy numbers mL^{-1} extracted MLVSS. Abundance of *amoA* gene copy number for AOB population in the pilot tank ranged from 4.30×10^5 to 2.29×10^6 copy numbers mL^{-1} extracted MLVSS (Table 6.4). The ratio of nitrifying bacteria among all bacteria represented by *amoA* to 16S rRNA ratio has a decreasing trend with increasing VSS concentrations. AOB cell numbers/16S rRNA bacterial cells ratio increased from 2.94 to 4.05 percent when the VSS concentration reached to 3750 mg L^{-1} . Afterwards, the fraction of AOB cells gradually declined to 1.15 percent when the VSS concentrations reached to $10,855 \text{ mg L}^{-1}$ throughout 148 days of operation (Table 6.5).

The number of *Nitrospira sp.* 16S rRNA gene (or cell numbers) was approximately 100 times greater than the number of *Nitrobacter* 16S rRNA gene (Table 6.4). Additionally, the fraction of *Nitrospira* cells was also considerably higher (5–10 times greater) than AOB population and there were not apparent differences throughout operational period. The proportion of Anammox bacteria with respect to total bacterial 16S rRNA gene copy number varied between 0.41 percent and 0.84 percent whereas the ammonia oxidizing archaea (AOA) ranged between 0.05 percent and 0.09 percent in the pilot tank (Table 6.5). Low fraction of AOA indicated that bacteria rather than archaea in the pilot plant drive the nitrogen conversion. Moreover, significant amount of Anammox bacteria considered that nitrogen removal through Anammox might occur in the tank.

In a study conducted by Yu and coworkers [160], the fraction of AOB among all bacteria at MBRs operated at different SRTs (30 d, 90 d, and infinite) is estimated by fluorescence in situ hybridization (FISH) analysis. Based on the results, authors indicated that detecting AOBs with FISH technique led to some inaccuracy in detection. They concluded that MBR having an infinite sludge age contained the highest fraction of AOB (4.9%) among all bacteria indicating that no sludge purge strategy led to the increase in AOB ratios. Similarly, Duan and coworkers [158] investigated the effects of short solids retention time (3 d, 5 d and 10 d) on microbial community in a lab-scale nitrifying MBR. They found that bacterial diversity as revealed by DGGE analysis decreased with decreasing SRT values and gene copy numbers as quantified by real-time

PCR analysis increased with increasing SRT. They also indicated that the increased sludge age could decrease the microbial activity in MBR. In the studies of Li and coworkers [161], a bench-scale MBR reactor with complete sludge retention is operated with decreasing hydraulic retention times and the microbial community dynamics was investigated by a combination of the MPN method, fluorescence in situ hybridization (FISH) and quinone profiles.

Table 6.4. The gene copy number of 16S rDNA bacteria, *amoA* AOB, *Nitrobacter*, *Nitrospira*, *amoA* AOA and Anammox bacteria in the MBR samples.

<i>Sample</i>	<i>Target gene copy number</i>					
	<i>16S rRNA</i>	<i>amoA AOB</i>	<i>Nitrobacter</i>	<i>Nitrospira</i>	<i>amoA AOA</i>	<i>Anammox</i>
Days 1	5.13×10^7	8.38×10^5	1.73×10^4	1.59×10^6	7.50×10^3	5.90×10^4
Days 22	1.02×10^8	2.29×10^6	4.83×10^4	3.40×10^6	2.62×10^4	1.22×10^5
Days 50	9.18×10^7	7.55×10^5	1.71×10^4	2.10×10^6	2.04×10^4	2.14×10^5
Days 71	9.24×10^7	7.70×10^5	3.20×10^4	3.34×10^6	2.16×10^4	1.20×10^5
Days 92	7.69×10^7	5.13×10^5	1.44×10^4	2.76×10^6	1.45×10^4	1.46×10^5
Days 127	6.58×10^7	4.30×10^5	1.56×10^4	1.75×10^6	1.25×10^4	1.01×10^5
Days 148	7.54×10^7	4.84×10^5	8.05×10^3	2.24×10^6	1.55×10^4	1.34×10^5

In contrast to previous studies, they have found a gradual increase in MLVSS concentration coupled with a decrease in the number of nitrifiers. Another study conducted by Han and coworkers [143] confirmed the negative influence of prolonged SRT on specific nitrification rate, which was explained by impeded transfer rate of both substrate and oxygen and accumulation of inert biomass due to endogenous respiration. However, the results of the real-time PCR study clearly showed that AOB fraction decreased with increasing MLVSS concentration. Lower fraction of nitrifiers in the bacterial community results in declining rate of specific nitrification (Table 6.3).

Table 6.5. Nitrogen converting microorganisms ratio in the MBR based on bacterial 16S rRNA gene.

<i>Sample</i>	<i>amoA AOB/</i> 16S rRNA	Nitrobacter/ 16S rRNA	Nitrospira/ 16S rRNA	<i>amoA AOA/</i> 16S rRNA	<i>Anammox/</i> 16S rRNA
Days 1	2.94 %	0.12 %	11.19 %	0.05 %	0.41 %
Days 22	4.05 %	0.17 %	12.02 %	0.09 %	0.43 %
Days 50	1.48 %	0.07 %	8.23 %	0.08 %	0.84 %
Days 71	1.50 %	0.12 %	13.01 %	0.08 %	0.47 %
Days 92	1.20 %	0.07 %	12.92 %	0.07 %	0.68 %
Days 127	1.18 %	0.09 %	9.57 %	0.07 %	0.55 %
Days 148	1.15 %	0.04 %	10.69 %	0.07 %	0.64 %

Phylogenetic analysis of the *amoA* sequences indicated that AOB populations in the initial sludge taken from the Pasakoy WWTP were phylogenetically related to uncultured bacterium clone NineSprings-83W, uncultured ammonia-oxidizing bacterium clone BXA-294, uncultured bacterium B-clone14, uncultured bacterium clone 4-17 and uncultured bacterium clone T58. On day 71, when the VSS concentration reached to about 7 g L^{-1} , *Nitrospira* related species appeared, uncultured *Nitrospira sp.* clone B2 and *Nitrospira sp.* LT2MFa. However, most of the clones were phylogenetically affiliated with *Nitrosomonas* lineage (Figure 6.2). Other ammonia oxidizing bacteria were phylogenetically related to uncultured bacterium clone NineSprings-83W, uncultured bacterium isolate DGGE gel band M33, uncultured ammonia-oxidizing bacterium clone BJ-082-6, uncultured bacterium clone B-clone14, uncultured ammonia-oxidizing beta proteobacterium clone Psedi-29, uncultured ammonia-oxidizing bacterium isolate DGGE gel band F2, uncultured ammonia-oxidizing bacterium clone AOBd-A4D2, uncultured bacterium clone 4-24 and uncultured bacterium clone 14-10. After 148 days of operation, uncultured bacterium clone T58 related to the *Nitrosomonas* lineage and *Nitrospira sp.* Nsp58 related to the *Nitrospira* lineage became dominant species in the MBR (Figure 6.2). Other ammonia oxidizing bacteria were phylogenetically related to uncultured ammonia-oxidizing bacterium clone AOB-F11, uncultured bacterium clone LM 3, uncultured ammonia-oxidizing bacterium clone BXA-141, uncultured bacterium clone RT-600-29 and uncultured bacterium clone M-amoA-31.

Previous studies have shown that members of the beta proteobacterial genera *Nitrosomonas* and *Nitrospira* are the dominant ammonia-oxidizing bacteria in wastewater treatment systems [135]. As shown in Figure 6.2, sequence analysis revealed that *Nitrosomonas* related AOB species were dominant in the seed sludge and *Nitrospira sp.* were the dominant AOB in the MBR after 148 days of operation. Similar to this study, Yu and coworkers [160] indicated that the fast-growing *Nitrosomonas sp.* were the dominant AOB at 30 days SRT, while considerable slow-growing *Nitrospira sp.* existed in MBR operated without sludge purge. The authors also indicated that in spite of the differences of the community structures of AOBs, MBR possibly possessed similar heterotrophic community structures. On the other hand, the authors thought that low specific ammonium-oxidizing and low specific nitrate forming rate caused by slow-

growing *Nitrosospira sp.* during non sludge purging period. However, the results of this study revealed that decreasing trend of AOB fraction might affect the specific activity of nitrifiers.

The sequence analysis of 16S rDNA *Nitrospira* gene revealed that all sequences were related to previously identified *Candidatus Nitrospira defluvii* (FP929003) with 99 –100 percent sequence similarity in the MBR sludge samples. The genus *Nitrospira* can be subdivided into at least four monophyletic sublineages I–IV [162]. So far, three different species of *Nitrospira* have been isolated; *Nitrospira marina* [163] *Nitrospira moscoviensis* [164] and *Candidatus Nitrospira defluvii* [165], which were isolated from seawater, freshwater and activated sludge environment, respectively. *Candidatus Nitrospira defluvii* was affiliated to *Nitrospira* sublineage I, which is most important for sewage treatment [166]. Sublineage I contained only sequences retrieved from nitrifying bioreactors. In comparison, the distribution of *Nitrospira*-like bacteria in Sublineage II ranged from WWTPs to natural habitats like soil, lake and freshwater environments and also an isolated representative, *Nitrospira moscoviensis* [162].

According to real-time PCR results high fraction of *Nitrospira* species in the pilot tank pointed out that *Candidatus Nitrospira defluvii* species probably have more functions than only nitrite oxidation. However, the usage of organic substrates as a carbon source or for energy generation by *Nitrospira* species, has not been proved by any scientist. Recently, Lücker and coworkers [167] speculated that the presence of *nirK* genes in *Ca. N. defluvii* indicates that this organism may denitrify NO_2^- by using organic substrates as an electron donor. However denitrification by *Ca. N. defluvii* has not been experimentally demonstrated yet. This unknown function of *Candidatus Nitrospira defluvii* can be the reason of high fraction of *Nitrospira* (up to 13.01%) in the MBR samples (Table 6.5).

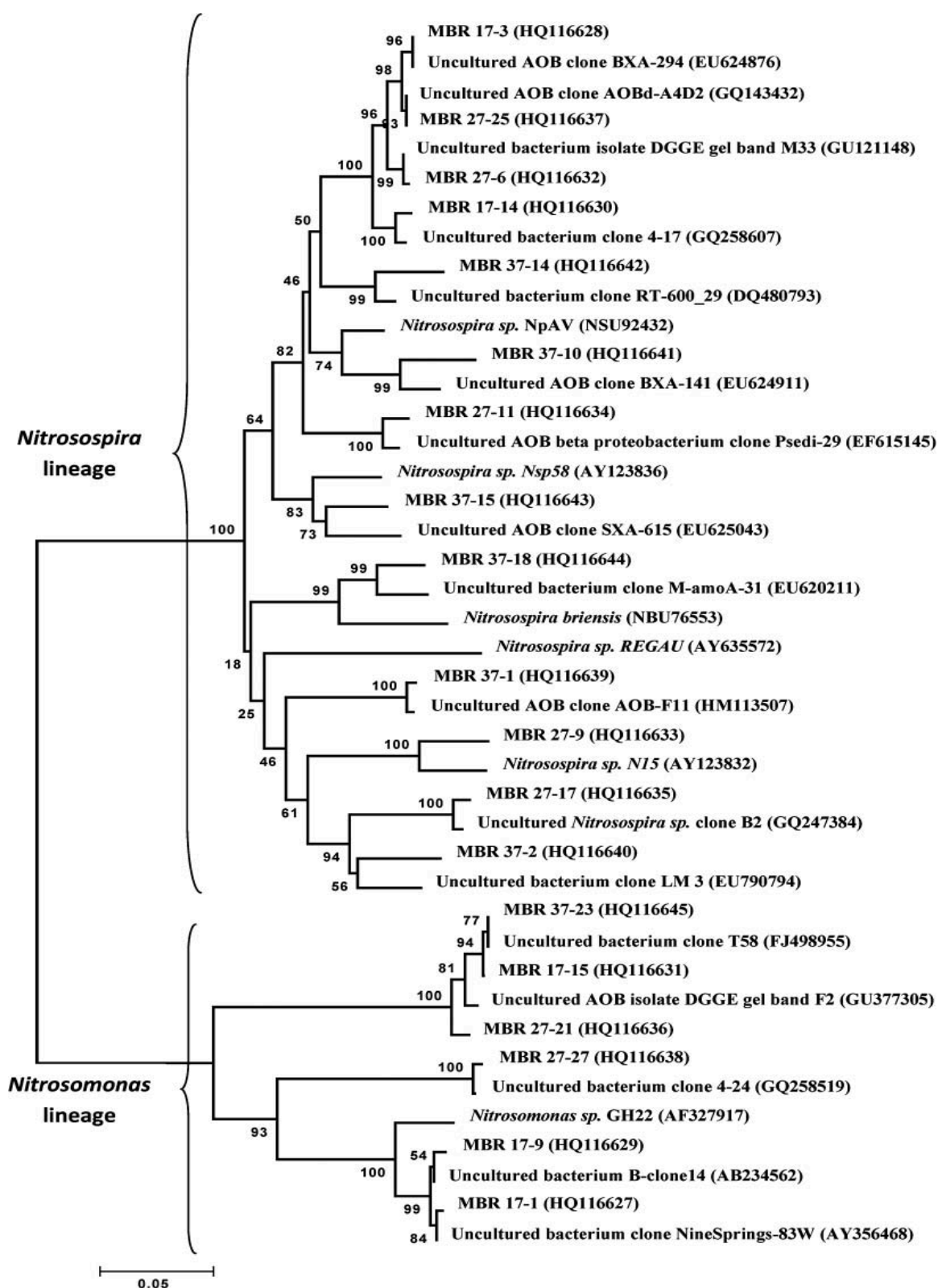


Figure 6.2. Neighbor-joining phylogenetic tree of AOB sequences generated from *amoA* gene. The significance of each branch is indicated by bootstrap values (1,000 replicates).

The scale bar represents 0.05 inferred substitutions/nucleotide positions.

7. HIGH BIOMASS FILTRATION SYSTEMS: ENERGY AND COST ANALYSIS OF SLUDGE PRODUCTION

7.1. Introduction

Since research on membrane bioreactor technology began over 30 years ago, several generations of biomass filtration systems have evolved to treat municipal wastewater and all has been reported to have chemical or biological oxygen demand (COD or BOD) and nitrogen removal efficiencies of more than 95 %. However, because of some disadvantages of MBR, such as high-energy consumption and membrane fouling, it has been seen as high-risk compared to conventional technologies. MBRs are viewed by many customers as high capital and operating expenditure, mainly due to membrane installation and replacement costs and higher energy demand compared to conventional activated sludge systems. Therefore, unless a high output quality is required, organisations generally do not perceive a need to invest large sums of money in an MBR [2, 168 – 171]. On the other hand, comparison cannot be done with a secondary treatment activated sludge system but with a system that provides same effluent quality. However, controversial comparison results of MBR to conventional activated sludge (CAS) system with tertiary filtration have been stated in different studies. 10 – 20 % higher MBR operating cost was described previously [172], while latter studies showed that MBR operation was less expensive than operating a combination of CAS and tertiary filtration [173, 174]. Yet limited reports have been published regarding the in-depth analysis of operating parameters over the lifetime of an MBR installation compared to that of CAS and tertiary filtration.

The most significant aspects of MBR operation cost are energy consumption and membrane material replacement; because the installation of many full-scale MBR plants is barely older than a decade, there is limited information available about impacts of operation

on membrane material's life [175]. Several manufacturers have modified different operational strategies so as to lower the expenses. One of the most efficient strategies to limit membrane fouling is the use of a gas/liquid two-phase flow to enhance the mass transfer [42]. However, the energy demand of membrane bioreactors in order for membrane scouring and cleaning or to filter water through the membrane has been reported to be a factor of two to four times higher, compared to the conventional activated sludge process (CASP) [176]. More than 50 % of the energy is used for aeration, which is approximately 30 to 40 % of the energy demand resulting from scouring air of the membrane [4, 177]. Generally there is a linear relationship between membrane permeability and membrane aeration up to a threshold value, beyond which permeability is unchanged with membrane aeration [178]. Scouring air is provided through coarse bubble diffuser system, which is 10 to 20 % less efficient than fine bubble aeration for supplying oxygen to the biomass (standard oxygen transfer efficiency, SOTE of 19 to 37 % at 5 m depth) but have the advantage of lower cost. In some operations, e.g. treatment of high strength liquors, coarse, and fine bubble aeration are used in combination [179]. On the other hand, aeration sequencing management is important: intermittent aeration, especially working with intermittent filtration, enables to save energy [42].

It has been shown through different researches, that the energy demand of municipal MBR could be as low as $0.7 - 0.8 \text{ kWh m}^{-3}$ or as high as $6 - 8 \text{ kWh m}^{-3}$. In submerged MBRs, it is the turbulent aeration which generates the cross flow at around 1 m s^{-1} (as compared with $2 - 4 \text{ m s}^{-1}$ in a side-stream system) without the need for a recirculation pump to remove the accumulated solids around the membranes, as well as scouring the membrane and providing oxygen to the biomass for aerobic biodegradation process [180, 181]. Hence, the energy consumption of submerged MBRs is potentially lower than that of side stream MBRs. Air demand for membrane scouring is usually higher than the actual biological demand. Around 0.2 kWh was reported to be used for oxygen supply of the activated sludge and 0.7 kWh for the deposit reduction by air scour in some applications. Depending on feed wastewater strength a further 10 to 50 % of energy is demanded for bio-treatment; it is also shown in literature that aeration is the main cost associated with submerged units [179]. Aeration is thus an important aspect of MBR because it has a dominant influence on operating

cost and filtration flux [182]. Hence, there is a need to reduce this fraction of air used for membrane surface scouring in order to make the filtration technology with high MLSS concentration more commercially applicable alternative to conventional wastewater treatment processes.

Despite the increased aeration cost, a possible strategy for operational cost limitation is reduction of sludge withdrawal. The cost of excess sludge treatment accounts for more than half of the total operating cost in CASs [183]. In comparison with CASs, MBRs can be operated in a wide range of MLSS concentrations and sludge retention time (SRT) because SRT can be controlled completely independently from hydraulic retention time (HRT) by membrane. Several researchers studied the possibility of operating MBR without sludge withdrawal. Theoretical investigations have showed that biomass production can be limited in MBR by appropriate operational strategies like limiting biomass withdrawal, consequently minimizing bacterial growth [124]. A major problem associated with MBRs for sludge reduction is the severe membrane fouling caused by the high concentrations of sludge and organic matter [183]. Long SRTs were also investigated for their effects on the biomass. These conditions may cause some modifications in the sludge properties and dynamic behavior, as a result of change in metabolic state of bacteria due to substrate limitation, lower enzymatic activity, smaller yield and decay coefficients, biomass loss by endogenous mechanisms, decay, lysis and predation [112]. However, the separating technique selects non floc-forming bacteria and modifies the nature and structure of bioflocs [184]. Some researchers emphasized the accumulation of organic inerts and inorganic material within the biomass under complete sludge retention [185, 186]. Separately, the stabilization of volatile suspended solids and the specific maintenance activities of biomass were reported, which means no accumulation of inert material was also possible [114].

As per the discussion above, the pilot scale high biomass filtration system was evaluated in terms of energy consumption and operational costs based on energy and sludge withdrawal. The system was compared to that of the full-scale conventional biological nutrient

removal (BNR) plant. The full-scale plant combined with tertiary filtration and disinfection for effluent reuse purposes.

7.2. Operational Cost Calculations

Operational costs were determined as follows: energy, sludge disposal, maintenance, laboratory, personnel and consumables. In addition, the energy demand analysis was composed of aeration, sludge disposal, wastewater pumping and others and a specific energy cost of $0.0751 \text{ € kWh}^{-1}$ was used. The energy consumption was measured with wattmeters.

7.2.1. Pilot Plant Operational Costs

The equipment of the pilot plant in which energy consumption varied were influent pump, drum screen, recirculation pump and fine bubble aeration blower; however the coarse bubble aeration blower consumed a constant amount of energy. The P&I diagram of the pilot plant is given in Figure 7.1.

The influence of MLSS concentration and aeration type on oxygen transfer and thereby the aeration energy was computed using the findings of Cornel and Krause [187] and Yoon and coworkers [188]. The average total aeration energy in kWh d^{-1} was obtained by summing blower power consumption for both membrane scouring and excess biological oxygen demand.

Pumping energy requirements comprised of inlet pumping (average headloss 5 m) and internal recirculation (average headloss 0.5 m). Because sludge wastage was possible through a branch and valve on the internal recirculation line, no additional pump was used. A constant mixing power of 2.5 kW was used in the anoxic tank and no mechanical mixing was required for the other zones.

The pilot plant was operated for over two years and results of a particular period (6 months), which comprises complete sludge retention time, were presented as the sludge yield as it was described in Chapter 5. Except for this particular period, some portion of sludge withdrawn weekly in order to maintain the MLSS concentration around 15,000 mg L⁻¹.

The membrane clean in place (CIP) protocol was applied every 6 to 8 months and the consumed chemical amount was taken into consideration in operational cost calculations; however no chemical consumed for cloth filter cleaning.

7.2.2. Full-scale Operational Costs

Operational cost comprise of the annual expenditure for personnel, maintenance, sludge disposal, laboratory, consumables and energy. A simple block diagram of the full-scale plant is given in Figure 7.2. Energy consumption was analysed considering the major demanding processes: inlet pumping (Pasakoy main, Uzundere, Mimar Sinan), aeration, sand filtration and UV disinfection, sludge processing (dewatering, drying) and the others. The daily electricity consumption was recorded separately from the power distribution units of these processes. The parameters involved in calculating the electricity cost is given in Table 7.1.

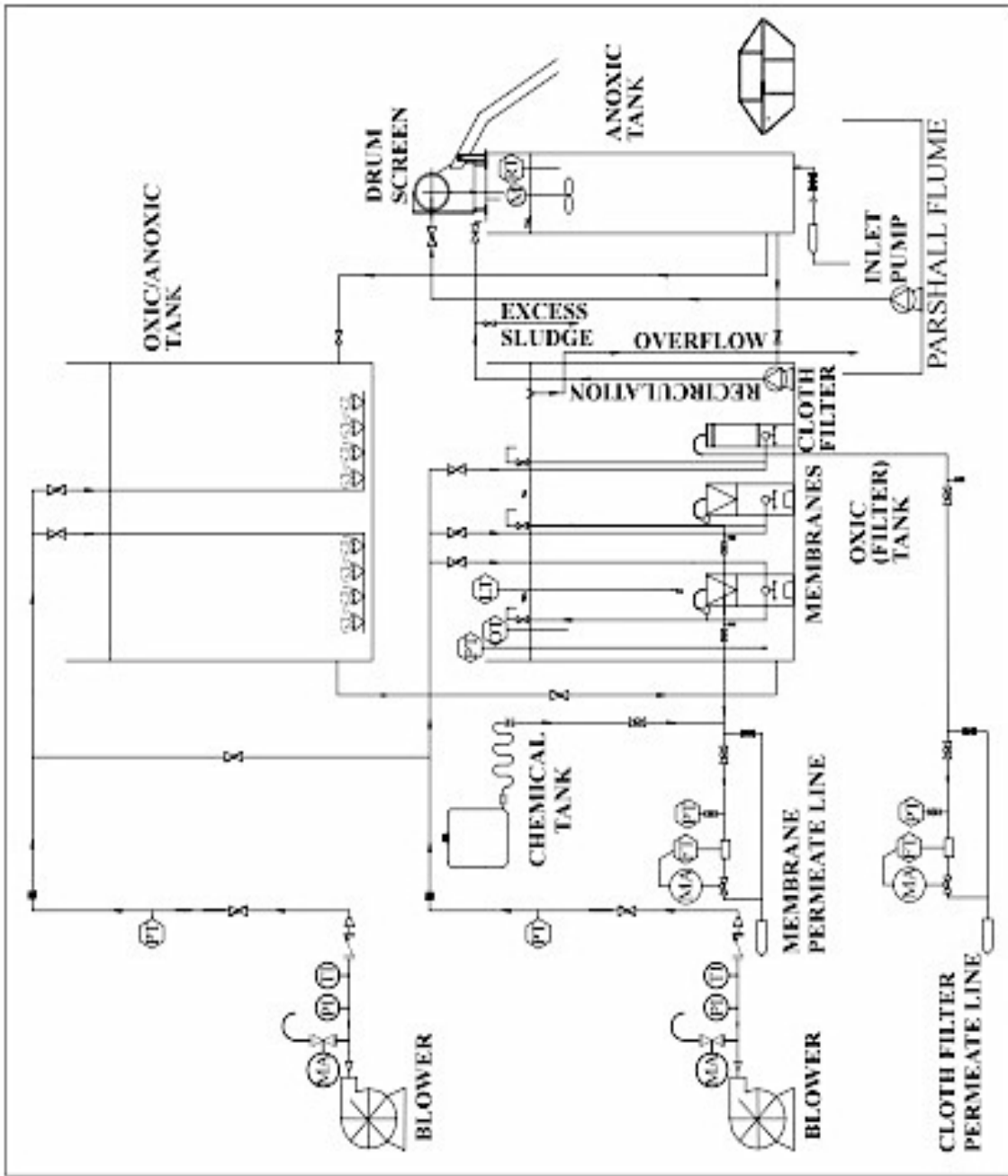


Figure 7.1. The P&I diagram of the pilot plant.

Because there is no primary sedimentation in the full-scale plant, the processed and disposed sludge is entirely waste activated sludge. Hence, wasted sludge has been dewatered directly without thickening and then dried. So, the sludge processing and disposal cost basically composed of energy consumed during the processes, personnel expenses, polymer cost for dewatering, maintenance, hauling cost (diesel oil, amortisation) and ultimate disposal price (Table 7.2). On the other hand, electricity has been produced in the cogeneration unit that consumes natural gas and sludge drying process has been carried out using the benefit of the water vapour produced in the turbine, however, the process is actually depended on the natural gas price (0.22 € m^{-3}).

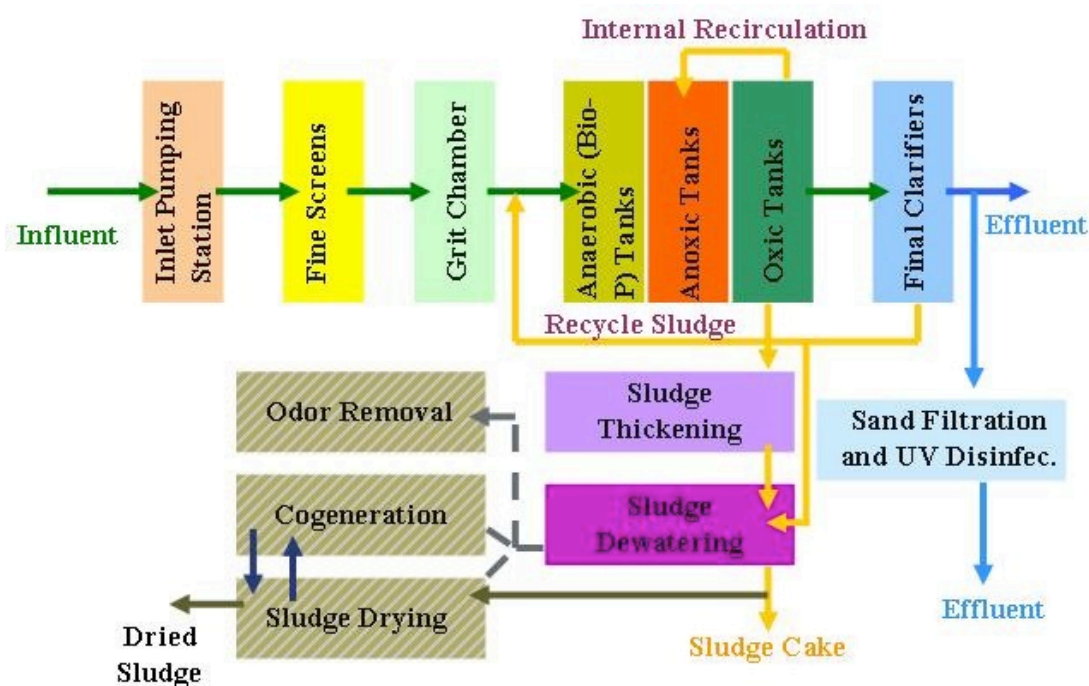


Figure 7.2. Block diagram of the BNR plant.

Table 7.1. Parameters involved in the energy cost.

Flow rate	$\text{m}^3 \text{d}^{-1}$
Consumed natural gas	$\text{m}^3 \text{d}^{-1}$
Consumed water vapour	kg d^{-1}
Electricity production in turbines	kWh d^{-1}
Electricity purchased from Ayedaş (in case of maintenance)	kWh d^{-1}
Consumed electricity in the plant	kWh d^{-1}
Average natural gas cost	€ d^{-1}
Ayedaş electricity cost	€ d^{-1}
Total electricity cost	€ d^{-1}
Unit electricity cost (per treated wastewater)	kWh m^{-3}

Table 7.2. Parameters involved in the ultimate sludge disposal (dry product cost from 1% to 99% dry solids, DS).

<i>SLUDGE DRYING</i>		
Daily energy consumption for sludge drying		kWh d^{-1}
Annual energy consumption for sludge drying		kWh year^{-1}
Annual energy cost for sludge drying		€ year^{-1}
Water Vapour	Turbine	kg year^{-1}
	Auxillary boiler	kg year^{-1}
Natural Gas	Turbine	$\text{m}^3 \text{year}^{-1}$
	Auxillary boiler	$\text{m}^3 \text{year}^{-1}$
Energy produced by turbine		kWh year^{-1}
Natural gas cost for turbine		€ year^{-1}
Cost (Ayedaş) of energy produced by turbine (if electricity was supplied from Ayedaş)		€ year^{-1}
Energy cost difference (Ayedaş-Turbine)		€ year^{-1}
Auxillary boiler energy cost		€ year^{-1}
Annual energy cost for drying		€ year^{-1}

Table 7.2. Parameters involved in the ultimate sludge disposal (dry product cost from 1% to 99% dry solids, DS) (continued)

Drying unit, Turbine, Boiler	Cost of one operator (worker)	€ month ⁻¹
	Number of operators	
	Monthly operator cost	€ month ⁻¹
	Annual operator cost	€ year ⁻¹
Total sludge drying cost		€ year ⁻¹
Total dry product (99% DS)		kg year ⁻¹
Drying (25% DS to 99% DS) cost per kg		€ kg ⁻¹
Drying (25% DS to 99% DS) cost per ton		€ ton ⁻¹
Drying cost of 3,960 kg sludge (25% DS to 99% DS)		€ kg ⁻¹
<i><u>SLUDGE DEWATERING</u></i>		
Sludge dewatering cost (1% DS to 25% DS)		€
Sludge Dewatering	Cost of one operator (worker)	€ month ⁻¹
	Number of operators	
	Hourly operator cost	€ h ⁻¹
	Operation period of operator	h
Operator cost		€ d ⁻¹
Total dewatering cost (1% DS to 25% DS) of sludge		€ d ⁻¹
Total dewatering cost (1% DS to 25% DS) of sludge		€ year ⁻¹
<i><u>MAINTENANCE (SLUDGE PROCESSING UNITS)</u></i>		
Maintenance cost of sludge processing		€ year ⁻¹
<i><u>SLUDGE DISPOSAL</u></i>		
Ultimate disposal unit price of 99% DS sludge		€ ton ⁻¹
Average amount of dry product (99% DS) hauled daily		ton d ⁻¹
Total daily dry product disposal cost		€ d ⁻¹
Total annual dry product disposal cost		€ year ⁻¹
Unit price of diesel oil		€ L ⁻¹
Diesel oil diesel oil consumption per ton of 99% DS sludge		L ton ⁻¹
Total daily diesel oil consumption		L d ⁻¹
Total daily diesel oil cost		€ d ⁻¹
Total annual diesel oil cost		€ year ⁻¹
Daily amortization		€ d ⁻¹
Annual amortization		€ year ⁻¹
Total daily dry product hauling cost		€ d ⁻¹
Total annual dry product hauling cost		€ year ⁻¹

Table 7.2. Parameters involved in the ultimate sludge disposal (dry product cost from 1% to 99% dry solids, DS) (continued)

Disposal cost per ton of dry product (99% DS)	€ year ⁻¹
<i>DRY PRODUCT COST</i>	
Daily dry product (1% DS to 99% DS) cost	€ d ⁻¹
Annual dry product (1% DS to 99% DS) cost	€ year ⁻¹
Dry product (1% DS to 99% DS) cost per ton	€ ton ⁻¹

7.3. Results and Discussion

7.3.1. Bioreactor Performance and Energy Consumption

The pilot plant was operated for 26 months. The rated power of two rotary-lobe blowers, which were installed for the pilot plant, was 7.5 kW each and for the average ambient air temperature, power consumption (absorbed power) of one blower was 3.66 kW (ambient temperature around 30 °C). Operation of 1 blower for scouring of filters consumed 0.88 kWh per m³ treated wastewater. Second blower was operated intermittently for fine bubble aeration, mostly 5 minutes on and 20 minutes off depending on the strength of incoming wastewater. The total energy consumption (at 15,000 mgMLSS L⁻¹) of inlet pump (7 m of water head), recirculation pump, drum screen, anoxic tank mixer and blowers together was about 1.03 – 1.17 kWh m⁻³ of permeate. 65 – 70 % of this energy was consumed for air scouring (unit price of electricity was 0.0751 € kWh⁻¹). On the other hand, the full-scale plant consumed 0.45 kWh m⁻³ of treated wastewater on the average. The full-scale plant included, 43 m of wastewater pumping, preliminary treatment, biological treatment (aeration with turbo blowers), clarification of treated wastewater, sand filtration and UV disinfection of effluent

water, sludge processing (waste activated sludge pumps, dewatering, drying), administration building, lightning of site etc.

7.3.2. Sludge Yield in the Bioreactor

High MLSS and SRT conditions decreased sludge production by 62 % in the pilot plant. Thus, 0.078 kg dry matter produced per 1 m³ of permeate in the pilot plant, while 0.204 kg dry matter produced per 1 m³ of treated wastewater in the full-scale plant (Chapter 5). This difference can provide a significant decrease in sludge processing and disposal cost in a larger scale wwtp like Pasakoy. Namely, total energy cost for sludge processing decreases by 45 % and daily polymer consumption cost for sludge dewatering decreases by 61 %. Including all parameters given in Table 7.2, the overall sludge processing and disposal cost, which is the dry product cost from one percent to 99 % DS, declines 43 %. The lower sludge processing energy demand leads to consume six percent less natural gas in the plant's electricity production. The contribution of sludge amount in operation cost and energy consumption in a larger scale plant is discussed in Section 7.3.3.

7.3.3. Effect of Biomass Filtration Instead of Gravity Removal in Final Clarifiers

The existing process of the full-scale plant and the option of operating it as a biomass filtration system were compared in accordance with the results of the pilot plant. Second stage of the Paşaköy WWTP has sand filtration and UV disinfection units. The effluent water quality of the plant is equivalent to that of a CFBR/MBR filtration plant. Turbidity in the BNR effluent water is decreased below 2 NTU in the sand filters (it is required < 10 NTU before entering the UV unit) and finally the filtered water is disinfected in the UV unit; the final quality of the treated wastewater is 0 – 14 total coliform and 0 – 4 fecal coliform.

The comparison of the two systems was done based on the concepts of aeration and sludge production, thus the operational cost for energy and sludge disposal. Common structures for a membrane filtration plant and a conventional BNR plant, like inlet pumping station, screens, grit chamber etc. were also taken into consideration; also, sludge drying process was included for both systems. The natural gas consumption of the co-generation unit for electricity production was calculated and the price of corresponding kWh energy consumption was given here as the energy cost. The items like personnel and maintenance were determined by calculating the number of equipment (pump, centrifuge, blower, drier, etc.) required in case of operating the full-scale plant as a biomass filtration system and estimating the number of operators needed to operate the system. So, the operation costs for items like these were found by adapting the unit costs in real case operation to the biomass filtration option.

The operational data shows the following differences. There is a need for scouring air in a submerged biomass filtration unit, which countervails some of the oxygen requirement for nitrification from time to time but generally higher than the actual requirement of a typical domestic wastewater. Besides, the MBR needed a relaxation period about five minutes, one to three times a day and no permeate was produced during relaxation; however, it needed chemical cleaning in six or eight months period. During a chemical cleaning process, approximately 3 L of 0.5 % sodium hypochlorite consumed per membrane cartridge. On the other hand, the cloth filter was operated without relaxation and chemical cleaning. In the full-scale BNR plant six pieces of sand filters were backwashed in turns in approximately every 18 hours and $2500 \text{ m}^3 \text{ h}^{-1}$ backwash water was used.

Because the above mentioned common aspects of two systems (gravity vs. filter separation) were taken into consideration, the term “operation cost” in the rest of the chapter represents the whole operating expenses, as well as a separate evaluation of sludge

disposal cost and the energy cost (for aeration, sludge processing and the sand filter-UV disinfection unit for the conventional BNR plant). Sludge disposal consists of processing (excess sludge pumping, dewatering, drying), transportation and ultimate disposal. The dried sludge has been disposed to a cement factory, where it has been used as fuel. Despite the huge construction cost distinction between the two filtration systems (the cost of CFBR was approximately 10 % of that of the MBR), the operation cost of CFBR and MBR assumed to be identical. Because the annual chemical cleaning cost was even less than one per thousands of the monthly operation cost and the relaxation periods caused about 0.6 % less permeate production. These slight cost differences were omitted. Moreover, the term “electricity cost” in the rest of the chapter represents the electricity consumed in the whole plant. The energy consumption of aeration system, sludge processing and the sand filter-UV disinfection units for the conventional BNR plant was presented separately.

Table 7.3 shows the comparison of three options for Paşaköy WWTP operation. Also, same comparison was done by eliminating the sludge drying, because it is not a requirement for sludge processing in every treatment plant (Table 7.4). Option 1 is the real case, which is a conventional BNR operation. Options 2 and 3 represent operation of the plant as a biomass filtration system with two different fluxes regarding the experience of the pilot unit. The fluxes in Option 2 and 3, which were considered to be feasible for the flat sheet membranes, were taken as $0.42 \text{ m}^3 \text{ m}^{-2} \text{ d}^{-1}$ (at peak flow: $0.52 \text{ m}^3 \text{ m}^{-2} \text{ d}^{-1}$) and $0.53 \text{ m}^3 \text{ m}^{-2} \text{ d}^{-1}$ (at peak flow: $0.65 \text{ m}^3 \text{ m}^{-2} \text{ d}^{-1}$) respectively. But, as it was exemplified in the pilot plant, the flux in Option 2 (or even slightly lower) was more likely to operate steadily in terms of trans-membrane pressure. The operation cost was calculated for existing inflow conditions: approximately $114,000 \text{ m}^3 \text{ d}^{-1}$ of flow rate for the 2nd stage plant.

Table 7.3. Proportional values of important operation parameters (with sludge drying).
 (Option 1: full-scale BNR plant; Option 2: biomass filtration, flux: $0.42 \text{ m}^3 \text{ m}^{-2} \text{ d}^{-1}$; Option 3:
 biomass filtration, flux: $0.53 \text{ m}^3 \text{ m}^{-2} \text{ d}^{-1}$) [189].

	<u>Option 1</u>	<u>Option 2</u>	<u>Option 3</u>	
Electricity cost for sludge processing / Electricity cost	22.92	11.14	12.72	%
Sludge disposal cost / Operation cost	35.79	24.57	26.28	%
Electricity cost / Operation cost	40.44	51.30	48.01	%
Sludge disposal cost / Aeration cost	88.50	47.90	54.73	%
Aeration cost / Operation cost	18.33	33.61	29.09	%
Aeration cost / Electricity cost	45.32	65.52	60.60	%

Table 7.4. Proportional values of important operation parameters (without sludge drying).
 (Option 1: full-scale BNR plant; Option 2: biomass filtration, flux: $0.42 \text{ m}^3 \text{ m}^{-2} \text{ d}^{-1}$; Option 3:
 biomass filtration, flux: $0.53 \text{ m}^3 \text{ m}^{-2} \text{ d}^{-1}$).

	<u>Option 1</u>	<u>Option 2</u>	<u>Option 3</u>	
Electricity cost for sludge processing / Electricity cost	8.72	2.51	2.91	%
Sludge disposal cost / Operation cost	29.36	16.51	17.63	%
Electricity cost / Operation cost	36.44	45.83	42.24	%
Sludge disposal cost / Aeration cost	80.58	36.03	41.74	%
Aeration cost / Operation cost	19.56	32.94	28.47	%
Aeration cost / Electricity cost	53.68	71.88	67.41	%

The oxygen transfer efficiency in process conditions (α .OTE) highly depends on MLSS concentration. The α factor, which is a ratio of mass transfer coefficients in process to clean water, decreases exponentially with increasing MLSS concentration [187, 190 – 193]. In addition, the OTE of aeration diffusers in clean water contributes to the overall efficiency of oxygen transfer. However, expansion of conventional activated sludge process with nitrification or nitrification/denitrification, and higher sludge ages improve the α .OTE [194]. The aeration demand declines, when SRT was increased by extending hydraulic retention time (HRT) at fixed MLSS concentrations [174]. Also, the α factor increases gradually from its lowest value through the length of an oxidation ditch [195]. The α .OTEs per meter for the two different MLSS concentrations were calculated by using the following expression [187, 188]:

$$\alpha\text{-OTE (\%/m)} = 9.00 - 8.63 \times 10^{-4} \times \text{MLSS} + 2.56 \times 10^{-8} \times \text{MLSS}^2 \quad (7.1)$$

During the period of the study, air requirement in Option 1 for nitrification and excess carbon removal after denitrification was 37,180 Nm³ h⁻¹ (specific oxygen transfer efficiency per meter, α .OTE/m: 4.74%). Scouring air amounts in Option 2 and Option 3 were calculated as 91,985 Nm³ h⁻¹ and 73,588 Nm³ h⁻¹ respectively. Because the biomass concentration in these two options was higher, the volume of air to be supplied for nitrification and carbon removal was higher (77,892 Nm³ h⁻¹, specific oxygen transfer efficiency per meter, α .OTE m⁻¹: 1.82%) as a consequence of lower oxygen transfer efficiency in the biomass. The amount of scouring air in Option 2 meets the oxygen demand of the treatment, however in Option 3, the biological oxygen requirement was higher. So, the scouring air volume in Option 2 was taken as the total air to be provided for both oxidation and membrane cleaning and in Option 3, the air requirement for treatment was taken into consideration.

Over the two years of operation, eight pieces of membrane sheets out 300 membranes have been damaged. Considering an approximate membrane cost of 50\$ m⁻², the contribution of membrane replacement cost for Option 2 and Option 3 would be less than one per thousand of the total full scale operation. So, membrane replacement costs for Option 2

and Option 3 were 1.08 % and 0.95 % of the operation cost respectively. Thus, a possible membrane replacement cost was accepted as a part of all consumables.

According to the above-mentioned calculations about operating the plant as a biomass filtration system, despite the increase in the electricity cost for aeration by 28 to 41 % as a result of membrane scouring air, the total operation cost decreases by 9 to 15 % because of the decrease in the expenses for sludge dewatering, drying and ultimate disposal. The unit energy consumption in the full-scale plant has been approximately 0.45 kWh m^{-3} ; the unit energy consumption in Option 2 and 3 was calculated as 0.54 kWh m^{-3} and 0.47 kWh m^{-3} respectively. Hence, assuming the electricity price was $0.0751 \text{ € kWh}^{-1}$, the electricity cost per treated wastewater of the full-scale plant, Option 2 and 3 was 0.034 € m^{-3} , 0.041 € m^{-3} and 0.035 € m^{-3} respectively.

Figures 7.3 to 7.8 show the distribution of operation and electricity costs for the three options. In the full-scale plant, the electricity cost is 36 % of the total operation cost; however, if a biomass filtration system with $0.42 \text{ m}^3 \text{ m}^{-2} \text{ d}^{-1}$ flux was designed this value would increase to 45 %. Increasing the flux by 25 % (decreasing the filter surface area) decreases the electricity cost to 42 % of the operation cost. But, at this condition sustainability of flux could not be maintained because of earlier fouling of membranes. Also, the period between two chemical cleaning in MBR extends 2 or 3 times at low flux conditions. Despite the higher electricity cost of the biomass filtration design that is advisable for operation, the total monthly operation cost is nine percent lower than that of the full-scale plant. Here the important point is verification of the decrease in total sludge production (observed yield coefficient) by two-thirds and its applicability in design of high biomass filtration systems. Because there are 40 % higher or lower values in literature than the average $0.25 \text{ mg}_{\text{MLSS}} \text{ mg}_{\text{COD}}^{-1}$ of biosolids yield at $15,000 \text{ mg L}^{-1}$ MLSS concentration in the pilot plant. However, according to the results in the pilot plant, it is possible to reduce monthly sludge processing cost of the full-scale plant by switching the process to a high biomass filtration system.

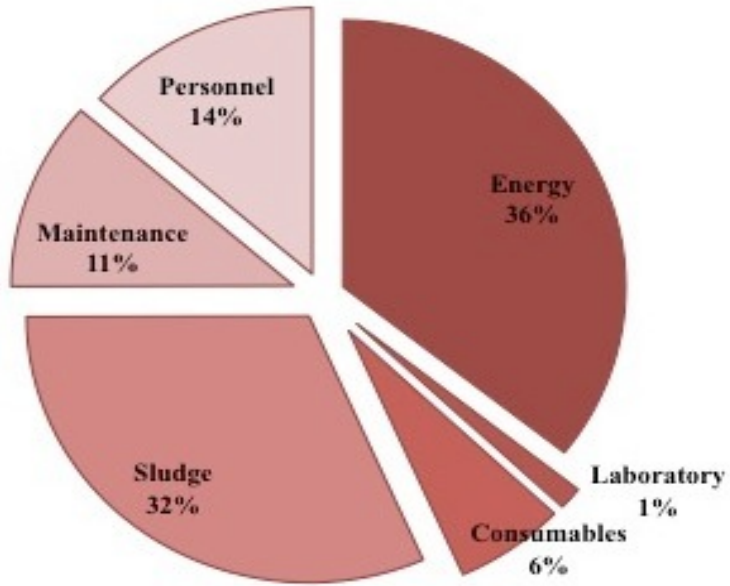


Figure 7.3. Distribution of important items in total operation cost for Option 1.

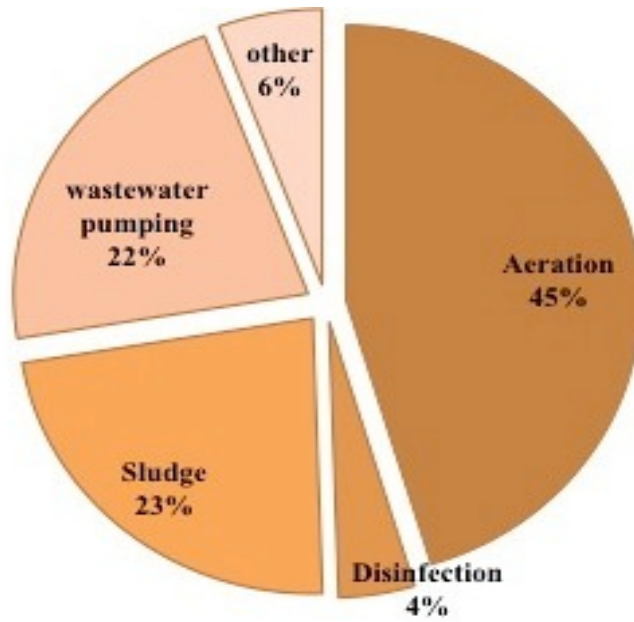


Figure 7.4. Distribution of electricity costs for Option 1.

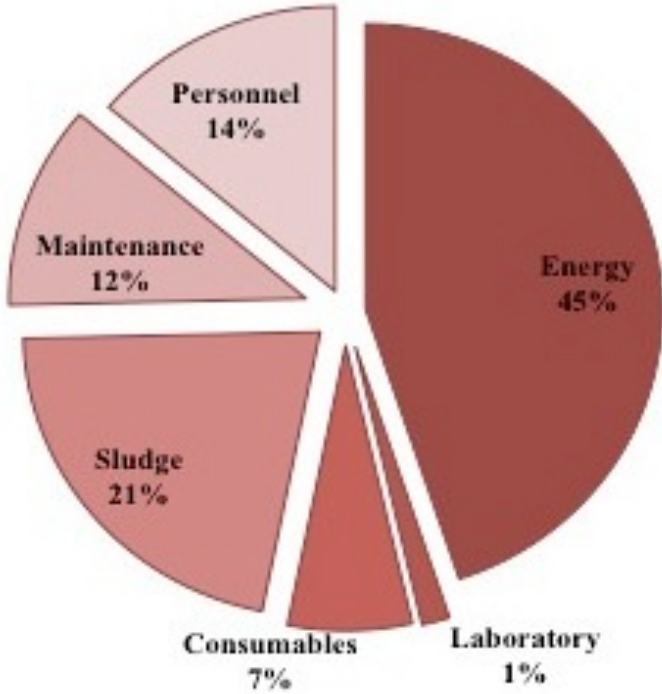


Figure 7.5. Distribution of important items in total operation cost for Option 2.

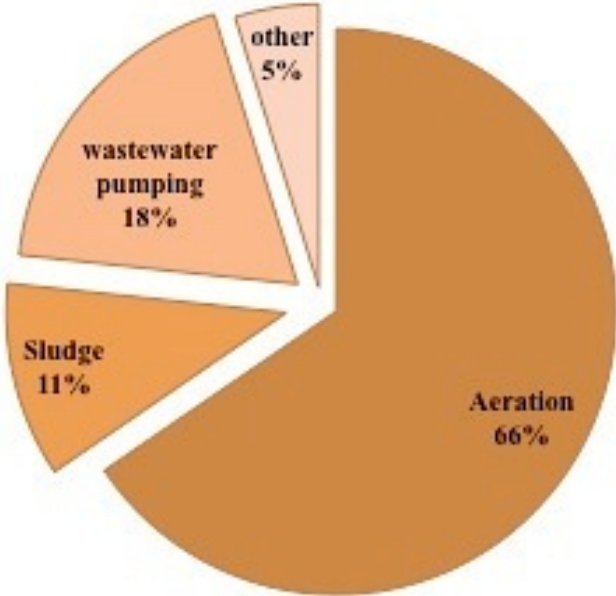


Figure 7.6. Distribution of electricity costs for Option 2.

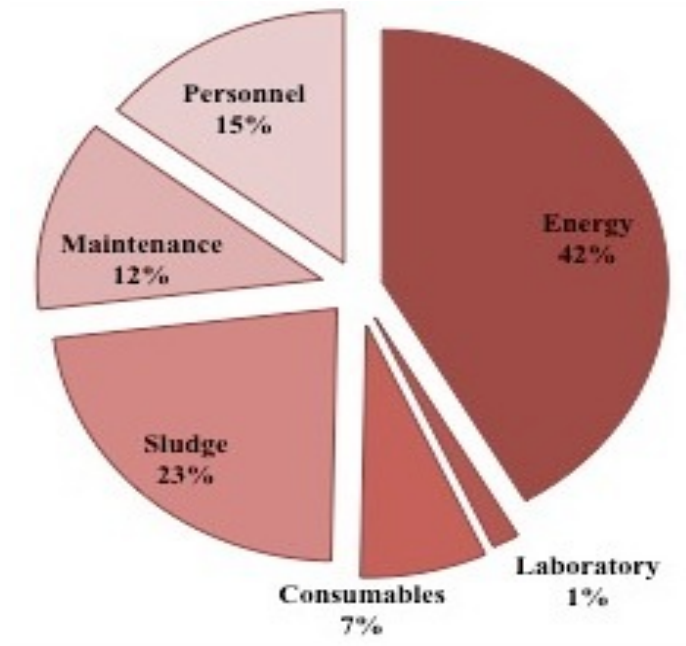


Figure 7.7. Distribution of important items in total operation cost for Option 3.

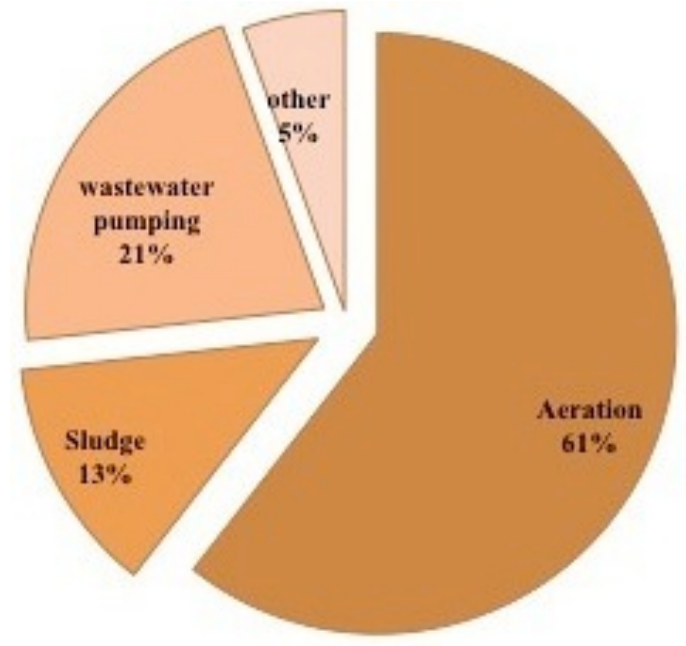


Figure 7.8. Distribution of electricity costs for Option 3.

8. CONCLUSIONS

The main objectives of the study were to bring up a submerged filtration system that depends on cake filtration principles and evaluate the main features of the high MLSS cake filtration (nitrification – denitrification) bioreactor; namely, filtration and treatment efficiencies, low sludge production potential regarding the growth pattern of nitrogen converters and operating cost in comparison with a membrane bioreactor. The results of the long-term filtration behaviour and characterisation of the parallel CFBR and MBR pilot units in Pasakoy WWTP, were presented in Chapter 4. The 0.4 μm flat sheet microfiltration membranes and a polyester cloth filter were operated in same tank at a target MLSS concentration of 15,000 mg L^{-1} . The air scouring system used for the membrane also scoured the cloth filter (55 $\text{m}^3 \text{h}^{-1}$ per 100 m^2 of filter area). Both the cloth filter and the membrane produced effluent with suspended solid concentrations less than 10 mg L^{-1} . Cloth filters can act as an alternative to final clarifiers while taking full advantage of the MBR systems, such as high MLSS operation, a smaller footprint, higher treatment efficiency depending on composition of biomass at higher concentrations and low sludge production.

The design operation flux of the commercial membrane used in this study was 17.5 $\text{L h}^{-1} \text{m}^{-2}$. The system was operated around design flux values; however, more stable operation was achieved when flux was around 9 $\text{L h}^{-1} \text{m}^{-2}$. The overall operating flux of the cloth filter was higher than that of a commercial membrane. The flux declined to 48 $\text{L h}^{-1} \text{m}^{-2}$ at the end of the one-year operation.

One year of continuous operation with the cloth filter showed that pressure differences across the cloth filter reached a steady value, after which no considerable changes

of Δp could be observed. The initial cost of a cloth filter is much less (approximately 90 %) than the cost of a membrane system.

Flux decline of the cross-flow cloth filter was observed in two steps, which were characterized by the deviation from the linear relationship between t/V and V . Initial filtration period was compatible with the standard blocking model, hence pore constriction and growth of a sufficiently thick cake layer over the media were considered as the basic fouling mechanisms. However, the latter period of filtration was considered as the stable cake filtration period.

In Chapter 5, the system efficiency and sludge production were monitored at constant volumetric loading rate in a pilot scale submerged CFBR and MBR unit. *AmoA* enzyme, which peaked in day 22, declined dramatically after one month of operation and stabilised in the latter period. However, the system showed insignificant and negligible deterioration of nitrification process, and stable COD and $\text{NH}_4\text{-N}$ removal efficiencies were achieved. Also, no deterioration of filtration was observed until $23000 \text{ mg}_{\text{MLSS}} \text{ L}^{-1}$. The results confirmed coexistence of aerobic and anaerobic ammonia oxidizers in a partially aerated system. Anammox bacteria grew at a significantly lower rate than that of aerobic ammonia oxidizers. However, they were more resistant to the effects of complete sludge retention (e.g. overgrazing on bacteria). The average observed sludge yield in the system was $0.25 \text{ kg}_{\text{MLSS}} \text{ kg}_{\text{COD}}^{-1}$ ($\text{MLSS} > 15,000 \text{ mg L}^{-1}$). Long-term experiments with complete solids retention showed that equilibrium conditions were reached after 3 months and could be maintained in terms of sludge production. MLVSS/MLSS ratio showed 3 different patterns: increasing, decreasing and finally increasing – stable. Stabilisation of the ratio, while constant inert material in wastewater was fed, evidenced that some portion of the inerts has become degradable at prolonged sludge retention. Hence, the study verified the feasibility of high MLSS filtration.

Moreover, the molecular study on the nitrogen converters at high MLSS concentrations (Chapter 6) showed that gradually increased VSS concentrations adversely affect the biomass fractions of AOB in the MBR, whereas fraction of NOB population did not change significantly. Phylogenetic analysis revealed that membrane bioreactor harbored diverse ammonia oxidizing community related to the *Nitrosomonas* and *Nitrospira* lineages. However, 16S rDNA *Nitrospira* gene analysis revealed that all clones were related to previously identified *Candidatus Nitrospira defluvii*. According to the quantitative real-time PCR results, *Nitrospira* species had the highest fraction of nitrogen-converting organism, which was up to 10-fold greater than AOB. It is considered that high fraction of *Nitrospira* species may have alternative functions than only nitrite oxidation. To understand the discrepancy between the number of bacterial genes and their known functions more investigations on the molecular tools are needed.

The system efficiency, sludge production and energetic parameters in a pilot scale submerged CFBR/MBR unit, and a full-scale BNR were analysed in Chapter 7. Also, three scenarios of a plant operation (conventional BNR plant and high biomass filtration plant with two different fluxes) were evaluated in terms of operation cost and energy consumption. The pilot plant provided a reliable operation except for the nitrate nitrogen removal. But the limited facilities of the pilot plant would be overcome in a real, larger scale plant and the contribution of oxygen from the coarse bubble aeration zone can be prevented resulting a robust nitrate nitrogen removal. The most important advantage of all in the pilot plant was low sludge production, which was approximately one thirds of the unit sludge production in the BNR plant. The disadvantage of operation with such elevated MLSS concentration was lower oxygen transfer efficiency, but the operation cost calculations showed that decreased sludge yield could overcome the handicap. Although the total energy cost increased by 6 to 9 % in the two scenarios of biomass filtration, the total operation cost was 9 to 15 % less than that of the full-scale plant.

REFERENCES

- [1] Gander, M.A., Jefferson, B., Judd, S.J., 2000. Membrane bioreactors for use in small wastewater treatment plants: membrane materials and effluent quality. *Water Science Technology*, 41 (1), 205 – 211.
- [2] Judd, S., 2006. *The MBR Book Principles and Applications of Membrane Bioreactors in Water and Wastewater Treatment*, First Edition, Elsevier, Great Britain.
- [3] Stephenson, T., Judd, S., Jefferson, B., Brindle, K., 2000. *Membrane Bioreactors for Wastewater Treatment*, IWA Publishing, London.
- [4] Ndinisa, N.V., Fane, A.G., Wiley, D.E., 2006. Fouling control in a submerged flat sheet membrane system: part I – bubbling and hydrodynamic effects. *Separation Science Technology*, 41, 1383 – 1409.
- [5] Cleasby, J.L., Logsdon, G.S., 1999. Granular Bed and Precoat Filtration. In *Water Quality and Treatment*, Fifth Edition, McGraw-Hill, New York.
- [6] Teoh, S.K., 2003. Studies in filter cake characterisation and modelling, Ph.D. Thesis, National University of Singapore.
- [7] Tiller, F.M., 1958. The role of porosity in filtration. Part 3: Variable pressure – variable-rate filtration. *American Institute of Chemical Engineers Journal*, 4 (2), 170 – 174.
- [8] Koch, M., 2008. Cake filtration modelling – Analytical cake filtration model and filter medium characterization, Ph.D. Thesis, Norwegian University of Science and Technology.

- [9] Campbell, R.W., 1983. Liquid/solid separation. Cake filters in batch filtration. *Plant/Operations Progress*, 2 (4), 216 – 221.
- [10] Ruth, B.F., 1935. Studies in filtration III. Derivation of general filtration equations. *Industrial and Engineering Chemistry*, 27, 708 – 723.
- [11] Tien, C., 2002. Cake filtration research – a personal view. *Powder Technology*, 127, 1 – 8.
- [12] Hillis, P., 2000. *Membrane Technology in Water and Wastewater Treatment*, the Royal Society of Chemistry.
- [13] Chu, H.P., Li, X., 2005. Membrane fouling in a membrane bioreactor (MBR): Sludge cake formation and fouling characteristics. *Biotechnology and Bioengineering*, 90 (3), 323 – 331.
- [14] Broeckmann, A., Busch, J., Wintgens, T., Marquardt, W., 2006. Modelling of pore blocking and cake layer formation in membrane filtration for wastewater treatment. *Desalination*, 189, 97 – 109.
- [15] Bai, R., Tien, C., 2005. Further work on cake filtration analysis. *Chemical Engineering Science*, 60, 301 – 313.
- [16] Tien, C., 2006. *Introduction to Cake Filtration: Analyses, Experiments and Applications*, Elsevier B.V., The Netherlands.
- [17] Dominiak, D., Christensen, M., Keiding, K., Nielsen, P.H., 2011. Gravity drainage of activated sludge: New experimental method and considerations of settling velocity, specific cake resistance and cake compressibility. *Water Research*, 45, 1941 – 1950.

- [18] Sveegaard, S.G., Keiding, K., Christensen, M.L., 2012. Compression and swelling of activated sludge cakes during dewatering. *Water Research*, 46, 4999 – 5008.
- [19] Svarovsky, L., 2001. *Solid liquid separation*, Fourth Edition, Elsevier Ltd., UK.
- [20] Tien, C., Teoh, S.K., Tan, R.B.H., 2001. Cake filtration analysis—the effect of the relationship between the pore liquid pressure and the cake compressive stress. *Chemical Engineering Science*, 56, 5361 – 5369.
- [21] McCabe, W., Smith, J.C., Harriott, P., 1956. *Unit operations of chemical engineering*, Fifth Edition, McGraw-Hill, Singapore.
- [22] Teoh, S.K., Tan, R.B.H., Tien, C., 2006. A new procedure for determining specific filter cake resistance from filtration data. *Chemical Engineering Science*, 61, 4957 – 4965.
- [23] Teoh, S.K., Tan, R.B.H., Tien, C., 2006. Analysis of cake filtration data – a critical assessment of conventional filtration theory. *American Institute of Chemical Engineers Journal*, 52 (10), 3427 – 3442.
- [24] Koenders, M.A., Wakeman, R.J., 1996. The initial stages of compact formation from suspensions by filtration. *Chemical Engineering Science*, 51, 3897 – 3908.
- [25] Hermans, P.H., Bredée, H.L., 1936. Principles of the mathematical treatment of constant pressure filtration. *Journal of the Society of Chemical Industry*, 55, 1 – 4.
- [26] Grace, H.P., 1956. Structure and performance of filter media. I. The internal structure of filter media. *American Institute of Chemical Engineers Journal*, 2, 307 – 315.
- [27] Hermia, J., 1982. Constant pressure blocking filtration laws. Application to power-law non-Newtonian fluids. *Transactions of the Institution of Chemical Engineers*, 60, 183 – 187.

- [28] Sonin, A.A., 2001. Fundamental laws of motion for particles, material volumes, and control volumes, http://web.mit.edu/2.25/www/pdf/fundamental_laws.pdf, (accessed January 2013).
- [29] Shirato, M., Iwata, M., 2006. Handbook of industrial drying / Solid-liquid separation for pretreatment of drying operation, Taylor&Francis Group LLC.
- [30] Meares, P., 1976. Membrane Separation Processes, Elsevier Scientific Publications, Amsterdam.
- [31] Le-Clech, P., Chen, V., Fane, A.G., 2006. Fouling in membrane bioreactors used in wastewater treatment. *Journal of Membrane Science*, 284, 17 – 53.
- [32] Mulder, J., 1996. Basic principles of membrane technology, Second Edition, Kluwer Academic Publishers, The Netherlands.
- [33] Chapman, S., Leslie, G., Law, I., 2007. Membrane Bioreactors (MBR) for Municipal Wastewater Treatment – An Australian Perspective, CH2M HILL, Australia.
- [34] Basile, A., Gallucci, F., 2011. Membranes for Membrane Reactors - Preparation, Optimization and Selection, John Wiley&Sons, UK.
- [35] Bemberis, I., Hubbard, P.J., Leonard, F.B., 1971. Membrane sewage treatment systems – potential for complete wastewater treatment. *American Society of Agricultural Engineers Winter Meeting*, 71 (878), 1 – 28.
- [36] Kraume, M., Drews, A., 2010. Membrane bioreactors in wastewater treatment – Status and trends. *Chemical Engineering and Technology*, 33 (8), 1251 – 1259.
- [37] EPA, 2005. Membrane filtration guidance manual, USA.

- [38] Chang, Y.J., 2006. Membrane applications. Surface water treatment workshop, www.mnawwa.org, (accessed March 2010).
- [39] Gupta, N., Jana, N., Majumder, C.B., 2008. Submerged membrane bioreactor system for municipal wastewater treatment process: An overview. *Indian Journal of Chemical Technology*, 15, 604 – 612.
- [40] Radjenovic, J., Matosic, M., Mijatovic, I., Petrovic, M., Barcelo, D., 2008. Membrane bioreactor (MBR) as an advanced wastewater treatment technology. *The Handbook of Environmental Chemistry*, 5, 37 – 101.
- [41] Roorda, J.H., van der Graaf, J.H., 2000. Understanding membrane fouling in ultrafiltration of WWTP-effluent. *Water Science Technology*, 41 (10-11), 345 – 353.
- [42] Braak, E., Alliet, M., Schetrite, S., Albasi, C., 2011. Aeration and hydrodynamics in submerged membrane bioreactors. *Journal of Membrane Science*, 379, 1 – 18.
- [43] Field, R.W., Wu, D., Howell, J.A., Gupta, B.B., 1995. Critical flux concept for microfiltration fouling. *Journal of Membrane Science*, 100, 259 – 272.
- [44] Ye, Y., Chen, V., 2005. Reversibility of heterogeneous deposits formed from yeast and proteins during microfiltration. *Journal Membrane Science*, 265, 20 – 28.
- [45] Zhang, T.C., Surampalli, R.Y., Vigneswaran, S., Tyagi, R.D., Ong, S.L., Kao, C.M., 2012. *Membrane Technology and Environmental Applications*, ASCE, USA.
- [46] Macphail, M.S., 2008. Cake dispersion for a submerged membrane bioreactor treating municipal wastewater, M.S. Thesis, The University of Guelph.

- [47] Kimura, K., Yamato, N., Yamamura, H., Watanabe, Y., 2005. Membrane fouling in pilot-scale membrane bioreactors (MBRs) treating municipal wastewater, *Environmental Science and Technology*, 39 (16), 6293 – 6299.
- [48] Chang, I.-S., Clech, P.L., Jefferson, B., Judd, S., 2002. Membrane fouling in membrane bioreactors for wastewater treatment. *Journal of Environmental Engineering*, 128 (11) 1018 – 1029.
- [49] Trussell, R.S., 2004. The effect of organic loading on process performance and membrane fouling in a submerged membrane bioreactor treating municipal wastewater, Ph.D. Thesis, University of California at Berkeley.
- [50] Scholz, W., Fuchs, W., 2000. Treatment of oil contaminated wastewater in a membrane bioreactor. *Water Research*, 34 (14), 3621 – 3629.
- [51] Acharya, C., Nakhla, G., Bassi, A., 2006. Optimization and mass balance in a two-stage MBR treating high strength pet food wastewater. *Journal of Environmental Engineering*, 132 (7) 810 – 817.
- [52] Hg, A.N.L., Kim, A.S., 2007. Mini-review of modelling studies on membrane bioreactor (MBR) treatment for municipal wastewaters. *Desalination*, 212, 261 – 281.
- [53] Knoblock, M.D., Sutton, P.M., Mishra, P.N., Gupta, K., Janson, A., 1994. Membrane biological reactor system for treatment of oily wastewaters. *Water Environment Research*, 66 (2), 133 – 139.
- [54] Satyawali, Y., Balakrishnan, M., 2008. Treatment of distillery effluent in a membrane bioreactor (MBR) equipped with mesh filter. *Separation and Purification Technology*, 63, 278 – 286.

- [55] Sun, D. D., Zang, J. L., Tay, J. H., 2002. A submerged tubular ceramic membrane bioreactor for high strength wastewater treatment. *Water Science and Technology*, 47 (1), 105 – 111.
- [56] Ghyoot, W., Verstraete, W., 1999. Reduced sludge production in a two-stage membrane-assisted bioreactor. *Water Research*, 34, 205 – 215.
- [57] Low, E.W., Chase, H.A., 1999. Reducing production of excess biomass during wastewater treatment. *Water Research*, 33, 1119 – 1132.
- [58] Jahan, K., Hoque, S., Ahmed, T., Turkdogan, I., Arslankaya, E., Patarkine, V., 2011. Activated sludge and other suspended culture processes. *Water Environment Research*, 83 (10), 1092 – 1149.
- [59] Wu, J., Huang, X., 2009. Effect of mixed liquor properties on fouling propensity in membrane bioreactors. *Journal of Membrane Science*, 342, 88 – 96.
- [60] Lousada-Ferreira, M., Geilvoet, S., Moreau, A., Atasoy, E., Krzeminski, P., van Nieuwenhuijzen, van der Graaf, J., 2010. MLSS concentration: Still poorly understood parameter in MBR filterability. *Desalination*, 250, 618 – 622.
- [61] Ng, H.Y., Tan, T.W., Ong, S.L., 2006. Membrane fouling of submerged membrane bioreactors: Impact of mean cell residence time and the contributing factors. *Environment Science and Technology*, 40, 2706 – 2713.
- [62] Giulio, M., Mori, G., Laura, S., Barberio, C., Claudio, L., 2008. Process efficiency and microbial monitoring in MBR (membrane bioreactor) and CASP (conventional activated sludge process) treatment of tannery wastewater. *Bioresource Technology*, 99, 8559 – 8564.

- [63] Teck, H.C., Loong, K.S., Sun, D.D., Leckie, J.O., 2009. Influence of a prolonged solid retention time environment on nitrification/denitrification and sludge production in a submerged membrane bioreactor. *Desalination*, 245, 28 – 43.
- [64] Yeom, I.T., Nah, Y.M., Ahn, K.H., 1999. Treatment of household wastewater using an intermittently aerated membrane bioreactor. *Desalination*, 124, 193 – 204.
- [65] Suwa, Y., Yamagishi, T., Urushigawa, Y., Hirai, M., 1989. Simultaneous organic carbon removal nitrification by an activated sludge process with crossflow filtration. *Journal of Fermentation and Bioengineering*, 67 (2), 119–125.
- [66] Ramphao, M., Wentzel, M.C., Merritt, R., Ekama, G.A., Young, T., Buckley, C.A., 2005. Impact of membrane solid-liquid separation on design of biological nutrient removal activated sludge systems. *Biotechnology and Bioengineering*, 89 (6), 630 – 646.
- [67] Sofia, A., Liu, W.T., Ong, S. L., Ng, W.J., 2004. In-situ characterization of microbial community in an A/O submerged membrane bioreactor with nitrogen removal. *Water Science and Technology*, 50, 41 – 48.
- [68] Mulder, A., Vandegraaf, A. A., Robertson, L. A., Kuenen, J. G., 1995. Anaerobic ammonium oxidation discovered in a denitrifying fluidized-bed reactor, *FEMS Microbiology Ecology*, 16, 177 – 183.
- [69] Rosenberger, S., Laabs, C., Lesjean, B., Gnirss, R., Amy, G., Jekel, M., Schrotter, J.-C., 2006. Impact of colloidal and soluble organic material on membrane performance in membrane bioreactors for municipal wastewater treatment. *Water Research*, 40, 710 – 720.
- [70] Drews, A., Vocks, M., Bracklow, U., Iversen, V., Kraume, M., 2008. Does fouling in MBR depend on SMP? *Desalination*, 231, 141 – 149.

- [71] Drews, A., Mante, J., Iversen, V., Vocks, M., Lesjean, B., Kraume, M., 2007. Impact of ambient conditions on SMP elimination and rejection in MBRs. *Water Reserach*, 41, 3850 – 3858.
- [72] Meng, F., Chae, S.R., Drews, A., Kraume, M., Shin, H.S., Yang, F., 2009. Recent advances in membrane bioreactors (MBRs): Membrane fouling and membrane material. *Water Research*, 43, 1489 – 1512.
- [73] Moghaddam, M.R.A., Guan, Y., Satoh, H., Mono, T., 2006. Filter clogging in coarse pore filtration activated sludge process under high MLSS concentration. *Water Science and Technology*, 15, 55 – 66.
- [74] Jeison, D., Diaz, I., van Lier, J.B., 2008. Anaerobic membrane bioreactors: Are membranes really necessary? *Electronic Journal of Biotechnology*, 11, 1 – 9.
- [75] Kiso, Y., Jung, Y.J., Ichinari, T., Park, M., Kitao, T., Nishimura, K., Min, K.S., 2000. Wastewater treatment performance of a filtration bio-reactor equipped with a mesh as a filter material. *Water Research*, 34, 4143 – 4150.
- [76] Chang, M.C., Horng, R.Y., Shao, H., Hu, Y.J., 2006. Performance and filtration characteristics of non-woven membranes used in a submerged membrane bioreactor for synthetic wastewater treatment. *Desalination*, 191, 8 – 15.
- [77] Chu, L.B., Li, S., 2006. Filtration capability and operational characteristics of dynamic membrane bioreactor for municipal wastewater treatment. *Separation and Purification Technology*, 51, 173 – 179.
- [78] Fan, B., Huang, X., 2002. Characteristics of a self-forming dynamic membrane coupled with a bioreactor for municipal wastewater treatment. *Environment Science and Technology*, 36, 5245 – 5251.

- [79] Fuchs, W., Resh, C., Kernstock, M., Mayer, M., Schoeberl, P., Braun, R., 2005. Influence of operational conditions on the performance of a mesh filter activated sludge process. *Water Research*, 39, 803 – 810.
- [80] Kiso, Y., Jung, Y.J., Park, M.S., Wang, W.H., Shimase, M., Yamada, T., Min, K.S., 2005. Coupling of sequencing batch bioreactor and mesh filtration: Operational parameters and wastewater treatment performance. *Water Research*, 39, 4887 – 4898.
- [81] Seo, G.T., Moon, B.H., Park, Y.M., Kim, S.H., 2007. Filtration characteristics of immersed coarse pore filters in an activated sludge system for domestic wastewater reclamation. *Water Science and Technology*, 55, 51 – 58.
- [82] Tooker, N.B., Darby, J.L., 2007. Cloth Media Filtration and Membrane Microfiltration: Serial Operation. *Water Environment Research*, 79, 125 – 130.
- [83] Walker, M., Banks, C.J., Heaven, S., 2009. Development of a coarse membrane bioreactor for two-stage anaerobic digestion of biodegradable municipal solid waste. *Water Science and Technology*, 59, 729 – 735.
- [84] Van Loosdrecht, M.C.M., Lykema, J., Norde, W., 1989. Bacterial Adhesion: A physicochemical approach. *Microbial Ecology*, 17, 1 – 15.
- [85] Koziarz, J., Yamazaki, H., 1998. Immobilization of bacteria on to polyester cloth. *Biotechnology Techniques*, 12 (5), 407 – 410.
- [86] Lee, D.J., Wang, C.H., 2000. Theories of cake filtration and consolidation and implications to sludge dewatering. *Water Research*, 34, 1 – 20.
- [87] Bowen, W.R., Yousef, H.N.S., Calvo, J.I., 2001. Dynamic crossflow ultrafiltration of colloids: a deposition probability cake filtration approach. *Separation and Purification Technology*, 24, 297 – 308.

- [88] T.S. Khean, 2003. Studies in filter cake characterisation and modelling, Ph.D. Thesis, National Uni. of Singapore.
- [89] Ho, J., Sung, S., 2009. Effects of solid concentrations and cross-flow hydrodynamics on microfiltration of anaerobic sludge. *Journal of Membrane Science*, 345, 142 – 147.
- [90] Grenier, A., Meireles, M., Aimar, P., Carvin, P., 2008. Analysing flux decline in dead-end nitration. *Chemical Engineering Research and Design*, 86, 1281 – 1293.
- [91] Grace, H.P., 1956. Structure and performance of filter media. I. The internal structure of filter media. *American Institute of Chemical Engineers Journal*, 2, 307 – 315.
- [92] Hermia, J., 1966. Etude analytique des lois de filtration à pression constant. *Revue Universelle des Mines*, 2, 45.
- [93] Sorensen, B.L., Sorensen, P.B., 1997. Applying cake filtration theory on membrane filtration data. *Water Research*, 31, 665 – 670.
- [94] Cheng, Y.L., Lee, D.J., Lai, J.Y., 2011. Filtration blocking laws: Revisited. *Journal of the Taiwan Institute of Chemical Engineers*, 42, 506 – 508.
- [95] Xu, W., Chellam, S., 2005. Initial stages of bacterial fouling during dead-end microfiltration. *Environmental Science and Technology*, 39, 6470 – 6476.
- [96] Standard Methods for the Examination of Water and Wastewater, 2005. Twentyfirst Edition, APHA, AWWA, WEF, Washington DC, USA.
- [97] Murase, T., Iritani, E., Cho, J.H., Nakanomori, S., Shirato, M., 1987. Determination of filtration characteristics due to sudden reduction in filtration area of filter cake surface. *Journal of Chemical Engineering of Japan*, 20, 246 – 251.

- [98] Tiller, M., Chow, R., Weber, W.H., Davies, O., 1981. Clogging Phenomena in the Filtration of Liquefied Coal. *Chemical Engineering Progress*, 77, 61 – 68.
- [99] Tiller, F.M., Cooper, H.R., 1960. The role of porosity in filtration: IV. Constant pressure filtration. *American Institute of Chemical Engineers Journal*, 6, 595 – 601.
- [100] Fenu, A., Guglielmi, G., Jimenez, J., Sperandio, M., Saroj, D., Lesjean, B., Brepols, C., Thoeye, C., Nopens, I., 2010. Activated sludge model (ASM) based modelling of membrane bioreactor (MBR) processes: A critical review with special regard to MBR specificities. *Water Research*, 44, 4272 – 4294.
- [101] Cronje, G.L., Beeharry, A.O., Wentzel, M.C., Ekama, G.A., 2002. Active biomass in activated sludge mixed liquor. *Water Research*, 36, 439 – 444.
- [102] Orhon, D., Karahan, O., Sozen, S., 1999. The effect of residual microbial products on the experimental assessment of the particulate inert cod in wastewaters. *Water Research*, 33, 3191–3203.
- [103] Ramdani, A., Dold, P., Gadbois, A., Deleris, S., Houweling, D., Comeau, Y., 2012. Characterization of the heterotrophic biomass and the endogenous residue of activated sludge. *Water Research*, 46, 653 – 668.
- [104] Sun, D.D., Khora, S.L., Haya, C.T., Leckie, J.O., 2007. Impact of prolonged sludge retention time on the performance of a submerged membrane bioreactor. *Desalination*, 208, 101 – 112.
- [105] Heran, M., Wisniewski, C., Orantes, J., Grasmick, A., 2008. Measurement of kinetic parameters in a submerged aerobic membrane bioreactor fed on acetate and operated without biomass discharge. *Biochemical Engineering Journal*, 38, 70 – 77.

- [106] Wei, Y., van Houten, R.T., Borger, AR., Eikelboom, DH., Fan, Y., 2003. Minimization of excess sludge production for biological wastewater treatment. *Water Research*, 37, 4453 – 4467.
- [107] Mason, C.A., Hamer, G., Bryers, J.D., 1986. The death and lysis of microorganism in environmental process. *FEMS Microbiology Reviews*, 39, 373 – 401.
- [108] Moussa, M.S., Hooijmans, C.M., Lubberding, H.J., Gijzen, H.J., van Loosdrecht, M.C.M., 2005. Modelling nitrification, heterotrophic growth and predation in activated sludge. *Water Research*, 39, 5080 – 5098.
- [109] Cote, P., Buisson, H., Pound, C., Arakki, G., 1997. Immersed membrane activated sludge for the reuse of municipal wastewater. *Desalination*, 113, 189 – 196.
- [110] Fan, X-J, Urbain, V., Quian, Y., Manem, J., 1996. Nitrification and mass balance with a membrane bioreactor for municipal wastewater treatment. *Water Science and Technology*, 34, 129 – 136.
- [111] Visvanathan, C., Aim, R.B., Parameshwaran, K., 2000. Membrane separation bioreactors for wastewater treatment. *Critical Reviews in Environmental Science and Technology*, 30 (1), 1 – 48.
- [112] Huang, X., Gui, P., Qian, Y., 2001. Effect of sludge retention time on microbial behaviour in a submerged membrane bioreactor. *Process Biochemistry*, 36, 1001 – 1006.
- [113] Liu, R., Huang, X., Xi, J., Qian, Y., 2005. Microbial behaviour in a membrane bioreactor with complete sludge retention. *Process Biochemistry*, 40, 3165 – 3170.
- [114] Laera, G., Pollice, A., Saturno, D., Giordano, C., Lopez, A., 2005. Zero net growth in a membrane bioreactor with complete sludge retention. *Water Research*, 39, 5241 – 5249.

- [115] Ni, B-J, Sheng, G-P, Yu, H-Q, 2011. Model-based characterization of endogenous maintenance, cell death and predation processes of activated sludge in sequencing batch reactors. *Chemical Engineering Science*, 66, 747 – 754.
- [116] Liang, P., Huang, X., Qian, Y., 2006. Excess sludge reduction in activated sludge process through predation of *Aeolosoma hemprichi*. *Biochemical Engineering Journal*, 28, 117 – 122.
- [117] van Loosdrecht, M,C.M., Henze, M., 1999. Maintenance, endogeneous respiration, lysis, decay and predation. *Water Science and Technology*, 39, 107 – 117.
- [118] Davey, H.M., Kaprelyants, A.S., Weichart, D.H., Kell, D.B., 1999. Approaches to the Estimation of Microbial Viability Using Flow Cytometry. *Current Protocols in Cytometry*, vol. 11, Microbial Cytometry, Wiley, New York.
- [119] Kaprelyants, A.S., Kell, D.B., 1996. Do bacteria need to communicate with each other for growth? *Trends in Biochemical Sciences*, 4, 237 – 242.
- [120] Kell, D.B., Young, M., 2000. Bacterial dormancy and culturability: the role of autocrine growth factors. *Current Opinion in Microbiology*, 3, 238 – 243.
- [121] Lubello, C., Caffaz, S., Gori, R., Munz, G., 2009. A modified activated sludge model to estimate solids production at low and high solids retention time. *Water Research*, 43 (18), 4539 – 4548.
- [122] Ramdani, A., Dold, P., Deleris, S., Lamarre, D., Gadbois, A., Comeau, Y., 2010. Biodegradation of the endogenous residue of activated sludge. *Water Research*, 44, 2179 – 2188.

- [123] Muller, E.B., Stouthamer, A.H., van Verseveld, H.W., Eikelboom, G.H., 1995. Aerobic domestic wastewater treatment in a pilot plant with complete sludge retention by cross-flow filtration. *Water Research*, 29 (4), 1179 – 1189.
- [124] Xing, CH., Wu, WZ., Qian, Y., Tardieu, E., 2003. Excess sludge production in membrane bioreactors: a theoretical investigation. *Journal of Environmental Engineering*, 129 (4), 291 – 297.
- [125] Duan, X., Zhou, J., Qiao, S., Yin, X., Tian, T., Xu, F., 2012. Start-up of the anammox process from the conventional activated sludge in a hybrid bioreactor. *Journal Environmental Sciences*, 24 (6), 1083 – 1090.
- [126] Strous, M., van Gerven, E., Kuenen, J.G., Jetten, M., 1997. Effects of aerobic and microaerobic conditions on anaerobic ammonium-oxidizing (anammox) sludge. *Applied and Environmental Microbiology*, 63 (6), 2446 – 2448.
- [127] Kuenen, J.G., 2008. Anammox bacteria: from discovery to application. *Nature Reviews Microbiology*, 6, 320 – 326.
- [128] Xiao, Y., Zeng, G.M., Yang, Z.H., Liu, YSh., Ma, YH., Yang, L., Wang, RJ., Xu, ZhY, 2009. Coexistence of nitrifiers, denitrifiers and Anammox bacteria in a sequencing batch biofilm reactor as revealed by PCR-DGGE. *Journal of Applied Microbiology*, 106, 496 – 505.
- [129] Yan, J.J., 2012. Interactions of marine nitrogen cycle microorganisms, Ph.D. Thesis, China: Radboud University Nijmegen.
- [130] Feng, Y-J, Tseng, S-K, Hsia, T-H, Ho, C-M, Chou, W-P, 2007. Partial Nitrification of Ammonium-Rich Wastewater as Pretreatment for Anaerobic Ammonium Oxidation (Anammox) Using Membrane Aeration Bioreactor. *Journal of Bioscience and Bioengineering*, 104, 182 – 187.

- [131] Hao, X., Heijnen, J.J., van Loosdrecht, MCM., 2002. Model-based evaluation of temperature and inflow variations on a partial nitrification–Anammox biofilm process. *Water Research*, 36, 4839 – 4849.
- [132] Nittami, T., Ootake, H., Imai, Y., Hosokai, Y., Takada, A., Matsumoto, K., 2011. Partial nitrification in a continuous pre-denitrification submerged membrane bioreactor and its nitrifying bacterial activity and community dynamics. *Biochemical Engineering Journal*, 55, 101 – 107.
- [133] Sliemers, A.O., Derwort, N., Campos Gomez, J.L., Strous, M., Kuenen, J.G., Jetten, M.S.M., 2002. Completely autotrophic nitrogen removal over nitrite in one single reactor. *Water Research*, 36, 2475 – 2482.
- [134] Zhang, L., Yang, J., Furukawa, K., 2010. Stable and high-rate nitrogen removal from reject water by partial nitrification and subsequent Anammox. *Journal of Bioscience and Bioengineering*, 110, 441 – 448.
- [135] Kowalchuk, G.A., Stephen, J.R., 2001. Ammonia-oxidizing bacteria: A model for molecular microbial ecology. *Annual Review of Microbiology*, 55, 485 – 529.
- [136] Strous, M., van Gerven, E., Zheng, P., Kuenen, J.G., Jetten, M.S.M., 1997. Ammonium removal from concentrated waste streams with the anaerobic ammonium oxidation (ANAMMOX) process in different reactor configurations. *Water Research*, 31, 1955 – 1962.
- [137] Francis, C.A., Beman, J.M., Kuypers, M.M.M., 2007. New processes and players in the nitrogen cycle: The microbial ecology of anaerobic and archaeal ammonia oxidation. *International Society of Microbial Ecology Journal*, 1, 19 – 27.
- [138] Grady, C.P.L., Lim, H.C., 1980. *Biological Wastewater Treatment. In: Theory and Applications*, Marcel Dekker, New York.

- [139] Geets, J., de Cooman, M., Wittebolle, L., Heylen, K., Vanparys, B., de Vos, P., Verstraete, W., Boon, N., 2007. Real-time PCR assay for the simultaneous quantification of nitrifying and denitrifying bacteria in activated sludge. *Applied Microbiology and Biotechnology*, 75, 211 – 221.
- [140] Yapsakli, K., Mertoglu, B., Cecen, F., 2010. Identification of nitrifiers and nitrification performance in drinking water Biological Activated Carbon (BAC) filtration. *Process Biochemistry*, 45 (9), 1543 – 1549.
- [141] Jie, H., Daping, L., Qiang, L., Yong, T., Xiaohong, H., Xiaomei, W., Xudong, L., Ping G., 2009. Effect of organic carbon on nitrification efficiency and community composition of nitrifying biofilms. *Journal of Environmental Sciences*, 21, 387 – 394.
- [142] Patel, J., Nakhla, G., Margaritis, A., 2005. Optimization of biological nutrient removal in a membrane bioreactor system. *Journal of Environmental Engineering- ASCE*, 131, 1021 – 1029.
- [143] Han, S.S., Bae, T.H., Jang, G.G., Tak, T.M., 2005. Influence of sludge retention time on membrane fouling and bioactivities in membrane bioreactor system. *Process Biochemistry*, 40, 2393 – 2400.
- [144] Tan, T.W., Ng, H.Y., Ong, S.L., 2008. Effect of mean cell residence time on the performance and microbial diversity of pre-denitrification submerged membrane bioreactors. *Chemosphere*, 70, 387 – 396.
- [145] Yoon, T.I., Lee, H.S., Kim, C.G., 2004. Comparison of pilot scale performances between membrane bioreactor and hybrid conventional wastewater treatment systems. *Journal of Membrane Science*, 242, 5 – 12.
- [146] Mertoglu, B., Calli, B., Inanc, B., Ozturk, I., 2006. Evaluation of in situ ammonia removal in an aerated landfill bioreactor. *Process Biochemistry*, 41 (12), 2359 – 2366.

- [147] Smith, C., Berg, D., Beaumont, S., Standley, N.T., Wells, D.N., Pfeffer, P.L., 2007. Simultaneous gene quantitation of multiple genes in individual bovine nuclear transfer blastocysts. *Reproduction*, 133 (1), 231 – 242.
- [148] National Center for Biotechnology Information. <http://www.ncbi.nlm.nih.gov> (accessed September 2010).
- [149] Muyzer, G., deWaal, E.C., Uitterlinden, A.G., 1993. Profiling of complex microbial populations by denaturing gradient gel electrophoresis analysis of polymerase chain reaction-amplified genes coding for 16S rRNA. *Applied Environmental Microbiology*, 59, 695 – 700.
- [150] Muyzer, G., Teske, A., Wirsén, C.O., Jannasch, H.W., 1995. Phylogenetic relationship of *Thiomicrospira* species and their identification in deep-sea hydrothermal vent samples by denaturing gradient gel electrophoresis of 16S rDNA fragments. *Archives of Microbiology*, 164, 165 – 172.
- [151] Rotthauwe, J.H., Witzel, K.P., Liesack, W., 1997. The ammonia monooxygenase structural gene *amoA* as a functional marker: molecular fine-scale analysis of natural ammonia oxidizing populations. *Applied Environmental Microbiology*, 63, 4704 – 4712.
- [152] Degrange, V., Bardin, R., 1995. Detection and counting of *Nitrobacter* populations in soil by PCR. *Applied Environmental Microbiology*, 61, 2093 – 2098.
- [153] Dionisi, H.M., Layton, A.C., Harms, G., Gregory, I.R., Robinson, K.G., Sayler, G.S., 2002. Quantification of *Nitrosomonas oligotrophalike* ammonia-oxidizing bacteria and *Nitrospira* spp. from full-scale wastewater treatment plants by competitive PCR. *Applied Environmental Microbiology*, 68, 245 – 253.

- [154] Neef, A., Amann, R., Schlesner, H., Schleifer, K.H., 1998. Monitoring a widespread bacterial group: In situ detection of planctomycetes with 16S rRNA-targeted probes. *Microbiology*, 144 (12), 3257 – 3266.
- [155] van der Star, W.R.L., Abma, W.R., Blommers, D., Mulder, J.W., Tokutomi, T., Strous, M., Picioreanu, C., van Loosdrecht, M.C.M., 2007. Startup of reactors for anoxic ammonium oxidation: Experiences from the first full-scale Anammox reactor in Rotterdam. *Water Research*, 41, 4149 – 4163.
- [156] Chiemchaisri, C., Wong, Y.K., Urase, T., Yamamoto, K., 1992. Organic stabilization and nitrogen removal in a membrane separation bioreactor for domestic wastewater treatment. *Water Science and Technology*, 25, 231 – 240.
- [157] Ng, H.Y., Hermanowicz, S.W., 2005. Membrane bioreactor operation at short solids retention times: Performance and biomass characteristics. *Water Research*, 39, 981 – 992.
- [158] Duan, L., Moreno-Andrade, I., Huang, C.L., Xia, S., Hermanowicz, S.W., 2009. Effects of short solids retention time on microbial community in a membrane bioreactor. *Bioresource Technology*, 100, 3489 – 3496.
- [159] Cicek, N., Macomber, J., Davel, J., Suidan, M.T., Audic, J., Genestet, P., 2001. Effect of solids retention time on the performance and biological characteristics of a membrane bioreactor. *Water Science and Technology*, 43(11), 43 – 50.
- [160] Yu, T., Qi, R., Li, D., Zhang, Y., Yang, M., 2010. Nitrifier characteristics in submerged membrane bioreactors under different sludge retention times. *Water Research*, 44, 2823 – 2830.
- [161] Li, H., Yang, M., Zhang, Y., Yu, T., Kamagata, Y., 2006. Nitrification performance and microbial community dynamics in a submerged membrane bioreactor with complete sludge retention. *Journal of Biotechnology*, 123, 60 – 70.

- [162] Daims, H., Maixner, F., Lucker, S., Stoecker, K., Hace, K., Wagner, M., 2006. Ecophysiology and niche differentiation of *Nitrospira*-like bacteria, the key nitrite oxidizers in wastewater treatment plants. *Water Science and Technology*, 54 (1), 21 – 27.
- [163] Watson, S.W., Bock, E., Valois, F.W., Waterbury, J.B., Schlosser, U., 1986. *Nitrospira marina* gen. nov. sp. nov.: A chemolithotrophic nitrite-oxidizing bacterium. *Archives of Microbiology*, 144, 1 – 7.
- [164] Ehrich, S., Behrens, D., Lebedeva, E., Ludwig, W., Bock, E., 1995. A new obligately chemolithoautotrophic, nitrite-oxidizing bacterium, *Nitrospira moscoviensis* sp. nov. and its phylogenetic relationship, *Archives of Microbiology*, 164, 16 – 23.
- [165] Spieck, E., Hartwig, C., McCormack, I., Maixner, F., Wagner, M., Lipski, A., Daims, H., 2006. Selective enrichment and molecular characterization of a previously uncultured *Nitrospira*-like bacterium from activated sludge. *Environmental Microbiology*, 8, 405 – 415.
- [166] Daims, H., Nielsen, J.L., Nielsen, P.H., Schleifer, K.H., Wagner, M., 2001. In situ characterization of *Nitrospira*-like nitrite-oxidizing bacteria active in wastewater treatment plants. *Applied Environmental Microbiology*, 67, 5273 – 5284.
- [167] Lucker, S., Wagner, M., Maixner, F., Pelletier, E., Koch, H., Vacherie, B., Rattei, T., Damsté, J.S.S., Spieck E., Paslier D., Daims, H., 2010. A *Nitrospira* metagenome illuminates the physiology and evolution of globally important nitrite-oxidizing bacteria. *Proceedings of the National Academy of Sciences*, 107, 13479 – 13484.
- [168] Cicek, N., Winna, H., Suidan, M.T., Wrenn, B.E., Urbain, V., Manem, J., 1998. Effectiveness of the membrane bioreactor in the biodegradation of high molecular weight compounds, *Water Research*, 32, 1553 – 1563.
- [169] EPA, 2010. Evaluation of Energy Conservation Measures for Wastewater Treatment Facilities, EPA 832-R-10-005, USA.

- [170] Chriemchaisri, C., Yamamoto, K., Vigneswaran, S., 1993. Household membrane bioreactor in domestic wastewater treatment. *Water Science and Technology*, 27, 171 – 178.
- [171] Verrecht, B., Maere, T., Brepols, C., Judd, S., 2010. The cost of a large-scale hollow fibre MBR. *Water Research*, 44, 5274 – 5283.
- [172] van der Roest, H.F., Lawrence, D.P., van Bentem, A.G., 2002a. Membrane Bioreactors for Municipal Wastewater Treatment (Water and Wastewater Practitioner Series: Stowa report), IWA, London.
- [173] Cote, P., Masini, M., Mourato, D., 2004. Comparison of membrane options for water reuse and reclamation, *Desalination*, 167, 1 – 11.
- [174] Brepols, C., Schafer, H., Engelhardt, N., 2010. Considerations on design and financial feasibility of full scale membrane bioreactors for municipal applications. *Water Science and Technology*, 61 (10), 2461 – 2468.
- [175] Churchouse, S.J., Warren, S., Floyd, M., 2007. Feedback from the Porlock MBR Plant in its 10th year of operation: an analysis of the flux, effluent quality and membrane lifetime data to date. Proceedings of the Seventh Aachen Water and Membrane Conference, Aachen, Germany.
- [176] Cornel, P., Wagner, M., Krause, S., 2003. Investigation of oxygen transfer rates in full scale membrane bioreactors. *Water Science and Technology*, 47 (11), 313 – 319.
- [177] Schoeberl, P., Brik, M., Bertoni, M., Braun, R., Fuchs, W., 2005. Optimization of operational parameters for a submerged membrane bioreactor treating dyehouse wastewater. *Separation and Purification Technology*, 44, 61 – 68.
- [178] Verrecht, B., Judd, S., Guglielmi, G., Brepols, C., Mulder, J.W., 2008. An aeration energy model for an immersed membrane bioreactor. *Water Research*, 42, 4761 – 4770.

- [179] Gander, M., Jefferson, B., Judd, S., 2000. Aerobic MBRs for domestic wastewater treatment: a review with cost considerations. *Separation and Purification Technology*, 18, 119 – 130.
- [180] Zhan, S., van Houten, R., Eikelboom, D.H., Doddema, H., Jiang, Z., Fan, Y., Wang, J., 2003. Sewage treatment by a low energy membrane bioreactor. *Bioresource Technology*, 90, 185 – 192.
- [181] Gil, J.A., Tua, L., Rueda, A., Montano, B., Rodriguez, M., Prats, D., 2010. Monitoring and analysis of the energy cost of an MBR. *Desalination*, 250, 997 – 1001.
- [182] Prieske, H., Drews, A., Kraume, M., 2008. Prediction of the circulation velocity in a membrane bioreactor. *Desalination*, 231, 219 – 226.
- [183] Meng, F., Chae, S.-R., Shin, H.-S., Yang, F., Zhou, Z., 2012. Recent advances in membrane bioreactors: configuration development, pollutant elimination, and sludge reduction. *Environmental Engineering Science*, 29 (3), 139 – 160.
- [184] Sperandio, M., Espinosa, M.C., 2008. Modelling an aerobic submerged membrane bioreactor with ASM models on a large range of sludge retention time. *Desalination*, 231, 82 – 90.
- [185] Rosenberger, S., Kruger, U., Witzig, R., Manz, W., Szewzyk, U., Kraume, M., 2002. Performance of a bioreactor with submerged membranes for aerobic treatment of municipal waste water. *Water Research*, 36, 413 – 420.
- [186] Pollice, A., Laera, G., Blonda, M., 2004. Biomass growth and activity in a membrane bioreactor with complete sludge retention. *Water Research*, 38 (7), 1799 – 1808.
- [187] Cornel, P., Krause, S., 2002, State of the Art on MBR in Europe, Darmstadt University of Technology, Institut WAR—Wastewater Treatment, Darmstadt, Germany.

- [188] Yoon, S.-H., Kim, H.-S., Yeom, I.-T., 2004. The Optimum Operational Condition of Membrane Bioreactor (MBR): Cost Estimation of Aeration and Sludge Treatment. *Water Research*, 38, 37 – 46.
- [189] Ozdemir, B., Yildiz, O., Demir, A., 2011. Membran Bioreaktörler: İstanbul'da işletme tecrübesi. 2.Ulusal Membran Teknolojileri ve Uygulamaları Sempozyumu Bildiriler Kitabı, İstanbul.
- [190] Gunder, B., 2001. The Membrane Coupled Activated Sludge Process in Municipal Wastewater Treatment, Technomic Publishing Company Inc., Lancaster.
- [191] Krampe J., Krauth, K., 2003. Oxygen Transfer into Activated Sludge with High MLSS Concentrations. *Water Science and Technology*, 47, 297 – 303.
- [192] Muller, E.B., Stouthamer, A.H., Vanverseveld, H.W., Eikelboom, D.H., 1995. Aerobic Domestic Wastewater Treatment in a Pilot Plant with Complete Sludge Retention by Cross-flow Filtration. *Water Research*, 29, 1179 – 1189.
- [193] Rosenberger, S., 2003. Charakterisierung von belebtem Schlamm in Membran belebungs reaktoren zur Abwasserreinigung, Dissertation, TU Berlin.
- [194] Rosso, D., Larson, L.E., Stenstrom, M.K., 2010. Aeration of Large-scale Municipal Wastewater Treatment Plants: State of the Art; Pier Final Project Report, A Digital Control System for Optimal Oxygen Transfer Efficiency Appendix F: Technical Papers, Los Angeles, CA.
- [195] Yunt, F.W., Stenstrom, M.K., 1996. Aeration Equipment Evaluation – Phase II: Process Water Test Results. EPA Report 68-03-2906, USA.